2006-08-28

Sound Absorption and Sound Power Measurements in Reverberation Chambers Using Energy Density Methods

David B. Nutter
Brigham Young University - Provo

SOUND ABSORPTION AND SOUND POWER MEASUREMENTS IN REVERBERATION CHAMBERS USING ENERGY DENSITY METHODS

by

David Benjamin Nutter

A thesis submitted to the faculty of

Brigham Young University

in partial fulfillment of the requirements for the degree of

Master of Science

Department of Physics and Astronomy

Brigham Young University

December 2006

BRIGHAM YOUNG UNIVERSITY

GRADUATE COMMITTEE APPROVAL

of a thesis submitted by

David Benjamin Nutter

This thesis has been read by each member of the following graduate committee and by majority vote has been found to be satisfactory.

Date	Timothy W. Leishman, Chair
Date	Scott D. Sommerfeldt
Date	Jonathan D. Blotter

BRIGHAM YOUNG UNIVERSITY

As chair of the candidate's graduate committee, I have read the thesis of David Benjamin Nutter in its final form and have found that (1) its format, citations, and bibliographical style are consistent and acceptable and fulfill university and department style requirements; (2) its illustrative materials including figures, tables, and charts are in place; and (3) the final manuscript is satisfactory to the graduate committee and is ready for submission to the university library.

Date

Timothy W. Leishman, Chair

Accepted for the Department

Ross L. Spencer
Graduate Coordinator
Department of Physics and Astronomy

Thomas W. Sederberg
Associate Dean, College of Physical and Mathematical Sciences

ABSTRACT

SOUND ABSORPTION AND SOUND POWER MEASUREMENTS IN REVERBERATION CHAMBERS USING ENERGY DENSITY METHODS

David B. Nutter

Department of Physics and Astronomy

Master of Science

Measurements in a reverberation chamber use spatially averaged squared pressure to calculate sound absorption, sound power, and other sound measurements. While a reverberation chamber provides an approximation of a diffuse sound field, variations in the measurements introduce uncertainty in measurement results. Room qualification procedures require a sufficient number of source-receiver locations to obtain suitable measurements. The total acoustic energy density provides greater spatial uniformity than squared pressure, which requires fewer source-receiver positions to produce similar or better accuracy in measurement results. This paper explores the possibility of using energy density in place of squared pressure, using methods outlined in current ISO standards, by describing several experimental and analytical results.

ACKNOWLEDGMENTS

I express gratitude to those who have helped me complete this research in any way. First and foremost, I appreciate my wife Tiffany for her constant support throughout this process. I thank my adviser, Dr. Timothy Leishman, for encouraging me through the difficult parts of the work. I thank the other members of my committee, Dr. Scott Sommerfeldt and Dr. Jonathan Blotter, for their helpful input. Thanks also to Dr. Kent Gee, Sarah Rollins, Ben Faber and Gordon Dix for assistance with my numerical analysis. I appreciate those who were involved with the qualification of the rooms and measurements, namely Micah Shephard, Ben Shafer, John Paul Abbott, and Ryan Chester. Finally, thanks to Diann Sorensen and to the members of the Acoustics Research Group for their support, and to NSF for funding this research.

TABLE OF CONTENTS

LIST OF TABLES

LIST OF FIGURES

CHAPTER 1 - INTRODUCTION

Energy-based acoustics research at Brigham Young University is currently encompassing many different areas of interest. These include active noise control in free and enclosed fields, near-field acoustic holography, equalization of one- and three-dimensional sound fields, and numerical modeling of diffuse fields. Recently, two reverberation chambers have been built by the university for experimental work in acoustics. It seemed appropriate to extend acoustic energy density research to include this experimental work. Progress made in the other areas of the energy-based research suggested that significant contributions could be made to the established field of reverberation room research. This thesis summarizes the role energy density may play in the improvement or simplification of reverberation chamber measurements in light of current qualification standards.

1.1 Background

In order to fully appreciate the significance of this research, this section contains a brief description of the basic theory of sound in enclosures, as well as pertinent research in reverberation room acoustics and other areas of acoustics.

1.1.1 Basic Theory and Concepts

Room acoustics is the study of sound propagation in enclosures. Three main theories have been developed to describe the sound field: wave (modal) theory, ray (geometric) theory, and diffuse field theory. In wave theory, the spatial and temporal relationship of vibrations in the medium caused by sound waves is expressed through the wave equation. The sound at any point in a room can be expressed by the superposition

of waves caused by direct and reflected sound. For simple room shapes, the complex acoustic pressure amplitude satisfying the reduced wave equation (Helmholtz equation) can be calculated from the modal eigenfunctions. The eigenfunctions satisfy the homogeneous Helmholtz equation and boundary conditions. In ray theory, for rooms with dimensions larger than half a wavelength, sound waves are replaced by rays. These sound rays act similarly to light rays in propagation, but neglect interference effects. Rays incident on a planar surface are reflected such that the angle of incidence equals the angle of reflection. Two methods that utilize geometric acoustics are the image source method and the ray tracing method. The image source method uses virtual sources at reflection boundaries, and creates an impulse response at a point by adding up the individual contributions from each source. Ray tracing involves projecting a number of possible ray paths from a source and tracking the times and energies of each path which pass through a specified region to generate an impulse response. The derivation and implementation of both wave theory and ray theory for practical situations are described by Kuttruff.[1]

Diffuse field theory is based on random incidence, a special case in room acoustics. It describes an ideal condition wherein the intensities of incident sound at a point are uniformly distributed over all possible directions, and the phase components of these waves are randomly distributed. This implies that the acoustic energy density is uniform throughout the sound field. While not perfectly realizable, this condition can be carefully approximated under specified conditions. The closest practical situation that resembles a diffuse field is within the central region of a qualified reverberation chamber.

The transition between wave theory and diffuse field theory is described by the Schroeder frequency.[2] Below this frequency, the sound field consists of individual, well-separated resonances, while above the Schroeder frequency, many normal modes overlap.

1.1.2 Relevant Work Done in the Past

Reverberation chambers have been a subject of great interest for the last 75 years. Ever since Sabine's famous reverberation experiments,[3] sound propagation in enclosures has been examined rigorously. Practical uses for a reverberation chamber include measurement of acoustical properties of sound sources and absorptive materials. The accuracy of these measurements has been under scrutiny for decades. Most of the research dealing with reverberation chambers is related to decreasing measurement uncertainty. The ISO standards are periodically updated to reflect new innovations and insights, which include both theoretical and experimental corrections to obtain results comparable to free-field measurements.

Current standards for measuring sound power and sound absorption rely on the use of spatially averaged squared pressure values. In a review of the standards in 1974, Tichy and Baade suggested that it would be more beneficial to use energy density measurements to reduce spatial variation of the sound field. However, since no reliable method of measuring kinetic energy density was available, the spatially averaged squared pressure has been continually used.[4]

Concerns about sound power measurements in reverberation rooms include underestimation of sound power at lower frequencies, changes in radiation impedance seen by the sound source, insufficient sampling of the sound field, and reproducibility at different source positions.[5] Some research has been devoted to solving these concerns.

Waterhouse investigated acoustic interference patterns at reflecting boundaries, which exist because of lack of phase randomness near room boundaries where the normal component of particle velocity of a plane wave vanishes.[6] The Waterhouse correction is applied to measurements taken in the diffuse field to account for the potential energy stored in these interference patterns. Schaffner has modified the correction to include absorption affects on the boundaries.[7] Another correction has been introduced by Vorlander to account for "missing sound level" using diffuse field equations.[8] Changes in radiation impedance are due to reflections from nearby surfaces and atmospheric conditions. Effects from the latter are applied to a correction term[5] which adjusts the measured levels to those that would be measured with a characteristic acoustic impedance of 400 $N \cdot s/m^3$. Schultz pointed out that measurement results are valid only for the source position used for the test.[9]

Use of stationary sound diffusers, a large room volume, and low-frequency absorption can reduce the effects of reflections. A rotating diffuser has also been shown to improve spatial averaging of the sound field, which reduces the number of receiver positions required for adequate sampling.[4] However, rotating diffusers are not permissible in some measurements, such as scattering coefficient measurements.[10] Averaging over several source positions may also reduce variation. Acceptable values of standard deviation are outlined in ISO standards 354 and 3741, and are based on models of statistical distribution of the squared pressure for high modal densities.[11, 12]

The most distinguishing characteristic of reverberation chambers is, of course, the long reverberation time. The reverberation time T_{60} was calculated by Sabine after a series of empirical measurements, which showed its relationship to the volume and total

absorption area of the room.[3] It is defined as the time, in seconds, that would be required for the sound pressure level to decrease by 60 dB after the sound source has stopped.[13] Other calculations of T_{60} are given by Eyring[14] and Norris, which result in smaller values at higher absorption. This quantity is used to determine the absorption coefficients of test materials. Diffuse field theory suggests that T_{60} is uniform at all points in a room. However, just as in steady-state sound pressure measurements, variation does exist in a reverberation chamber. It has been suggested by Hodgson that exponential decay (or a linear decay on a logarithmic scale), while predicted by the Eyring equation for a diffuse field, is actually dependent on room shape, room absorption, and the absorption coefficient of the sound diffusers.[15] Thus, sound may become "trapped" in certain regions of the room, which results in a decay that deviates from the theoretical prediction. One method of obtaining T_{60} is by performing backward integration of the squared impulse response.[16] Another way is to measure the decay curve at a point in a room after the source producing a steady-state sound field in a room has been turned off. Both the integrated impulse response method and the decay curve method are allowed by ISO 354.

Some interesting work has been done in obtaining energy density measurements, even as far back as the 1930's. Wolff and Massa[17] used a pressure gradient microphone to estimate the particle velocity, and compared variations of the potential, kinetic, and total energy density in a room. Others[18,19] used spaced microphones to estimate particle velocity from pressure differences. Elko[20] similarly used many microphones embedded in a sphere to reduce bias errors of these estimates. The usable frequency range depends on the size of the sphere. The recent introduction of the Microflown™ sensor, a micro-machined sensor that directly measures particle velocity, has provided a means of

obtaining energy density measurements up to 20 kHz. The accuracy of these measurements is treated in several publications.[21]

At the time of this writing, no published work on accurate experimental measurements of sound absorption or sound power using energy density in reverberation chambers is known by the author. However, several applications of energy density and intensity measurements, which also rely on particle velocity, have been published. Active Noise Control using energy density in three-dimensional enclosures was originally pursued by Parkins and Sommerfeldt.[22] Microflown® has provided a method of calibration of its velocity sensors for several acoustic environments, including a reverberation room technique.[21] A reverberation chamber was used to measure the absorption coefficients of materials, by placing the Microflown™ sensor very close to the surface and measuring the absorbed intensity due to the diffuse excitation.[23] A so-called "quadraphonic impulse response" is mentioned by Bonsi,[24] which is essentially the energy density impulse response derived in this thesis. Bonsi's use is not for precision measurements, but for the acoustic enhancement of audio tracks.

1.2 Motivations for Research

Because the sound field in enclosures can be extremely complex, research in reverberant rooms continues to expand. Even with the utmost care given to comply with the latest versions of ISO standards, a level of measurement uncertainty is unavoidable. Because of this, the standards contain values of acceptable measurement standard deviations. Deviation values considered acceptable could be greatly reduced if there were means of obtaining consistent results. The identification of problems associated

with previous research may lead to effective use of new technology to meet the needs of research and industry.

1.2.1 Problems or Shortfalls of Past Work

As previously mentioned, the lack of accurate methods to obtain kinetic energy density from particle velocity has necessitated the use of spatially averaged squared pressure measurements to calculate sound levels and absorption characteristics. The use of pressure gradient microphones to estimate particle velocity and total energy density is limited by the physical dimensions of the transducer. Energy density probes using spaced microphones suffer from the similar restrictions. Furthermore, the reproducibility of measurements in different reverberation chambers is still under investigation, since sound source location, receiver location, and changes in atmospheric conditions affect the measurements. Steps taken to qualify a room for sound power measurements, such as a rotating diffuser and low-frequency absorbers, compromise conditions necessary for other measurements (e.g., sound absorption and scattering). These qualification steps can also be quite time consuming.

1.2.2 Needs of Researchers and Industry

Due to the number of factors that increase measurement uncertainty even in qualified chambers, both academic and professional groups would benefit from methods that effectively minimize one or more sources of error. If it were possible to extend the usable low-frequency range of a chamber without adding more absorption to increase modal overlap, reverberation chambers could service additional measurements with little or no modifications. Perhaps smaller rooms which do not meet current volume requirements could be used with reasonable accuracy at lower frequencies. In addition, if

measurements were taken using a quantity that is more uniform than squared pressure, less reverberant rooms that fail to satisfy current standards might also be used to obtain comparable measurements, providing a means for those who do not have access to such facilities.

1.2.3 Uniqueness of Research Required to Address the Needs

The application of an energy density sensor in a reverberation chamber to measure the sound power of a source and the absorption coefficient of a test material looks promising. Previous research suggesting greater uniformity of total energy density than that of squared pressure can be verified with the recent availability of an accurate particle velocity sensor, especially at higher frequencies. Measurements taken in several environments can also aid in determining if the strict methods required in the current standards can be adapted if total energy density is used instead of squared pressure.

1.3 Objectives of Research

The following important questions will be answered by this thesis;

- Can energy density measurements achieve comparable or better results for reverberation chamber measurements than the methods described by current standards?
- If so, what is the minimum number of energy density measurements required to obtain these results?
- Can the use of energy density extend the usable range of reverberation rooms at frequencies below the Schroeder frequency?
- Can the use of energy density allow smaller reverberation chambers to be used with greater accuracy?

- Can energy density be used in rooms that are not reverberation chambers to obtain comparable measurement results?

The answers to these questions could have an effect on future revisions of the standards for precision measurements in reverberation chambers. They may also lead to results with a higher degree of confidence than that obtained from current methods.

The aims of this research are to answer the questions posed above. The answers to these questions may be found by completing the following goals:

- Qualify a reverberation chamber for current absorption and sound power measurement methods, using standards ISO 354 and 3741.
- Measure the sound power and absorption of two samples using standard methods.
- Using results from procedures outlined in the standards, the number of energy density sensors required to achieve the same values for sound absorption and sound power as standard microphone will be determined.
- Determine whether the use of energy density sensors can extend the usable frequency range of the room, particularly below the Schroeder frequency. If this extension is possible, determine the new frequency range.
- Determine the possibility of obtaining similar measurement results in a smaller reverberation chamber.
- Determine the possibility of extending measurements to rooms that are not reverberation chambers.

1.4 Scope of Research

This thesis discusses current methods of obtaining measurements for sound power and sound absorption in a reverberation chamber. It explores the use of energy density

for these measurements. While other important measurements, such as sound transmission loss and scattering, can also be made in a reverberation chamber, they are not discussed. The qualification process of the chamber used is included for clarity.

1.5 Plan of Development

This chapter has explained the background and motivations for the research, as well as the objectives and scope of the paper. Chapter two will discuss the methods used to obtain the measurement results. Chapter three will detail the measured data and chapter four will provide an analysis of these results. Finally, chapter five will provide conclusions and the impact of the work on current methods, as well as recommendations for future work.

CHAPTER 2 – METHODS

Two rectangular chambers were constructed for the purpose of obtaining sound measurements including sound absorption of various materials, sound power of sources under test, sound scattering properties of surfaces, and sound transmission through partitions. When this research began, the reverberation chambers had not been qualified for measurements, according to established standards. The first step, therefore, was to qualify the chambers. This chapter outlines the qualification process for preparing a chamber for both sound absorption and sound power measurements, including instrumentation, data acquisition, and analysis. Because only the larger chamber meets volume conditions specified in the ISO standards for these measurements, it was selected to obtain the primary objectives of this research. The steps for calculation of the sound absorption and sound power of test sources and materials in a qualified chamber will then be discussed. A new approach for calculation of the impulse response and sound power using energy density is also introduced.

2.1 Qualification for Sound Absorption Measurements (ISO 354)

For sound absorption measurements, ISO 354[13] specifies room parameters including volume, spatial dimensions, atmospheric conditions, and diffusivity. The qualification procedure includes the use of a test material, directions for positioning the sound source and receivers, and the calculation of T_{60}.

2.1.1 Acceptable Room Parameters

The absorption coefficients of the material under test are measured in 1/3rd-octave bands, between 100 Hz and 5000 Hz. In order to obtain sufficient accuracy at the

lowest frequencies, the volume of the chamber must be at least 150 m^3. The standard suggests that the volume should be at least 200 m^3 but not exceed 500 m^3 because excessive air absorption can cause inaccuracies at higher frequencies. Similarly, rooms with smaller volumes are useful for obtaining accurate high frequency data, but suffer at low frequencies. The spatial dimensions of the room must be such that the length of the longest straight line within the boundary of the room, denoted $I_{\max}$, must not exceed a value given by the inequality

$$I_{\max} < 1.9V^{1/3}, \tag{2.1}$$

where V is the room volume.[13] The dimensions of the chamber are 4.96 m × 5.89 m × 6.98 m. The maximum allowable straight line value for the chamber is then 11.18 m, while the measured value is 10.39 m. The standard requirement that no two dimensions can be a ratio of small numbers[13] is also satisfied.

Atmospheric conditions during any measurement process in the chamber are to be closely monitored. It is desirable to have similar room conditions during measurements both with and without the test specimen. Changes in temperature and humidity affect reverberation time values, which can alter the apparent absorption coefficients of the test material if unaccounted for. It is recommended that values of the relative humidity be at least 30% for all measurements. The ambient temperature should not drop below 15° C.

Diffusivity in the chamber is achieved by adding stationary or rotating elements with hard, reflecting surfaces. Stationary diffusers are positioned randomly in the room. The material used for the diffusers should have a density of at least 5 kg/m^2, with small absorption coefficients.[13] They should have individual surface areas between 0.8 m^2 to 3 m^2. Using a test specimen with a frequency dependent absorption coefficient greater than

0.9 over the frequency range from 500 Hz to 4000 Hz, diffusers are added to the room, and the average sound absorption coefficient is calculated by averaging the reverberation times, or decay curves, of the room with and without the test specimen. This process is repeated until the sound absorption coefficient reaches a consistent maximum value.

2.1.2 Room Qualification

The large chamber was outfitted with stationary diffuser panels of varying surface areas, suspended from the ceiling (see Fig. 2.1). They were created from acrylic sheets that were slightly curved by using a heat gun. A Genie Lift™ was used to access the 23 foot ceiling, and several holes were drilled to place anchors and corresponding eyebolts. Wire rope of differing lengths were attached to these eyebolts and suspended to prepare for the addition of the diffuser panels. For practical reasons, the Genie Lift™ was kept in a corner of the room throughout the qualification process. It was treated as a diffuser itself,

FIG. 2.1. Ceiling view of suspended diffuser panels in large chamber.

and its exposed surface area was included in the measurements (see Fig. 2.2). The use of rotating vanes is suggested to keep the shape of the room changing. This breaks up modal patterns and reduces measurement variation. However, since standards for measuring sound scattering properties of surfaces state that rotating vanes must not be used[10], they were not included.

The test material used in the qualification was a 5 cm thick fiberglass planar absorber. The allowable surface area of rectangular-shaped absorbers must be between 10 m^2 and 12 m^2, but can be larger if the volume of the room exceeds 200 m^3. The width-to-length ratio of the absorber must be between 0.7 and 1. During measurements, the edges of the test specimen are not to be parallel to the nearest edge of the room. Also, no part of the test specimen is allowed to be closer than 0.75 m to any room boundary. The material was placed in a Type A mounting (on the floor). In order to fit the test specimen inside the chamber under these constraints, it was cut into several pieces and arranged in a rectangular shape.

FIG. 2.2. Genie Lift™ positioned as a diffuser during room qualification.

The joints of the pieces were covered with tape, as directed, in order to prevent exposed air spaces (see Fig. 2.3). The outer edges of the specimen were exposed; therefore, as required, the additional surface area was included in the total value, which was 10.65 m^2.

The two specified ways to measure T_{60} are the interrupted noise method and the integrated impulse response method. The interrupted noise method involves a statistical process in which at least three decay curves are measured at one microphone or loudspeaker position and then averaged. To obtain a desired repeatability comparable to the integrated impulse response method, at least ten decay curves should be used. An omni-directional noise source is turned on until the room reaches a steady state condition. The noise is then abruptly turned off, and the sound pressure level at that position decays until it reaches the ambient noise level of the room.

FIG. 2.3. Test material placed in Type A mounting.

The slope of the average of these decays is used to calculate T_{60}. This is repeated at several positions (at least 12) to obtain a spatially averaged T_{60}.

The integrated impulse response method, or IIR method, is a deterministic function which requires more sophisticated instrumentation and data processing than the interrupted noise method. A pseudo-random noise signal is produced from a signal generator and sent to a sound source through an amplifier. The signal is then retrieved by the microphone, where it is sent to an analyzer and processed. The retrieval of the pseudo-random noise gives the analyzer information about the room, from which the impulse response of the room between the source and receiver is created. The impulse response is filtered into 1/3rd-octave bands. The filtered impulse responses are then backward integrated using the Schroeder method,[16] computed by

$$E_p(t) = \int_t^\infty h_p^2(t) d(-t), \tag{2.2}$$

where $h_p^2(t)$ is the squared pressure impulse response. This integration is equivalent to averaging an infinite number of decay curves using the interrupted noise method. The slope of the integrated curve is then used to determine T_{60}. For either method, the evaluation of the decay curves or integrated impulse responses are to be started 5 dB below the initial sound pressure level, and are to have a range of 20 dB. The bottom of the evaluation range must be at least 10 dB above the background noise level. The T_{60} values are extrapolated from this region using a least-squares-fit line over the evaluation range.[25] These values are then spatially averaged from the multiple measurement positions.

The IIR method was chosen for room qualification. A TEF Analyzer was used with SoundLab™, a software package that includes a maximum-length sequence impulse response measurement package. Six Larson Davis ½-inch ICP Microphones were used to record the impulse responses at discrete locations. These microphones were powered by an ICP power supply, with individual gains for each channel. A dodecahedron loudspeaker (see Fig. 2.4) was used as the sound source. The loudspeaker amplifier, TEF, and ICP power supply were in the control room, and the signals were sent via a patch panel (see Fig. 2.5).

The standard calls for at least 12 source-receiver locations (see Fig. 2.6), where the source must be placed in at least two different positions, and the microphones must be in at least three different positions. Because the sound field close to the room boundaries and other reflecting surfaces is not diffuse, the microphones must be at least 1 m from these surfaces. The microphone positions are also to be at least 1.5 m apart, 2 m from the

FIG. 2.4. Dodecahedron sound source.

FIG. 2.5. Reverberation chamber control room.

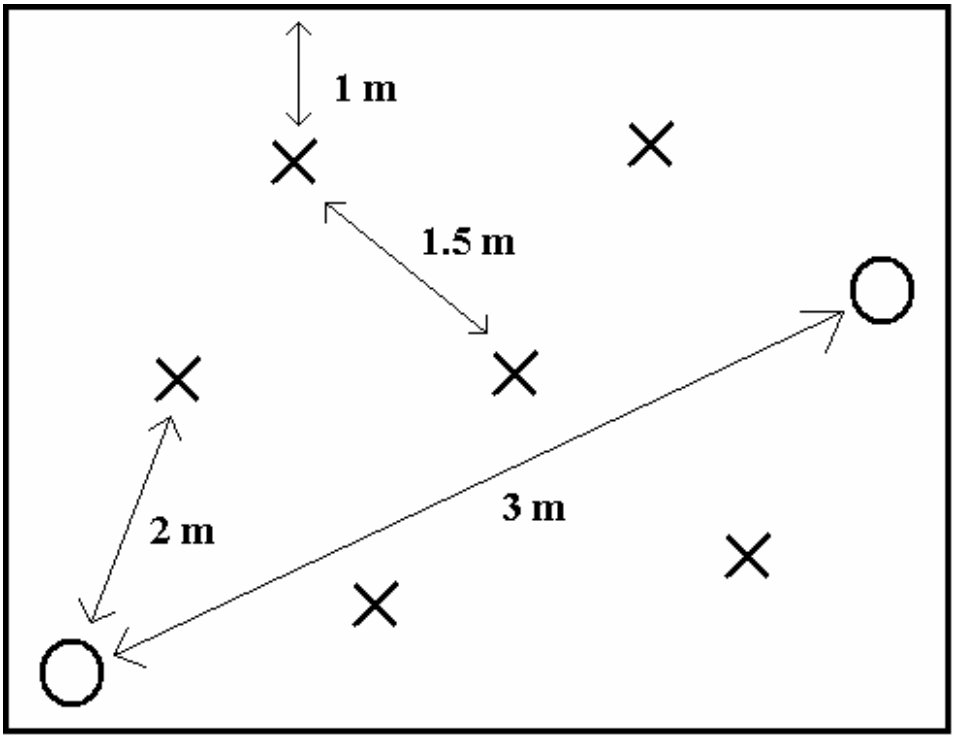

FIG. 2.6. Schematic of source-receiver positions. The O's are sources and the X's are receivers.

sound source, and 1 m from the test material. Source positions should be 3 m apart. During qualification, two source positions were used, with six microphone positions for each source position.

Atmospheric conditions were monitored using a LI-COR temperature/humidity sensor. Because the door to the chamber had to be opened to change the source position, each set of measurements was taken after the room was given adequate time to reach its equilibrium state. Another unfortunate issue was the amount of time required to take the measurements. Each impulse response measurement took slightly more than two minutes to complete. After six measurements were completed, the source position was moved, time was given to allow atmospheric equilibrium, and six more measurements were completed. This process took about 45 minutes for the empty chamber, and the measurements which included the test material took slightly longer. As a result, each set of measurements for a given amount of diffuser material present in the chamber required almost two hours of data acquisition. The temperature and humidity were averaged between the 12 measurements for both the empty and occupied states.

From ISO 354, the equivalent sound absorption area of the test specimen for a given frequency band is

$$A_T = 55.3V\left(\frac{1}{c_2 T_2} - \frac{1}{c_1 T_1}\right) - 4V(m_2 - m_1), \tag{2.3}$$

where T denotes the arithmetic mean value of T_{60}, c is the speed of sound, V is the room volume, and m is the power attenuation coefficient. The subscripts *1* and *2* refer to values of the chamber when empty and with the test specimen, respectively. The value for m can be obtained by the relationship

$$m = \frac{\alpha}{10\log(e)}, \tag{2.4}$$

where α is the pure-tone sound-attenuation coefficient for atmospheric absorption, in decibels per meter. This coefficient is obtained by inserting the values of temperature, relative humidity, and barometric pressure into Eqs. (2.5) through (2.10), detailed in ISO 9613.[26] This document provides a method to account for the absorption of sound by the atmosphere. It assumes an atmosphere free from significant fog or pollutants, with uniform meteorological conditions. For a given temperature and pressure, the molar concentration, h, of water vapor, as a percentage value, is obtained from

$$h = h_r \frac{p_{sat}/p_r}{p_a/p_r}, \tag{2.5}$$

where h_r is the relative humidity, as a percentage value, p_a is the measured atmospheric pressure in kilopascals, p_r is the reference ambient atmospheric pressure in kilopascals, and p_{sat} is the saturation vapor pressure. The ratio p_{sat}/p_r is obtained from the relationship

$$\frac{p_{sat}}{p_r} = 10^C, \tag{2.6}$$

where

$$C = -6.8346\left(T_{01}/T\right)^{1.261} + 4.6151, \tag{2.7}$$

and where T is the temperature in Kelvin, and T_{01} is the triple-point isotherm temperature 273.16 K. Equations (2.6) and (2.7) are close approximations to values obtained by the World Meteorological Organization. Once h is known, the attenuation due to

atmospheric absorption can be described as a function of the oxygen and nitrogen relaxation frequencies (f_{rO} and f_{rN}). The relaxation frequencies, in Hz, are obtained by

$$f_{rO} = \frac{p_a}{p_r}\left(24 + 4.04\times10^4 h \frac{0.02+h}{0.391+h}\right), \tag{2.8}$$

$$f_{rN} = \frac{p_a}{p_r}\left(\frac{T}{T_0}\right)^{-1/2}\left(9 + 280h\cdot e^{\left\{-4.170\left[\left(\frac{T}{T_0}\right)^{-1/3}-1\right]\right\}}\right), \tag{2.9}$$

where T_0 is 293.15 K (room temperature). The attenuation coefficient α in Eq. (2.4) has units of reciprocal meters and is computed for a given one-third octave band f by

$$\alpha = 8.686 f^2\left(\begin{array}{l} 1.84\times10^{-11}\left(\frac{p_a}{p_r}\right)^{-1}\left(\frac{T}{T_0}\right)^{1/2} + \left(\frac{T}{T_0}\right)^{-5/2} \\ \left\{0.01275\cdot e^{\left(\frac{-2239.1}{T}\right)}\left(f_{rO}+\frac{f^2}{f_{rO}}\right)^{-1} + 0.1068\cdot e^{\left(\frac{-3352}{T}\right)}\left(f_{rN}+\frac{f^2}{f_{rN}}\right)^{-1}\right\} \end{array}\right). \tag{2.10}$$

Of special interest is the accuracy level obtained from these calculations. According to ISO 9613 the accuracy of the pure-tone attenuation coefficient is estimated to be ±10% under optimum atmospheric conditions. This has drastic effects on measurements at higher frequencies, and will be discussed later.

The sound absorption coefficient of a plane absorber is

$$\alpha_s = \frac{A_T}{S_T}, \tag{2.11}$$

where S_T is the area, in square meters, covered by the test specimen. α_s is not expressed as a percentage because it can have values larger than 1.0 (e.g. because of diffraction effects) when evaluated from reverberation time measurements.[13] Ten sets of diffusers

were added, for a total surface area of 48.95 m^2. This value included the surface area of the Genie Lift™. The observed absorption coefficient reached a maximum value after the addition of the ninth set of diffusers at 45.92 m^2. This frequency-averaged value was calculated and plotted for each incremental addition of diffusers, as can be seen in Fig. 2.7. After the addition of the tenth set of diffusers, the coefficient decreased slightly. Once the Genie Lift™ was removed, the total diffusing surface area dropped to 45.83 m^2, 22% of the surface area of the room. This was close to the 45.92 m^2 optimum value. The standard indicates that sound absorption coefficient values between 15%-25% are expected for qualification. It has been observed that the installation of diffusers beyond a sufficient number can actually reduce the absorption coefficient[27], and since the surface

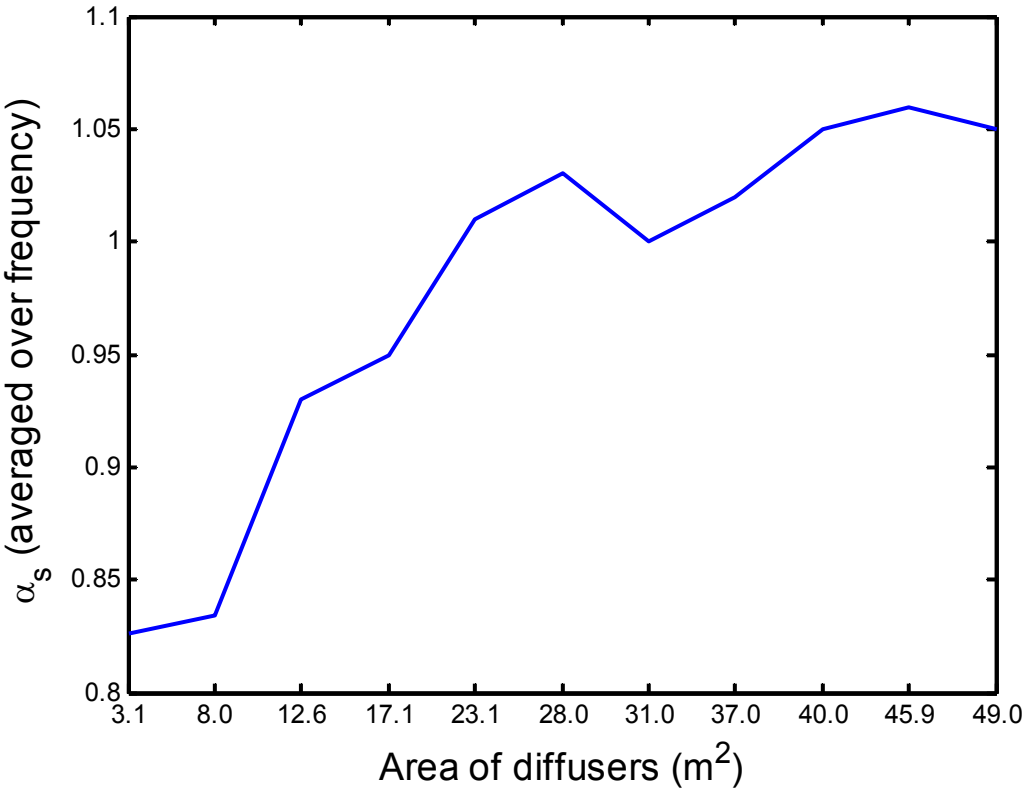

FIG. 2.7. Average absorption coefficient of test material as diffusers are installed for qualification.

area of the diffusers were within the expected values, it was decided not to add more diffusers.

The addition of diffusers to the chamber increases the total absorption in the room, which decreases T_{60}. The standard dictates maximum allowed equivalent sound absorption areas for each 1/3rd-octave band for the empty chamber. Also, the values for each frequency band are to be within 15% of the mean value of the adjacent values. Figure 2.8 shows the measured and calculated absorption coefficients overlaid with the allowed coefficients, showing that the empty chamber with diffusers meets the standard criteria.

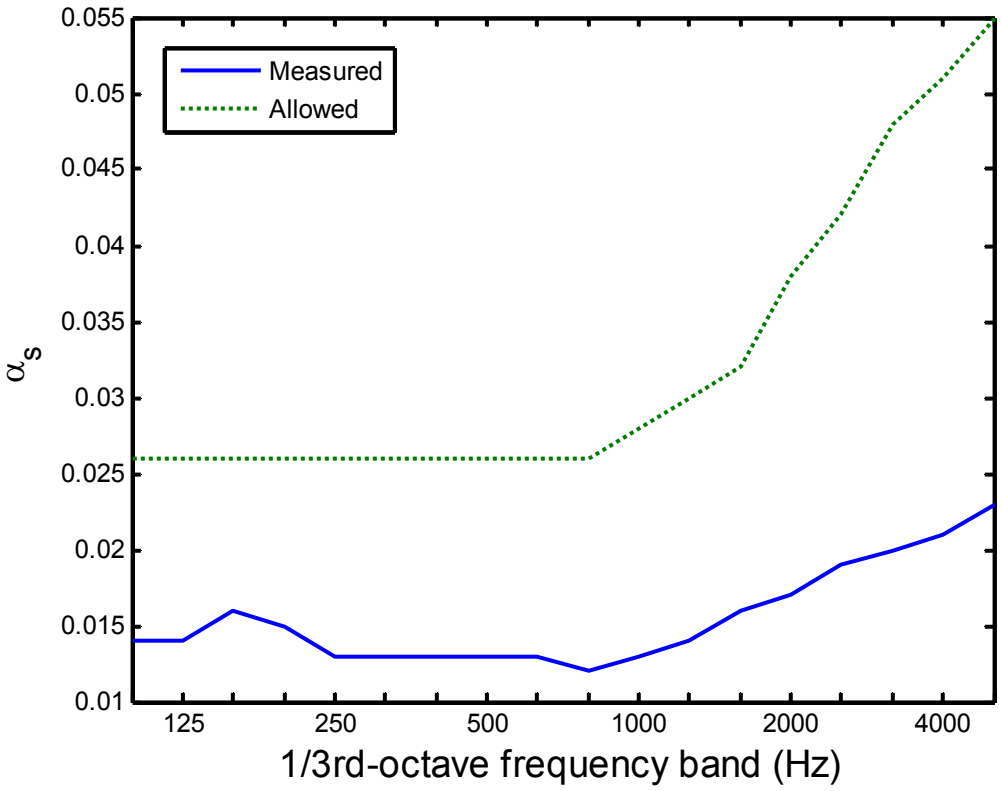

FIG. 2.8. Measured vs. allowed absorption coefficient of empty chamber.

2.2 Qualification for Sound Power Measurements (ISO 3741)

The methods in the ISO 3741 standard for sound power measurements[5] are applicable to steady noise with broadband, narrowband and discrete-frequency components. Like ISO 354, qualification of the reverberation room for sound power requires adequate volume, diffusing elements, suitably small sound absorption over the frequency range of interest, and sufficiently low background noise levels. The standard discusses measurement uncertainty, acceptable atmospheric conditions, source and receiver location and mounting, and determination of sound power levels. It also gives discusses the need for additional source and/or receiver positions based on the standard deviation of the obtained sound pressure levels.

2.2.1 Acceptable Room Parameters

The frequency range of interest is between 100 Hz and 10 kHz, in 1/3rd octave bands. Methods for determining accurate readings at higher frequencies are available in ISO 9295.[28] For the lowest frequency band of interest, the minimum volume required of the test room is 200 m^3. Requirements for absorption of the test room are to be "neither too large nor extremely small."[5] The sound radiation of the source and the frequency response characteristics of the test space are influenced by the absorption. The absorption also affects the minimum distance required between the noise source and microphone positions. This is shown[2] from the relationship of the diffuse-field distance $r_{c,}$ in meters, to the total absorption A in the room, by

$$r_c = \sqrt{\frac{A}{16\pi}} \,. \tag{2.12}$$

The surfaces of the room closest to the source must have an absorption coefficient less than 0.06. The remaining surfaces must be treated such that the numerical value of the reverberation time of the empty room is greater than the ratio of V and the total surface area of the room S, in each 1/3rd-octave band, by

$$T_{60} > \frac{V}{S}. \tag{2.13}$$

The V/S ratio for the large chamber, after qualification according to ISO 354, is 0.8. The addition of low-frequency absorbers will alter this value. Higher frequencies correspond to lower reverberation times due to air absorption, and should be closely monitored. Conversely, the sound absorption coefficient must be large enough to minimize the effect of room modes on the sound power produced by the source below a frequency f, where

$$f = \frac{2000}{V^{1/3}} Hz. \tag{2.14}$$

This frequency is roughly 340 Hz for the large chamber. Equation (2.14) resembles the equation for the Schroeder frequency[2]

$$f_c = 2000 \cdot \sqrt{\frac{T_{60}}{V}}. \tag{2.15}$$

The calculated value of f_c is 410 Hz, with a T_{60} value of about 8.5 s. The average sound absorption coefficient of all the surfaces of the room should not exceed 0.16. All values above f should not exceed 0.06. Pushing the absorption limits for sound power measurements is useful because it effectively increases modal overlap below f_c, which allows measurements below this value to be used in diffuse field calculations. Figure 2.8 shows that the chamber currently meets these restrictions. However, the addition of maximum allowable low-frequency absorption will push the absorption coefficients

higher than the allowed values given in ISO 354. Because of this, the absorbers must be designed for easy removal, for a variety of measurements in the multi-purpose reverberation chamber.

Requirements for background noise level depend on the measurement method used (direct or comparison). For the direct method, the level is required to be at least 10 dB below the sound pressure level of the test source in all bands within the frequency range of interest. If the comparison method is used, this difference is required to be at least 15 dB. For the measurement of low noise equipment, in which the 10 dB difference may not be achievable for all bands, any bands for which the A-weighted SPL of the test source is more than 15 dB below the highest A-weighted SPL may be excluded from the frequency range of interest. Atmospheric conditions pertinent to this standard include temperature, relative humidity and pressure. Acceptable variations of temperature and relative humidity are specified according to different ranges of these values. These limits are shown in Table 2.1. Interestingly, these ranges are more lenient than those found in ISO 354. Atmospheric pressure measurements are to be made within ± 1.5 kPa.

TABLE 2.1. Allowable changes in atmospheric conditions during sound power measurements. From ISO 3741.

Ranges of temperature θ °C	**Ranges of relative humidity** %		
	< 30%	30% to 50%	> 50%
	Allowable limits for temperature and relative humidity		
- 5 ≤ θ < 10	± 1 °C ± 3 %	± 1 °C ± 5 %	± 3 °C ± 10 %
10 ≤ θ < 20		± 3 °C ± 5 %	
20 ≤ θ < 50	± 2 °C ± 3 %	± 5 °C ± 5 %	± 5 °C ± 10 %

2.2.2 Room Qualification

Even with strict adherence to the standard, measurement uncertainty exists. The largest sources of uncertainty include possible deviations from the theoretical model (direct method), calibration errors of the reference sound source (comparison method), inadequate sampling of the sound field, and variations in acoustic coupling from the noise source to the sound field. This uncertainty can be reduced by using multiple source locations, increasing the number of microphone positions, adding low-frequency sound absorbers, and using moving diffuser elements. The choice to not use a moving diffuser has already been discussed.

Figure 2.9 shows a typical setup for sound power measurements. The sound source should be placed in one or more locations in the room that resemble a normal installation. If no particular position is specified, the source must be placed on the floor at least 1.5 m away from any wall of the room. If more than one source position is used,

FIG. 2.9. Placement of sound source in a reverberation chamber.

the distance between different positions must be equal to or larger than the half wavelength of sound corresponding to the lowest mid-band frequency of measurement. For 100 Hz this distance must be 1.72 m. In rectangular rooms, the source should be placed asymmetrically on the floor

Several microphone positions are required for measuring the sound pressure level and determining the radiated sound power. For each frequency band of interest, the minimum distance, $d_{\min}$, between the noise source and the nearest microphone position must not be less than

$$d_{\min} = C_1 \sqrt{V / T_{60}}, \tag{2.16}$$

where C_1 is a constant with a given value of 0.08, and $d_{\min}$ is in meters. Using the comparison method, this value can be obtained from

$$d_{\min} = C_2 \times 10^{(L_{Wr} - L_{pt})/20}, \tag{2.17}$$

where C_2 is equal to 0.4, L_{Wr} is the known sound power level of the reference sound source, and L_{pt} is the average sound pressure level when the reference sound source is operated in the test room. The latter two values are expressed in dB. The standard suggests that the values C_1 and C_2 be multiplied by two in order to minimize the near-field bias error. The microphones must also be more than 1 m from any room surfaces, and spaced at least half the wavelength of the lowest mid-band frequency of interest from each other.

The qualification procedure differs for the measurement of discrete-frequency components or for broadband sound. Qualification for broadband sound is only necessary if the room volume is less than specified for the lowest 1/3rd-octave band frequency of interest, or if it is larger than 300 m^3. Since the large chamber is of

acceptable volume, only the qualification procedure for the measurement of discrete-frequency components was necessary. Problems in measurement may occur when testing sound sources with discrete-frequency components. This is caused by much larger spatial variance of the sound field, and both spectral and spatial variances of the coupling of the sound source to the modes of a reverberation room, than would exist for broadband sound. At low frequencies, only a small number of room modes can be significantly excited at any given frequency. One solution to this problem is to add damping to the room in order to broaden the frequency response of each mode. For high frequencies, the number of microphone positions used impacts the accuracy. The standard suggests either an array of discrete microphone positions together with a rotating diffuser, or a long, circular microphone traverse.

The standard indicates that a suitable sound source should be used for qualification. This should be a loudspeaker with a cone diameter of 200 mm or less and an airtight backing enclosure. To determine suitability, it should be placed on the floor of a hemi-anechoic chamber with the loudspeaker cone facing upwards. The same type of microphone used in the reverberation chamber is to be placed 10 mm to 20 mm on axis above the loudspeaker. The SPL, or L_p, is obtained by

$$L_p = 10\log\left(\frac{p^2}{p_{ref}^2}\right)dB, \tag{2.18}$$

where p is the measured acoustic pressure and p_{ref} is the reference acoustic pressure with a value of 20 μPa. The SPL is to be calculated and recorded at certain test frequencies to the nearest 0.5 dB. These test frequencies are listed in Table 2.2. If L_p for adjacent frequency bins does not differ by more than 1 dB, the loudspeaker may be used for the

room test. This loudspeaker is then placed in the room at the location of the source to be qualified. The cone must be facing away from the nearest room surface, including the floor. The energetic average SPL is calculated at fixed source locations for each test frequency according to the relationship

$$(\overline{L_p})_j = 10\log\left[\frac{1}{N_M}\sum_{i=1}^{N_M} 10^{0.1L_{pi}}\right] dB - K_1, \tag{2.19}$$

where $(\overline{L_p})_j$ is the SPL for the j^{th} source position (assuming more than one source position exists), averaged over all N_M fixed microphone positions, L_{pi} is the time-averaged SPL measured at the i^{th} microphone, and K_1 is the background noise correction. If more than one source position is used, L_p is averaged for each frequency by

$$\overline{L_p} = 10\log\left[\frac{1}{N_S}\sum_{j=1}^{N_S} 10^{0.1(\overline{L_p})_j}\right] dB, \tag{2.20}$$

where $\overline{L_p}$ is the SPL in a given frequency band, averaged over all source and microphone positions, and N_S is the number of source positions. To obtain K_1, the background noise level in the room is measured with the source off, immediately before or after the SPL measurement of the test source. This is given by

$$K_1 = -10\log(1 - 10^{-0.1\Delta L}) dB, \tag{2.21}$$

where ΔL is the difference of the levels of mean-square sound pressure of the source under test in operation and of the background sound pressure. If this value is greater than 15 dB, no corrections are made, and K_1 is neglected in Eq. (2.19). This same set of source locations is to be used for the equipment test.

TABLE 2.2. Test frequencies for alternative qualification of reverberation room for measuring sound power levels of noise sources containing significant discrete-frequency components. From ISO 3741, with typographical corrections.

Center frequency of one-third-octave bands (Hz)															
	100	125	160	200	250	315	400	500	630	800	1000	1250	1600	2000	2500
	-	-	147	-	-	-	361	-	-	-	-	-	1470	-	-
	-	113	148	-	226	-	364	-	-	-	-	1130	1480	-	2260
	-	114	149	-	228	-	367	445	564	712	-	1140	1490	-	2280
	90	115	150	180	230	285	370	450	570	720	900	1150	1500	1800	2300
	91	116	151	182	232	288	373	455	576	728	910	1160	1510	1820	2320
	92	117	152	184	234	291	376	460	582	736	920	1170	1520	1840	2340
	93	118	153	186	236	294	379	465	588	744	930	1180	1530	1860	2360
	94	119	154	188	238	297	382	470	594	752	940	1190	1540	1880	2380
	95	120	155	190	240	300	385	475	600	760	950	1200	1550	1900	2400
	96	121	156	192	242	303	388	480	606	768	960	1210	1560	1920	2420
	97	122	157	194	244	306	391	485	612	776	970	1220	1570	1940	2440
	98	123	158	196	246	309	394	490	618	784	980	1230	1580	1960	2460
	99	124	159	198	248	312	397	495	624	792	990	1240	1590	1980	2480
	100	125	160	200	250	315	400	500	630	800	1000	1250	1600	2000	2500
	101	126	161	202	252	318	403	505	636	808	1010	1260	1610	2020	2520
	102	127	162	204	254	321	406	510	642	816	1020	1270	1620	2040	2540
	103	128	163	206	256	324	409	515	648	824	1030	1280	1630	2060	2560
	104	129	164	208	258	327	412	520	654	832	1040	1290	1640	2080	2580
	105	130	165	210	260	330	415	525	660	840	1050	1300	1650	2100	2600
	106	131	166	212	262	333	418	530	666	848	1060	1310	1660	2120	2620
	107	132	167	214	264	336	421	535	672	856	1070	1320	1670	2140	2640
	108	133	168	216	266	339	424	540	678	864	1080	1330	1680	2160	2660
	109	134	169	218	268	342	427	545	684	872	1090	1340	1690	2180	2680
	110	135	170	220	270	345	430	550	690	880	1100	1350	1700	2200	2700
	111	136	171	222	272	348	433	555	696	888	1110	1360	1710	2220	2720
	-	137	172	-	274	-	436	-	702	-	-	1370	1720	-	2740
	-	138	173	-	276	-	439	-	-	-	-	1380	1730	-	2760
Increment, Hz	1	1	1	2	2	3	3	5	6	8	10	10	10	20	20
Tolerance of increment, Hz	±0.3	±0.3	±0.3	±0.5	±0.5	±1	±1	±1.5	±2	±3	±3	±5	±5	±5	±5
Number of test frequencies, N_f	22	26	27	22	26	22	27	23	24	23	22	26	23	22	26

Once the room levels are obtained, they are corrected to remove the influence of near-field loudspeaker characteristics by subtracting the loudspeaker levels at each frequency taken in the hemi-anechoic chamber. For each 1/3rd-octave-band, the corrected room sound pressure levels are arithmetically averaged, and the standard deviation s_f of the difference between the corrected room levels and the mean level is computed. This is given by

$$s_f = \sqrt{\frac{\sum_{n=1}^{N_f} \left[\left(\overline{L}_p \right)_n - L_{pm} \right]^2}{N_f - 1}}, \tag{2.22}$$

where $\left(\overline{L}_p \right)_n$ is the average corrected SPL produced in the test room by the source obtained from Eq. (2.19) (or (2.20) if multiple source positions are used) when excited at the n^{th} test frequency, averaged over all microphone and source positions, N_f is the number of test frequencies, and L_{pm} is the arithmetic mean of $\left(\overline{L}_p \right)_n$, averaged over all N_f test frequencies. The room is qualified for each 1/3rd-octave band at the specific source locations, and for the given instrumentation and microphone positions, if the computed standard deviation does not exceed the limits given in Table 2.2. The standard states that it is not necessary to qualify the room at frequencies above the 2500 Hz 1/3rd-octave band.

The number of microphone positions necessary for qualification is at least six. If the standard deviations exceed the values in Table 2.3, more microphone positions must be used. The qualification should take place after the addition of low-frequency absorbers. However, the design and installation of the absorbers is not yet complete. Accordingly, a decision has not yet been reached as to whether the room will indeed be

TABLE 2.3. Maximum allowable standard deviations of sound pressure level. From ISO 3741.
Maximum allowable sample standard deviations, s_f

Octave-band center frequency Hz	1/3rd-octave-band center frequencies Hz	Maximum allowable standard deviations dB
125	100 to 160	3.0
250	200 to 315	2.0
500	400 to 630	1.5
1000 and 2000	800 to 2500	1.0

qualified for discrete-frequency measurements, or if the room will be left to a case-by-case scenario as explained above. As a result, qualification of the chamber for sound power measurements is currently limited to broad-band sources.

2.3 Measuring Sound Absorption of a Test Material

Once a reverberation chamber has been qualified according to ISO 354, the sound absorption of a test material can be measured. The process of measuring the absorption coefficient is very similar to the qualification procedure of the room. The frequency range of interest is between 100 Hz to 5000 Hz, in 1/3rd-octave bands. For this research, two different types of materials were measured. The first material was the planar absorber used in the room qualification. The second consisted of several upholstered office chairs. Planar absorbers are generally placed directly against a room surface, such as the floor of the reverberation room (Type A Mounting). Discrete objects, such as chairs, are placed in a fashion that represents typical use (on the floor), but they cannot be closer than 1 m to any other boundary. A sufficient number of these individual objects should be used to provide an appreciable change in sound absorption area. They are to be placed randomly in the chamber, spaced at least 2 m apart. The floor dimensions of the reverberation chamber only allowed 3 chairs to be used.

The temperature, relative humidity, and barometric pressure of the chamber were monitored with an Oregon Scientific WM-918 Electronic Weather Station, which was placed on the floor of the chamber. The outdoor temperature and humidity sensor was positioned close to the microphones during measurement. Just as in room qualification, the TEF Analyzer was used to generate the room impulse responses for 12 source-receiver locations. Equations (2.3) and (2.11) were used to calculate the sound absorption.

2.4 Energy Density Impulse Response

The behavior of a linear time-invariant system may be characterized by its impulse response *h(τ)*, defined as the output of the system at any time due to the application of a unit impulse function (Dirac delta function) $\delta(t)$ at the input a time τ beforehand. For an arbitrary input function $a(t)$, the output $b(t)$ is given by the convolution integral

$$b(t) = \int_{-\infty}^{\infty} h(\tau)a(t-\tau)d\tau\,, \tag{2.23}$$

Such that if $a(t) = \delta(t)$,

$$b(t) = \int_{-\infty}^{\infty} h_p(\tau)\delta(t-\tau)d\tau = h_p(t)\,. \tag{2.24}$$

In an enclosed sound field, the impulse response $h_p(\tau)$ between a source and a receiver is typically considered in terms of the acoustic pressure *p(t)* at the "output" position of the latter. However, the individual Cartesian components of the particle velocity [$u_x(t)$, $u_y(t)$, and $u_z(t)$] also satisfy the linear wave equation[29] and can therefore be used for the definition of additional impulse responses. For the *x* component of the particle velocity, the convolution integral becomes

$$u_x(t) = \int_{-\infty}^{\infty} h_{u_x}(\tau) a(t-\tau) d\tau \,, \tag{2.25}$$

where the impulse response $h_{u_x}(\tau)$ is defined by the application of the unit impulse:

$$u_x(t) = \int_{-\infty}^{\infty} h_{u_x}(\tau) \delta(t-\tau) d\tau = h_{u_x}(t) \,. \tag{2.26}$$

Similar relationships follow for the y and z components of the particle velocity. Since the square of the vector particle velocity magnitude is

$$u^2(t) = \left|\vec{u}(t)\right|^2 = u_x^2(t) + u_y^2(t) + u_z^2(t) \,, \tag{2.27}$$

one can analogously define a squared impulse response for the particle velocity vector magnitude:

$$h_u^2(t) = h_{u_x}^2(t) + h_{u_y}^2(t) + h_{u_z}^2(t) \,. \tag{2.28}$$

An impulse response associated with total energy density then follows with appropriate weightings. Interchanging for *t* one can write it as

$$h_w(t) = \frac{h_p^2(t)}{2\rho_0 c^2} + \frac{\rho_0}{2} h_u^2(t) \,. \tag{2.29}$$

The impulse responses obtained in Eqs. (2.28) and (2.29) are then used in Eq. (2.2), replacing $h_p^2(t)$.

Because the data is to be observed in filtered 1/3rd-octave frequency bands, the primary impulse responses must be filtered before they are squared in order to preserve frequency data. Figure 2.10 shows an example of the pressure, velocity magnitude, and energy density impulse responses obtained at one position, filtered at 250 Hz. The impulse responses are displayed on a logarithmic scale.

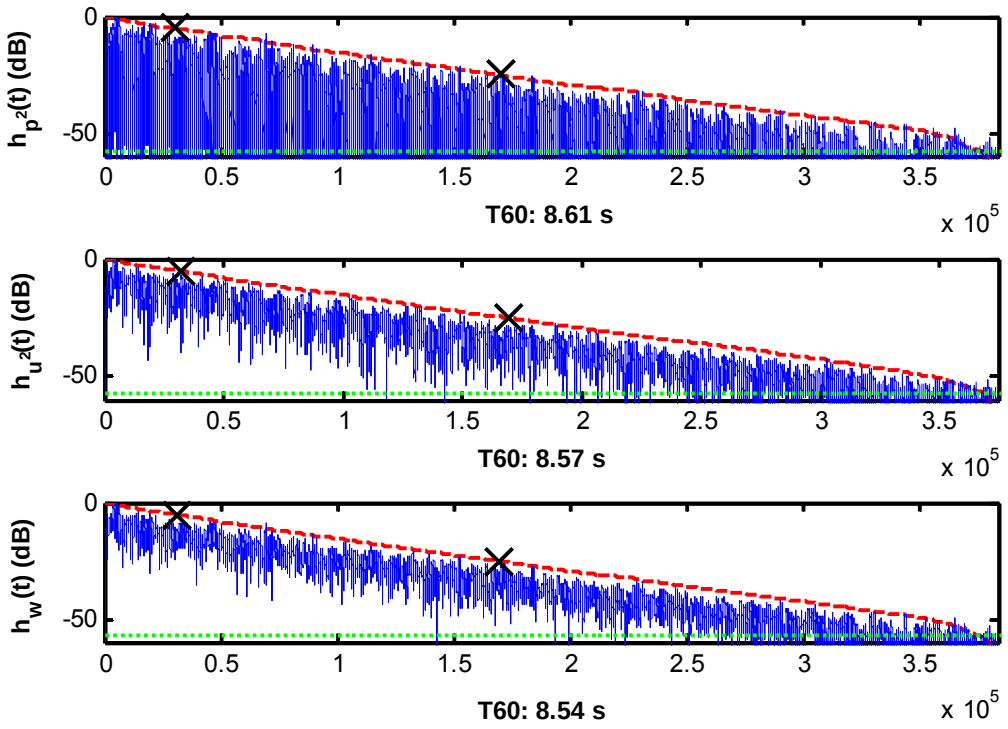

FIG. 2.10. Impulse responses of pressure, particle velocity magnitude, and total energy density obtained at one position, at 250 Hz. The red dashed line is the Schroeder integration curve. The horizontal green dotted line shows the noise floor, and the integration starts where this line intersects with the Schroeder curve. The black cross marks show the -5dB and -25dB down points.

A commercial sensor developed by Microflown® (see Fig. 2.11) was used to obtain the pressure and velocity measurements. This sensor was moved after each source-receiver measurement. It consists of one pressure sensor and three orthogonal velocity sensors for each Cartesian component. The voltage response of each transducer is output to a signal conditioning box, which corrects for amplitude and phase mismatch, and provides power for the sensors. The signal conditioning box outputs the data via four discrete channels, which are sent through the patch panel and received into the control room. It is then digitized and stored on a computer for later processing.

FIG. 2.11. Detailed view of Microflown™ sensor.

For a given frequency *f*, the sensitivity *M* of each velocity sensor is obtained by

$$M = \frac{LFS}{\sqrt{1+\frac{f_{CF1}^2}{f^2}}\sqrt{1+\frac{f^2}{f_{CF2}^2}}\sqrt{1+\frac{f^2}{f_{CF3}^2}}}, \tag{2.30}$$

where *LFS* is the sensitivity at 250 Hz, and f_{CF1}^2, f_{CF2}^2, and f_{CF3}^2 are the corner frequencies of the sensor. The calibrated *LFS* value is provided by the manufacturer in units of mV/Pa*, where

$$1Pa^* = \frac{1Pa}{\rho_0 c} \tag{2.31}$$

This value is then corrected for atmospheric conditions during measurements.

Of practical concern is the error introduced with the terms ρ_o and *c*. Normally, the amplitude of the squared impulse response is not important, since T_{60} is calculated by the slope of the integration curve. However, the combination of several impulse responses which are weighted by these variables suggests that errors of the measured atmospheric values inevitably lead to errors in the energy density impulse response. The significance of these errors will be treated in a later chapter.

2.5 Measuring the Sound Power of a Source

Following procedures given in ISO 3741, the sound power level of a source under test is obtained in the following fashion. The sound pressure level of the source is obtained at several fixed microphone positions in the reverberation chamber. For a given frequency band, the average sound pressure level in the room for the j^{th} source position is obtained by Eq. (2.19). If multiple source positions are used, the sound pressure level, averaged over all source and microphone positions, is given by Eq. (2.20). Using the equivalent sound absorption area A of the test room, the sound power level L_W of the sound source under test is given in dB by

$$L_W = \overline{L}_p + \left[\begin{array}{l} 10\log\frac{A}{A_0} + 4.34\frac{A}{S} + 10\log\left(1+\frac{S\cdot c}{8V\cdot f}\right) \\ -25\log\left(\frac{427}{400}\sqrt{\frac{273}{273+T_c}}\cdot\frac{B}{B_0}\right) - 6 \end{array} \right], \tag{2.32}$$

where A_0 is 1 m^2, S is the total surface area of all room surfaces[30] (in m^2), V is the room volume (in m^3), f is the mid-band frequency of the measurement (in Hz), c is the speed of sound in m/s at temperature T_c (in °C) (m/s), B is the atmospheric pressure (in Pa), and B_0 is the reference atmospheric pressure, 1.013×10^5 Pa. The first and last terms in the square brackets are from the relationship between sound power level and sound pressure level in a diffuse field. The second term was introduced by Vörlander to compensate for an underestimation of the sound field using Sabine's equation,. The third term is the Waterhouse correction, which includes the interference patterns of potential energy density near room surfaces. The fourth term accounts for atmospheric effects in the room, and corrects the value to what would be measured with a specific acoustic impedance of 400 Pa·s/m.

2.6 Obtaining Sound Power Level from Other Quantities

One of the purposes of this research is to determine if quantities other than sound pressure level can be used to obtain the sound power level of a source under test. Two are considered here: sound velocity level (SVL, or L_u) and sound energy density level (SEDL, or L_{ED}). The sound velocity level is defined as ten times the base 10 logarithm of the ratio of the time-mean-square particle velocity of a given sound or vibration to the square of a specified reference particle velocity.[31] It is expressed in the form

$$L_u = 10\log\left(\frac{u^2}{u_{ref}^2}\right) dB\,. \tag{2.33}$$

The reference value u_{ref} has not been clearly defined. Clause A.1 of ANSI S18-1989 notes that a reference particle velocity of 10 nanometers per second (10 nm/s) is used in ANSI S1.8-1969, in contrast with 1 nm/s preferred by ISO 1683-1983. Plane wave conditions describe the relationship between particle velocity and acoustic pressure as

$$u = \frac{p}{\rho_0 c}\,. \tag{2.34}$$

It is reasonable then to assume that the reference velocity should be related to the reference pressure in the same way, such that

$$u_{ref} = \frac{p_{ref}}{\rho_0 c}\,. \tag{2.35}$$

If the characteristic impedance, $\rho_0 c$, is estimated at 400 Pa·s/m, and $p_{ref} = 20\mu Pa$, the reference velocity is 50 nm/s. This value is much greater than either the ANSI or ISO suggestions. In any case, if p_{ref} is considered the primary standard, a fixed u_{ref} is not sufficiently accurate since ambient atmospheric conditions determine $\rho_0 c$. To illustrate

a possible range in the reference value, two conditions are explored. The first uses metrics of elevation at sea level, room temperature (20 °C), and dry air, with a reference barometric pressure of 101.325 kPa. In this case, ρ_0 becomes 1.204 kg/m^3, c becomes 343.37 m/s, and

$$u_{ref_1} = \frac{20\mu Pa}{(1.204 kg/m^3)(343.37 m/s)} = 48.38 \frac{nm}{s}. \quad (2.36)$$

A second case reflects conditions that are typical of those found in the reverberation chamber used in the study. It typically has a much lower barometric pressure due to the higher elevation. If the reference barometric pressure is 85.15 kPa, the relative humidity is 25%, and we assume a room temperature of 20 °C, we obtain values of ρ_o = 1.009 kg/m^3, c = 343.75 m/s, and

$$u_{ref_2} = \frac{20\mu Pa}{(1.009 kg/m^3)(343.75 m/s)} = 57.66 \frac{nm}{s}. \quad (2.37)$$

The sound energy density level can be expressed as

$$L_{ED} = 10 \log\left(\frac{w}{w_{ref}}\right) dB. \quad (2.38)$$

To obtain the reference value w_{ref} of energy density, the reference values of pressure and velocity can be added with appropriate weightings, such that

$$w_{ref} = \frac{\rho_0}{2} u_{ref}^{\ 2} + \frac{p_{ref}^{\ 2}}{2\rho_0 c^2}. \quad (2.39)$$

Using values from the sea-level case and the reverberation room case, we then obtain

$$w_{ref_1} = \frac{1.204 \frac{kg}{m^3}}{2}\left(48.38 \frac{nm}{s}\right)^2 + \frac{(20\mu Pa)^2}{2\left(1.204 \frac{kg}{m^3}\right)\left(343.37 \frac{m}{s}\right)^2} = 2.82 \times 10^{-15} \frac{J}{m^3}, \quad (2.40)$$

$$w_{ref\,2} = \frac{1.009\,\frac{kg}{m^3}}{2}\left(57.66\,\frac{nm}{s}\right)^2 + \frac{(20\,\mu Pa)^2}{2\left(1.009\,\frac{kg}{m^3}\right)\left(343.75\,\frac{m}{s}\right)^2} = 3.36\times10^{-15}\,\frac{J}{m^3}. \quad (2.41)$$

For a plane wave, sound pressure level, sound velocity level, and sound energy density level are equal, as long as the correct reference values are used. Thus, once L_u and L_{ED} have been calculated, the sound power level can be determined from either of these values by replacing L_p in Eq. (2.32). The Waterhouse correction term remains the same when L_u is used because the value of the integrated interference pattern for kinetic energy density is the same as potential energy density.[6] When L_{ED} is used the number 8 in the denominator of the term is replaced by 4, due to the combination of the potential and kinetic ED interference patterns. The other correction terms remain the same. The actual levels obtained in an enclosure are contingent on the diffusivity of the sound field. Because the variation in the sound field is different for each quantity, the average sound levels will also be different.

2.7 Chapter Summary

The qualification procedures for sound power and sound absorption measurements in reverberation chambers have been explained. A new method of measuring sound absorption and sound power involving energy density has been introduced. Energy density impulse responses can be obtained by combining the impulse responses of the squared pressure and squared velocity magnitude impulse responses. Sound power level can be calculated by obtaining the Sound Energy Density Level (SEDL). The procedures for implementing these measurements have been described.

The implication of error from atmospheric variables has also been considered. The results of related measurements will be treated in the next chapter.

CHAPTER 3 – EXPERIMENTAL RESULTS

Sound absorption and sound power measurements were taken in three rooms (see Fig. 3.1). The first was a qualified reverberation chamber with a volume of about 204 m^3 (4.96 m × 5.89 m × 6.98 m) and a Schroeder frequency of 410 Hz. The second room was a smaller reverberation chamber with a volume of about 61 m^3 (5.7 m × 4.3 m × 2.5 m) and a Schroeder frequency of 552 Hz. The third room was a classroom with a volume of about 235 m^3 (3.6 m × 6.3 m × 10.3 m) and a Schroeder frequency of 110 Hz. The second and third rooms were used to see how well ED could perform in non-ideal environments. The volume of the smaller reverberation chamber does not meet qualification standards. Low-frequency measurements in this room suffer in accuracy. The classroom contains many surface areas with different absorption coefficients. The lack of diffusers in such a room prevents a random distribution of sound energy, and a diffuse sound field cannot be assumed. The results for the three rooms are grouped into reverberation time, absorption coefficients, and sound power measurements.

3.1 Reverberation Time

For all T_{60} measurements, 12 source-receiver positions were used in each room for averaging. The average T_{60} values were obtained from squared pressure (p^2), squared particle velocity magnitude (u^2), and total energy density (ED) impulse responses. The T_{60} values for each quantity were then compared and examined. The probabilities of one quantity outperforming another were obtained for various scenarios. These methods were repeated with and without the inclusion of test materials.

(a)

(b)

(c)

FIG. 3.1. a) Large chamber. b) Small chamber. c) Classroom.

3.1.1 Large Chamber – Empty

The standard deviation σ of a set of data is

$$\sigma = \sqrt{\sum_{i=1}^{N} \frac{(x_i - \bar{x})^2}{N-1}}, \tag{3.1}$$

where N is the total number of data points, x_i is the i^{th} data point, and $\bar{x}$ is the arithmetic average of the data. Figure 3.2 shows the average and standard deviations of T_{60} obtained in the empty chamber using all 12 measurement positions. The dip at 160 Hz appears to be either due to the peak in the absorption coefficient illustrated in Fig. 2.3, or due to the positions being located at a node in the vertical plane. The average T_{60} values agree, particularly at higher frequencies. Most noticeable differences occur at 125 Hz and 160 Hz.

On the other hand, ED is observed to have a notably lower standard deviation than p^2 at all frequencies. Based on previous ED studies, this was an anticipated result. However, a striking and unexpected result is that u^2 outperforms p^2, particularly at higher frequencies. In fact, it appears to be as good as, if not better than, ED. This phenomenon is repeated in later observations. At lower frequencies, u^2 performs poorer than p^2.

To further investigate the performances of u^2 and ED, probability tests were conducted to analyze the minimum number of positions required to achieve results as good as those for twelve measurement positions from p^2. Using the measurement results, all possible combinations of the data were evaluated for an increasing number of positions used. The number of possible combinations C_r^n of objects r taken from a total objects n is given by the combinatorial formula[32]

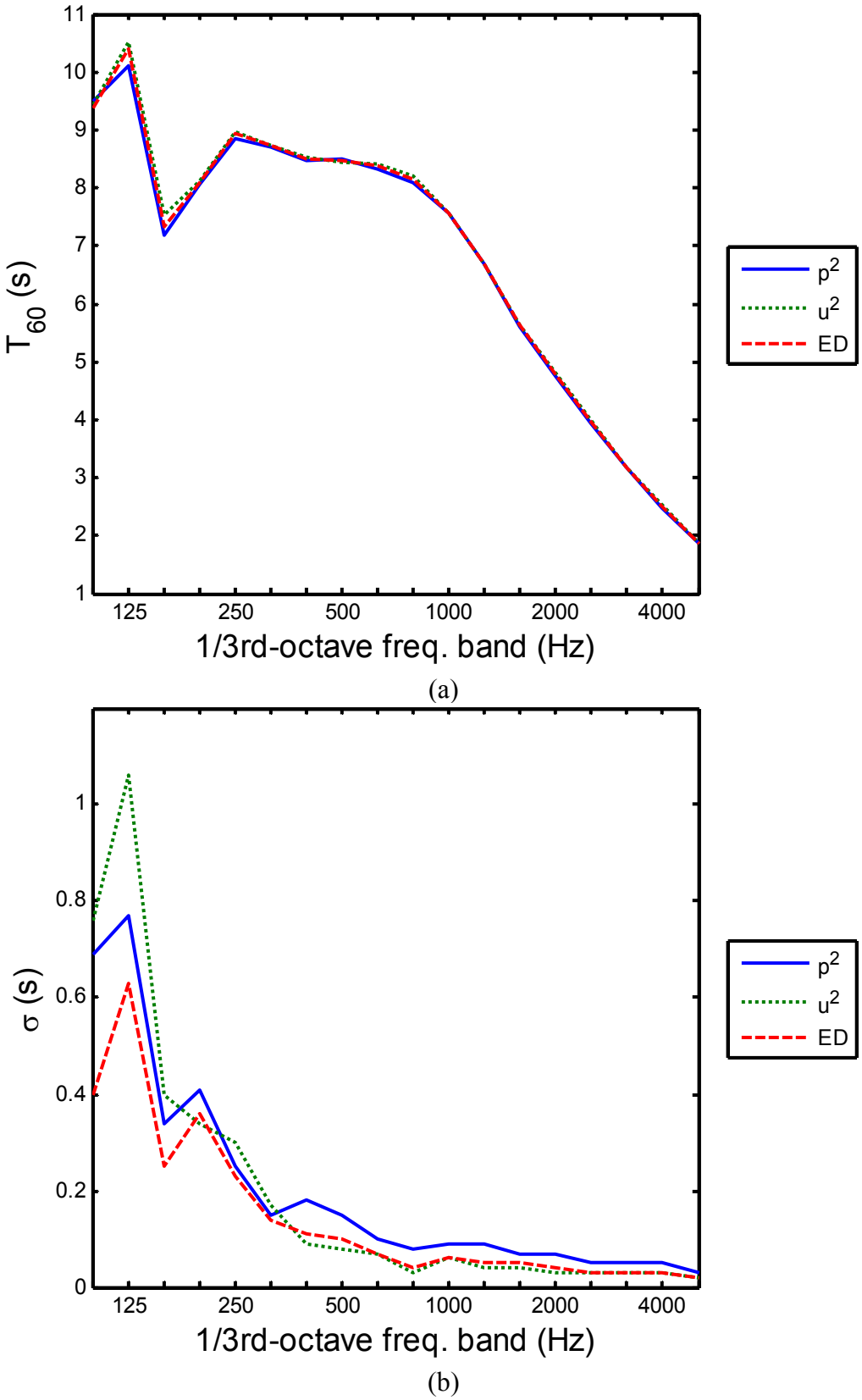

FIG. 3.2. T_{60} measurements in empty large chamber. a) Average. b) Standard deviation.

$$C_r^n = \frac{n!}{r!(n-r)!}. \tag{3.2}$$

The probability P that the standard deviation of T_{60} from r randomly chosen ED and u^2 positions is lower than the standard deviation of T_{60} from all twelve p^2 positions is shown in Fig. 3.3. Of the two quantities, ED consistently performs the best over all frequencies. At higher frequencies, six positions ensure a lower standard deviation than p^2. Standard deviation values for u^2 also do remarkably well at higher frequencies; seven positions are enough to outperform p^2.

A further comparison was made by determining the probability that any number of randomly chosen positions for one quantity led to a lower variation than the same number of randomly chosen positions for any other quantity. Three relationships were plotted: u^2 vs. p^2, ED vs. p^2, and u^2 vs. ED. The results are given in Figs. 3.4 through 3.6. As can be seen, the probabilities that variation is lower for both u^2 and ED vs. p^2 increase with the number of positions. For the case of u^2 vs. ED, it appears that the probability gravitates toward 50% at first; as more positions are used, results show lower probability at lower frequencies, and higher probability at higher frequencies. Even so, the sharp changes from one 1/3rd-octave band to the next indicate a frequency dependence of variation and that different sensor locations will produce different results.

To see if the performance of u^2 vs. ED was indeed significant, an F-test of unequal variances[32] was used. The test revealed that the standard deviation values were, in fact, statistically equal. This phenomenon was further investigated analytically, and will be discussed in the next chapter.

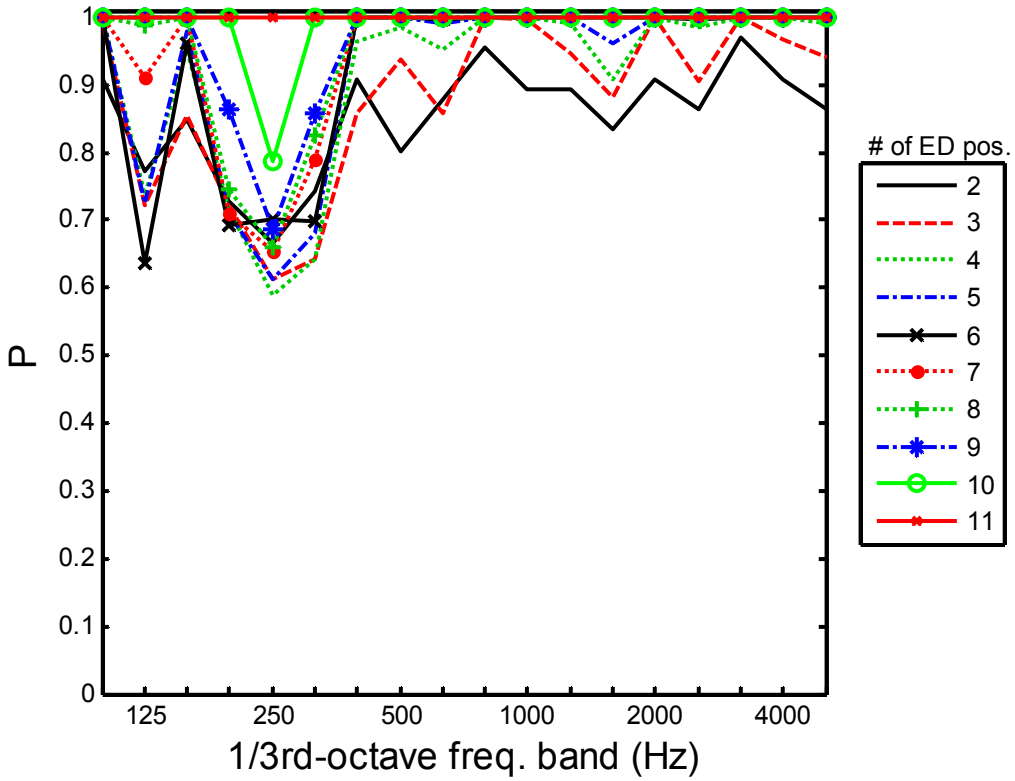

(a)

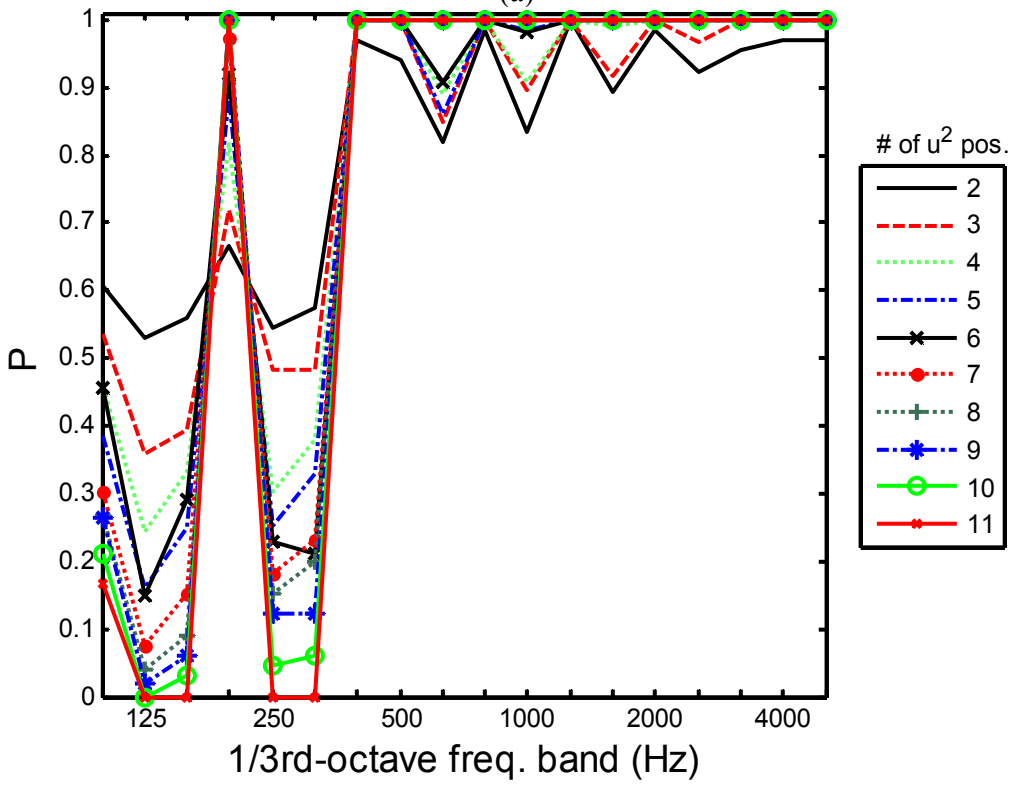

(b)

FIG. 3.3. Probabilities that a given number of positions of one quantity outperforms 12 p^2 meaurements in the empty chamber. a) ED. b) u^2.

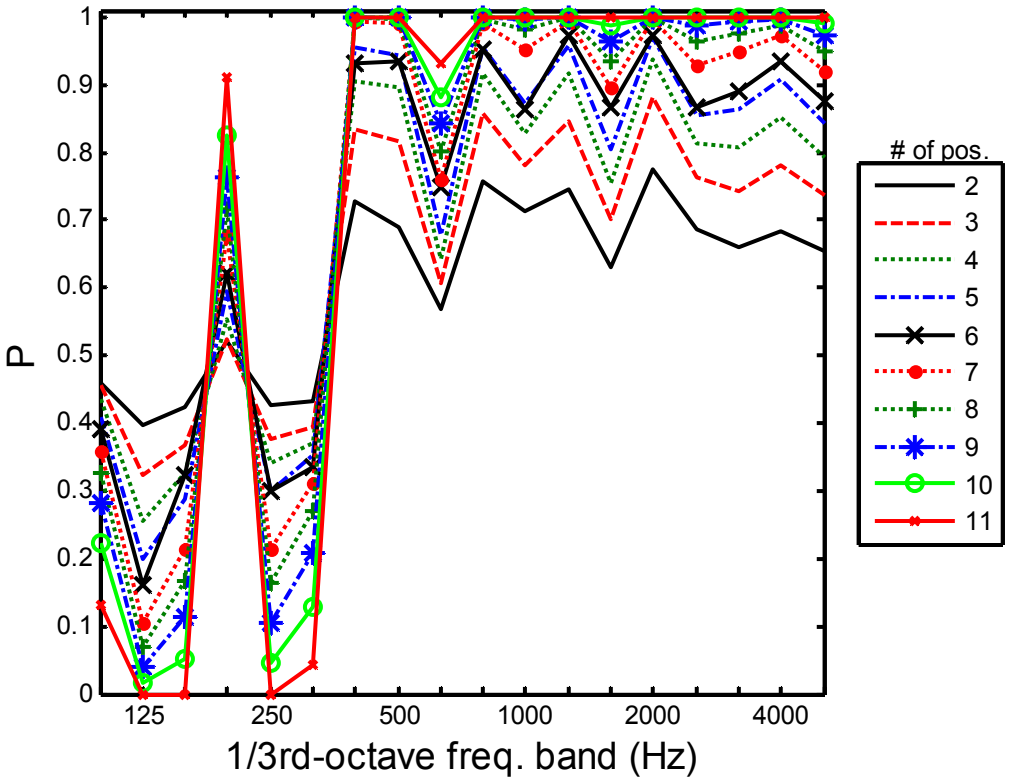

FIG. 3.4. Probability of lower variation in u^2 vs. p^2, in the empty large chamber.

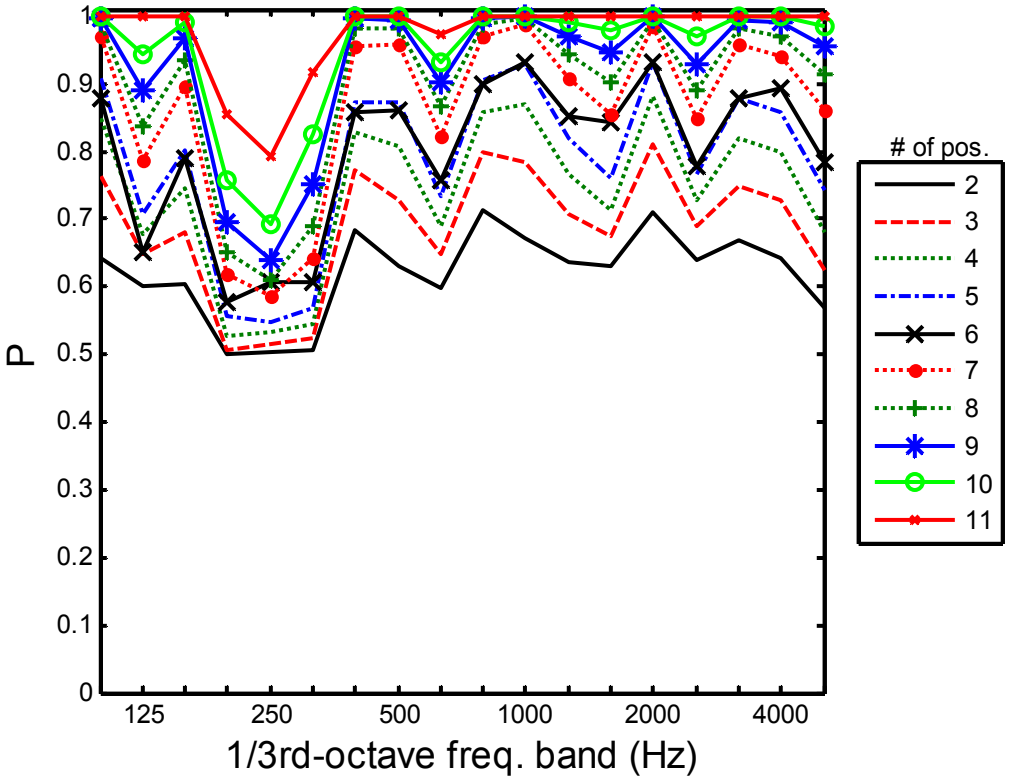

FIG. 3.5. Probability of lower variation in ED vs. p^2 in the empty large chamber.

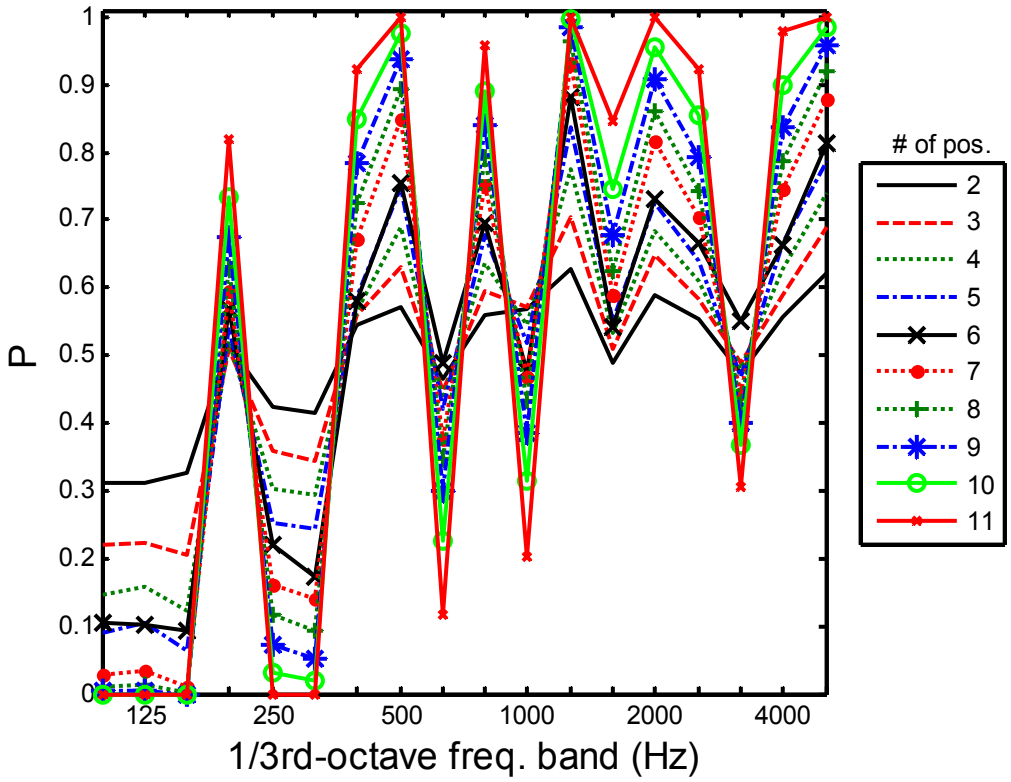

FIG. 3.6. Probability of lower variation in u^2 vs. ED in the empty large chamber.

3.1.2 Large Chamber – Fiberglass

The T_{60} measurements taken in the large chamber with the addition of the fiberglass absorption material were compared next. The total exposed surface area of the material, including the edges, was 10.65 m^2. It rested on the floor, at least 0.75 m from each wall, in an A-mounting (see ISO 354). Figure 3.7 shows the average and standard deviations of T_{60} obtained from all quantities, for twelve measurement positions. The results are extremely similar for all energy quantities, except at the lowest frequency band. As observed for the empty chamber, the variation from ED is lower than that of p^2. However, in this case, the ED is not better at 160 Hz. Below 200 Hz, u^2 does not perform better than p^2. Overall, the pattern resembles the results for the empty chamber.

Probability tests were also carried out as before, with similar results. For a given number of random measurement positions, Fig. 3.8 shows the probabilities of lower

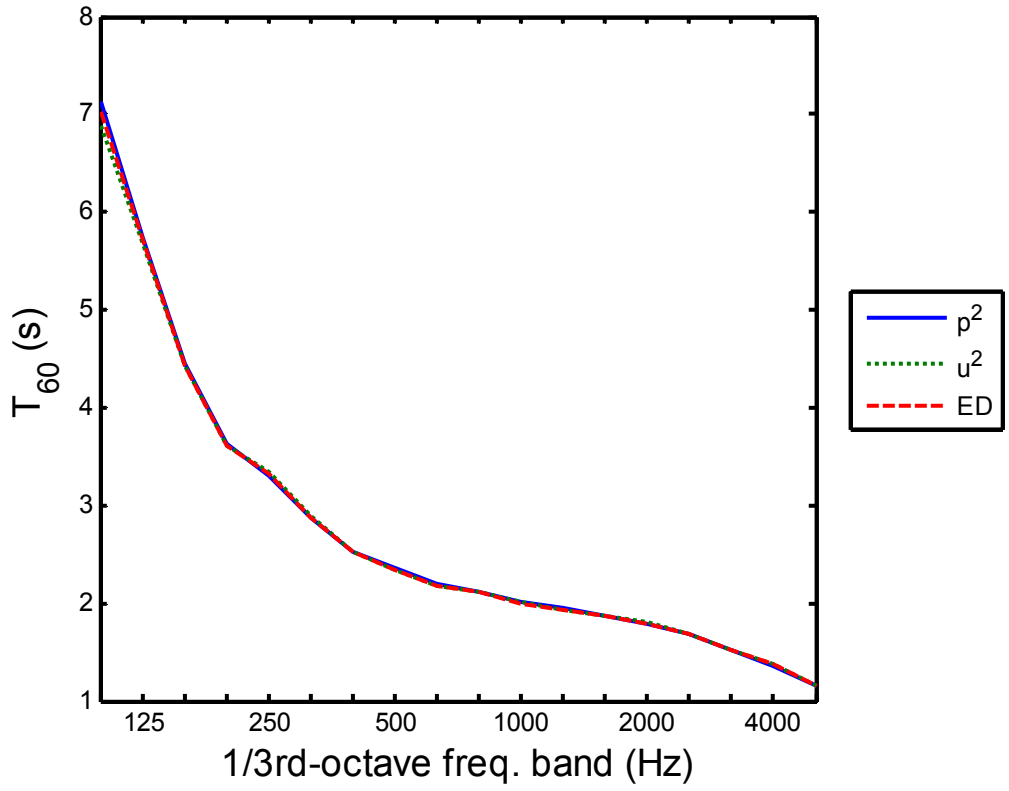

(a)

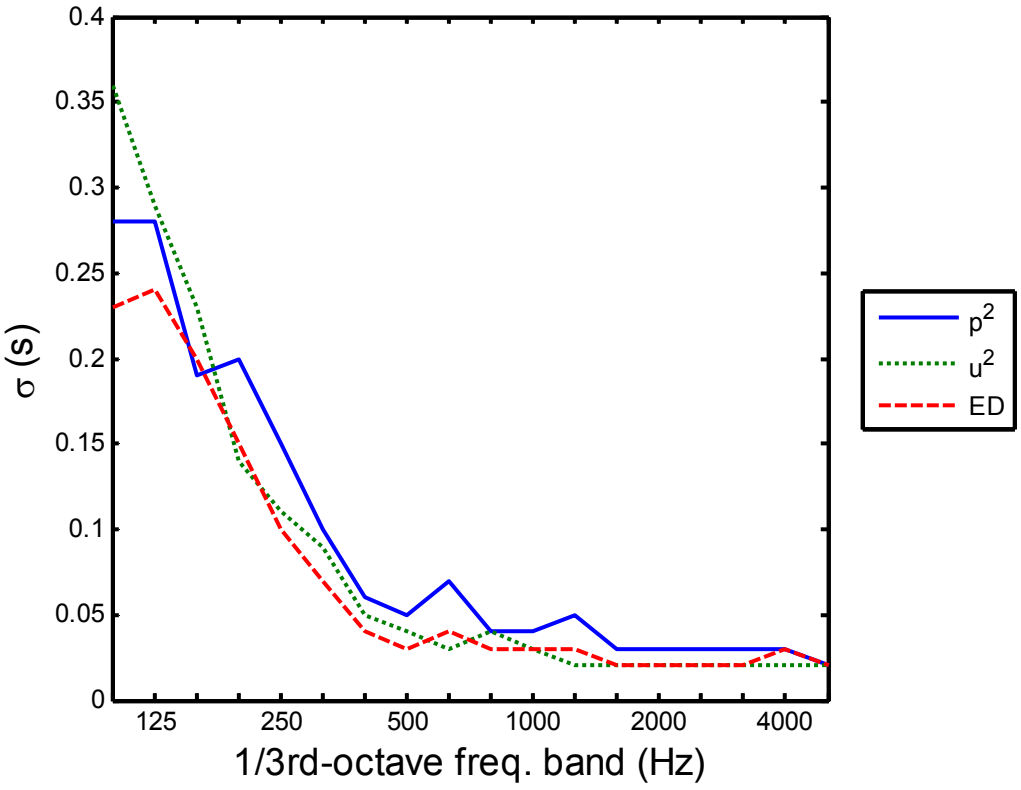

(b)

FIG. 3.7. T_{60} measurements with fiberglass in large chamber. a) Average. b) Standard deviation.

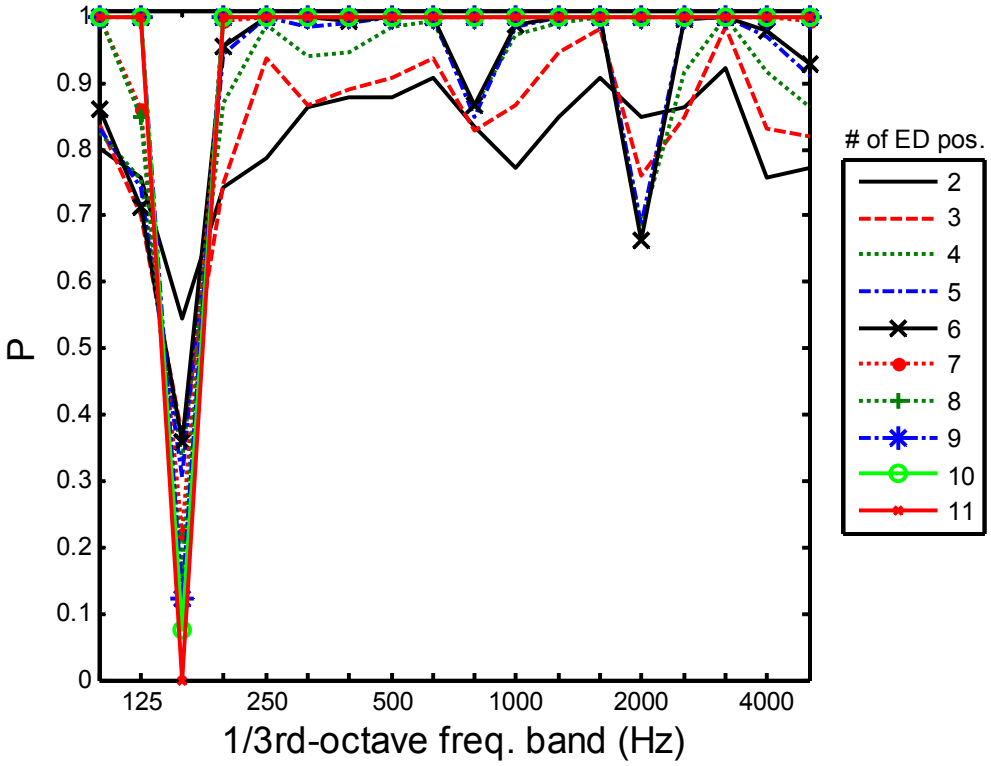

(a)

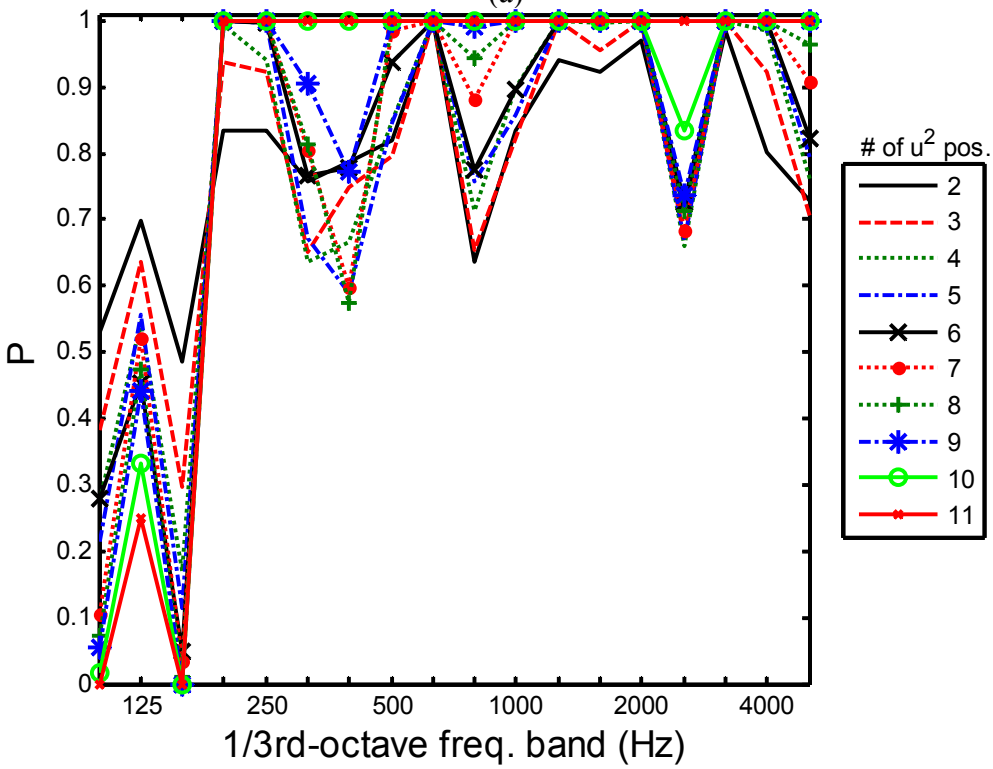

(b)

FIG. 3.8. Probabilities of one quantity with a given number of positions outperforming 12 p^2 positions in the large chamber with fiberglass. a) ED. b) u^2.

variation for a given random number of positions using both ED and u^2, vs. 12 p^2 positions. At higher frequency bands, ED generally performs better than u^2, with some exceptions. Figures 3.9 through 3.11 plot the probabilities for one energy quantity performing better than another, for a given number of randomly chosen positions. When the fiberglass was present, it took seven ED positions to guarantee 100% probability of lower variation in T_{60} than all 12 p^2 positions, above the Schroeder frequency (410 Hz). It took eleven u^2 positions to make this same guarantee. When comparing u^2 vs. ED, the quantity with the lowest variation depends strongly on frequency.

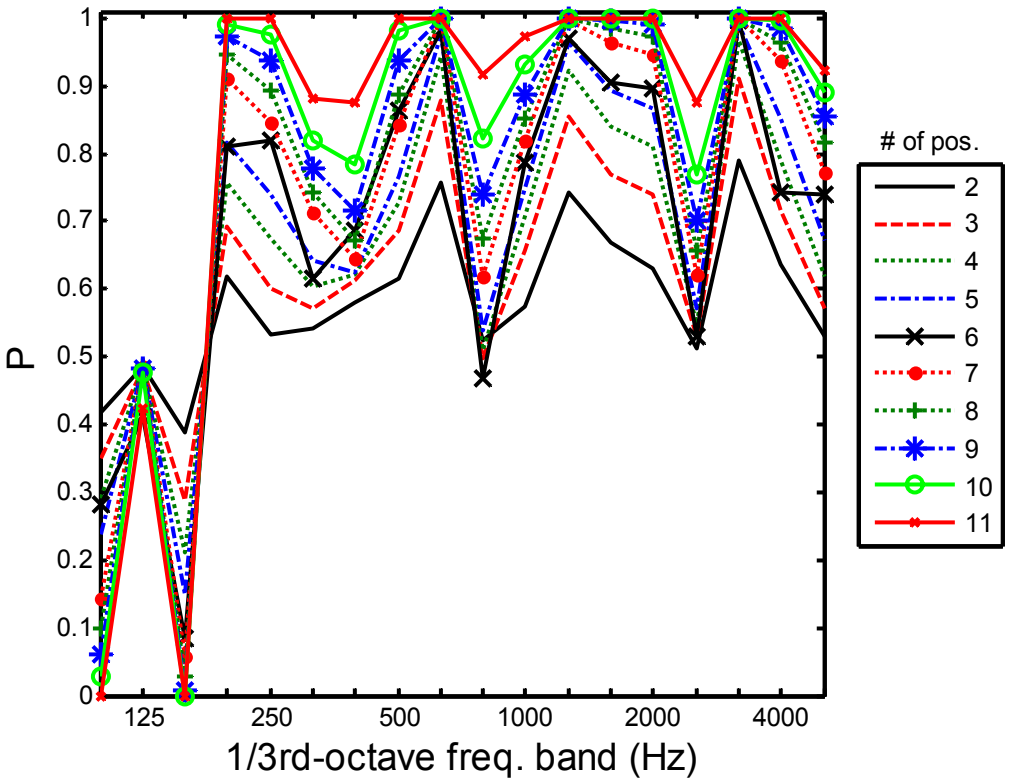

FIG. 3.9. Probability of lower variation in u^2 vs. p^2 for a given number of positions, in the large chamber with fiberglass.

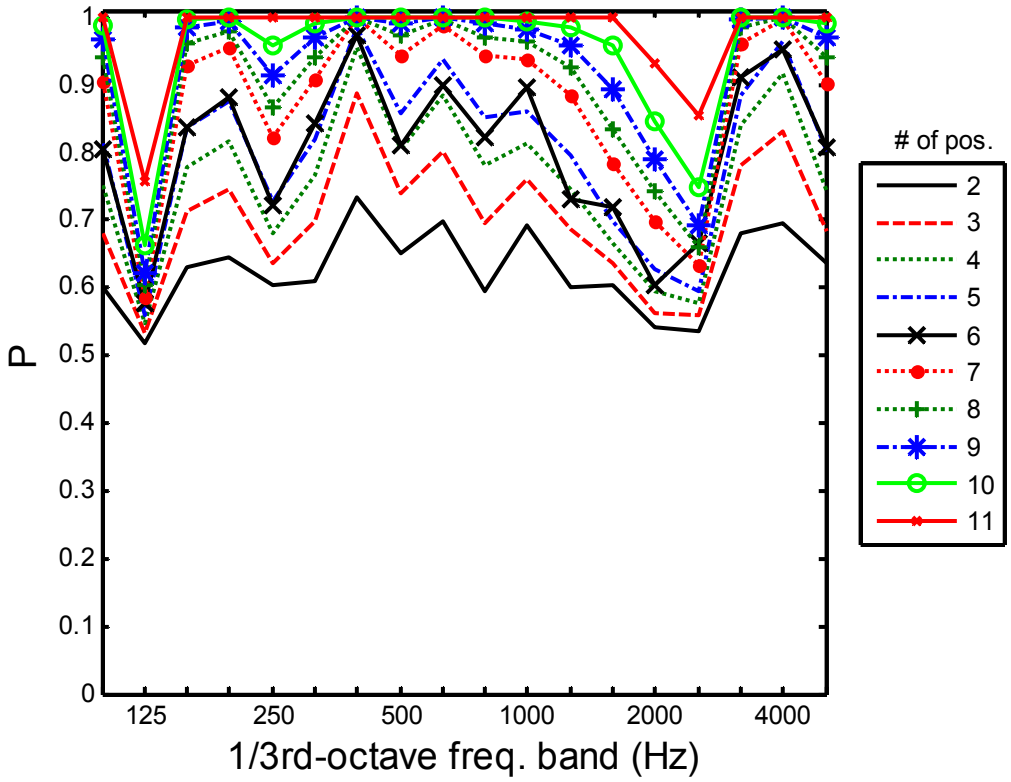

FIG. 3.10. Probability of lower variation in ED vs. p^2 for a given number of positions, in large chamber with fiberglass.

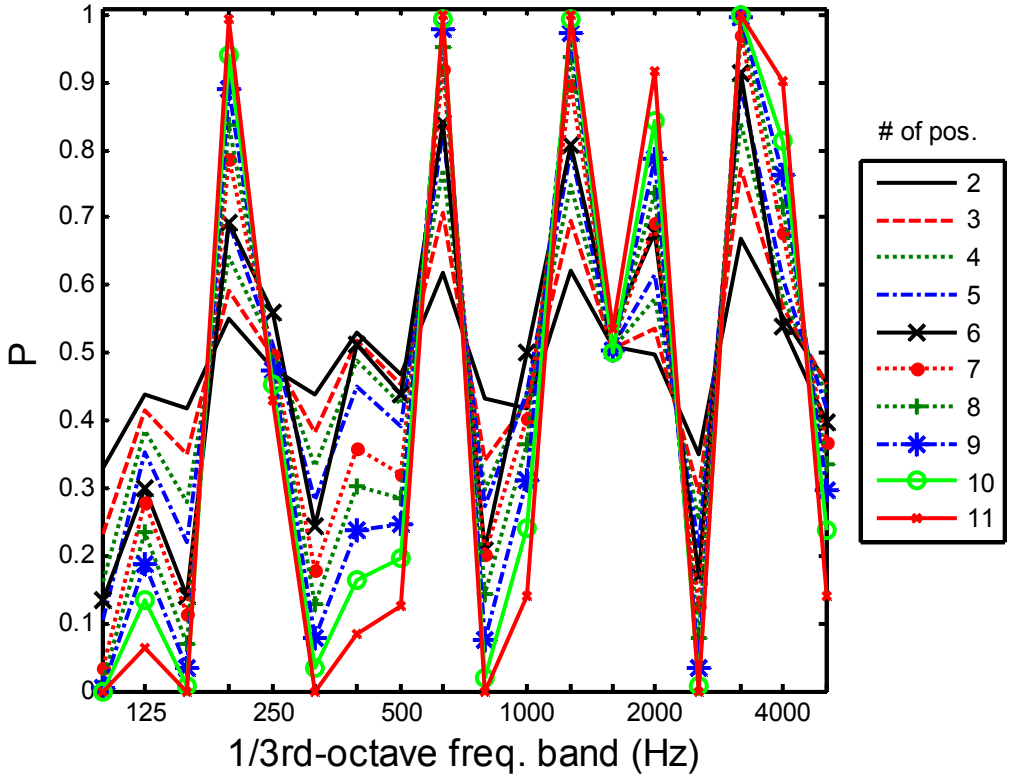

FIG. 3.11. Probability of lower variation in u^2 vs. ED for a given number of positions, in large chamber with fiberglass.

3.1.3 Large Chamber – Chairs

Another scenario was carried out using office chairs as absorption samples. Three identical office chairs were placed in the chamber in a fashion dictated by ISO 354. Due to the restrictions of distance from one object to another, only three chairs could be placed within the room. The average and standard deviations of the T_{60} measurements are shown in Fig. 3.12. The only noticeable difference in average value occurs at 125 Hz. Also, the dip at 160 Hz is present, apparently due to the small amount of total absorption. ED consistently has lower variation than p^2, whereas u^2 performs better at high frequencies, and poorer at low frequencies.

The probabilities for u^2 and ED performing better than 12 p^2 positions are shown in Fig. 3.13. As observed before, fewer ED positions are required at lower frequencies, and ED is more consistent across the entire spectrum. Figs. 3.14 through 3.16 present the probabilities of one energy quantity outperforming another energy quantity, for a randomly chosen number of positions. As in the cases before, the outcomes of u^2 vs. ED are not statistically significant.

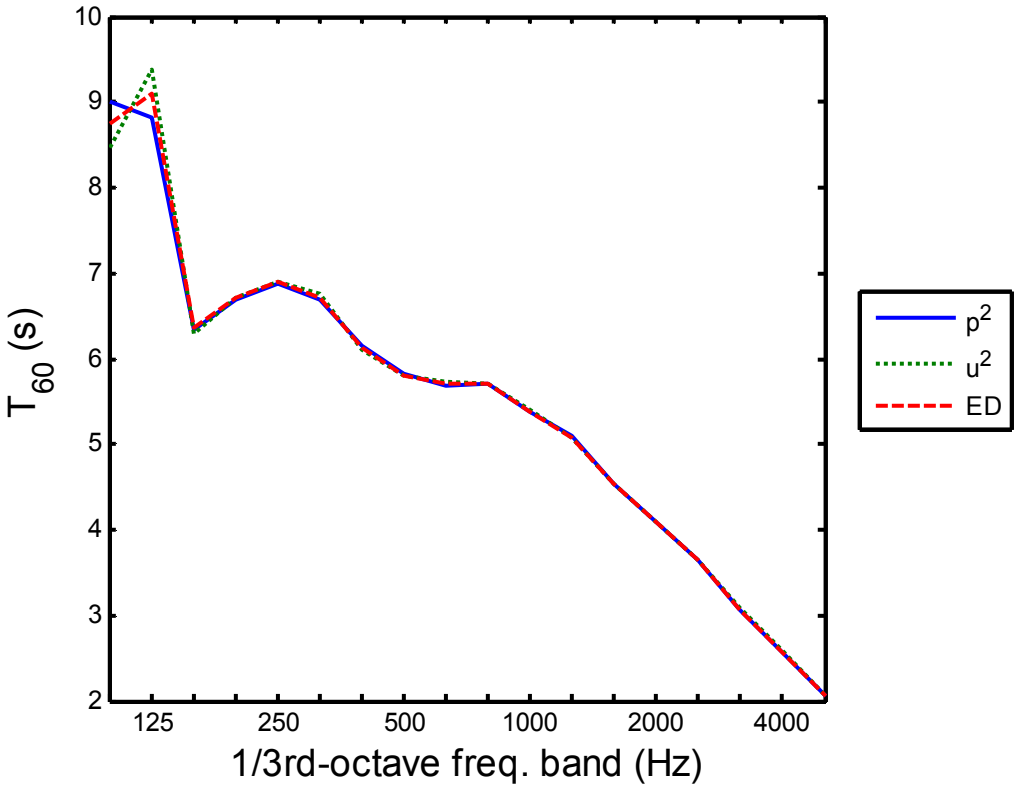

(a)

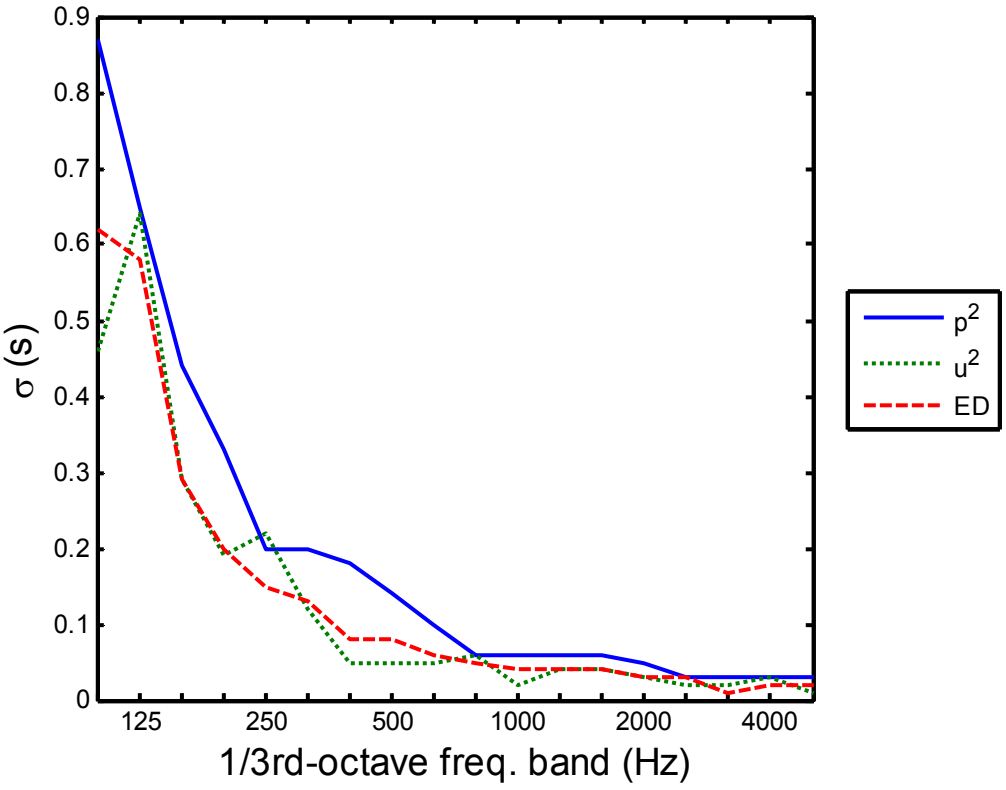

(b)

FIG. 3.12. T_{60} measurements in large chamber with chairs. a) Average. b) Standard deviation.

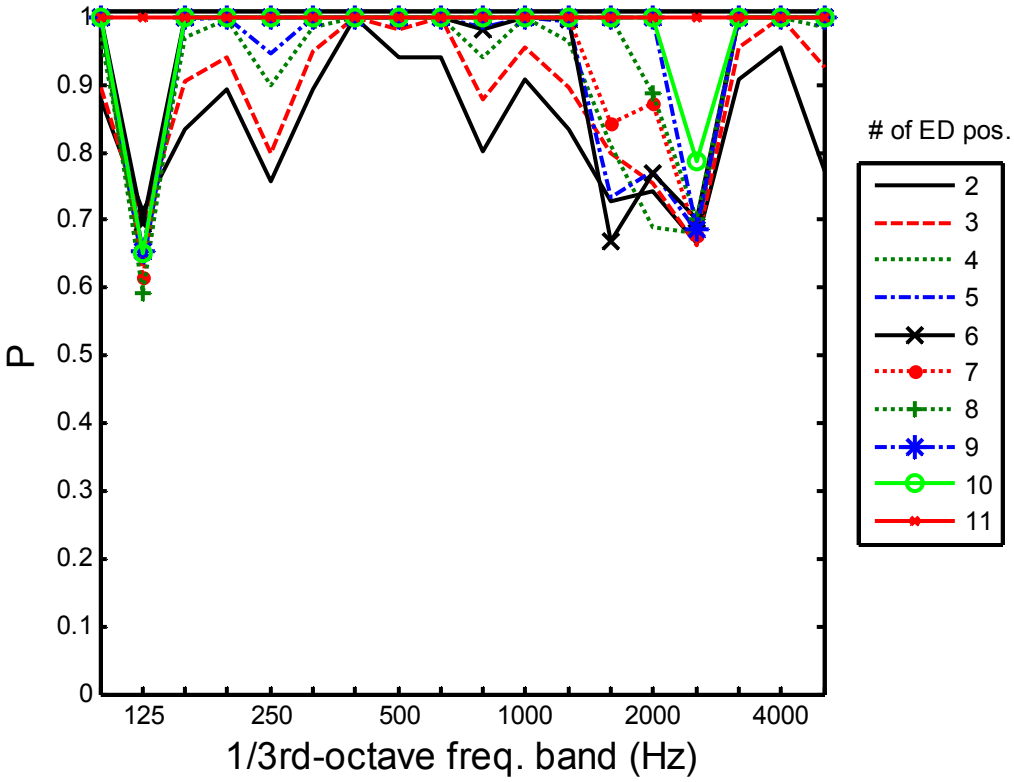

(a)

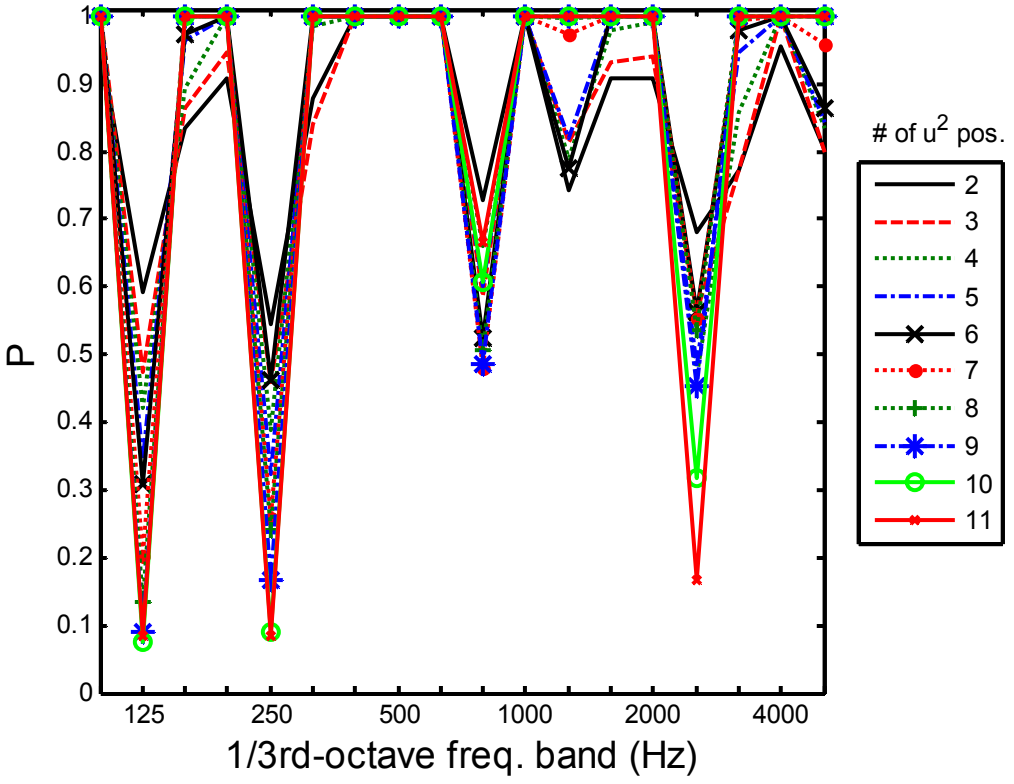

(b)

FIG. 3.13. Probabilities that a given number of positions of one quantity outperforms 12 p^2 positions in large chamber with chairs. a) ED. b) u^2.

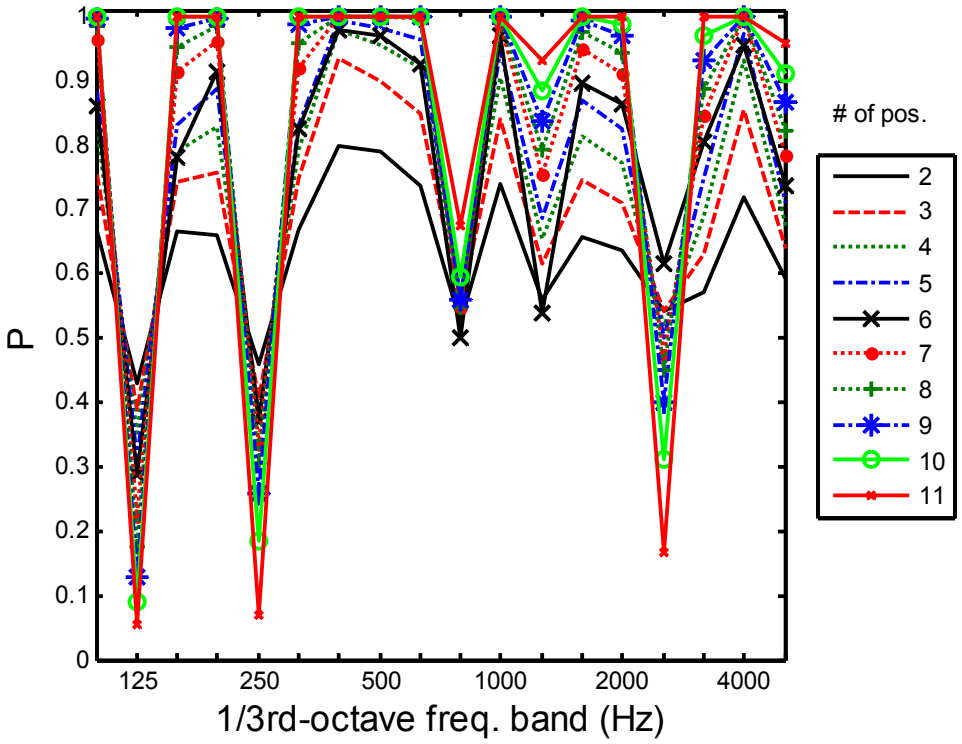

FIG. 3.14. Probability of lower variation in u^2 vs. p^2 for a given number of positions, in the large chamber with chairs.

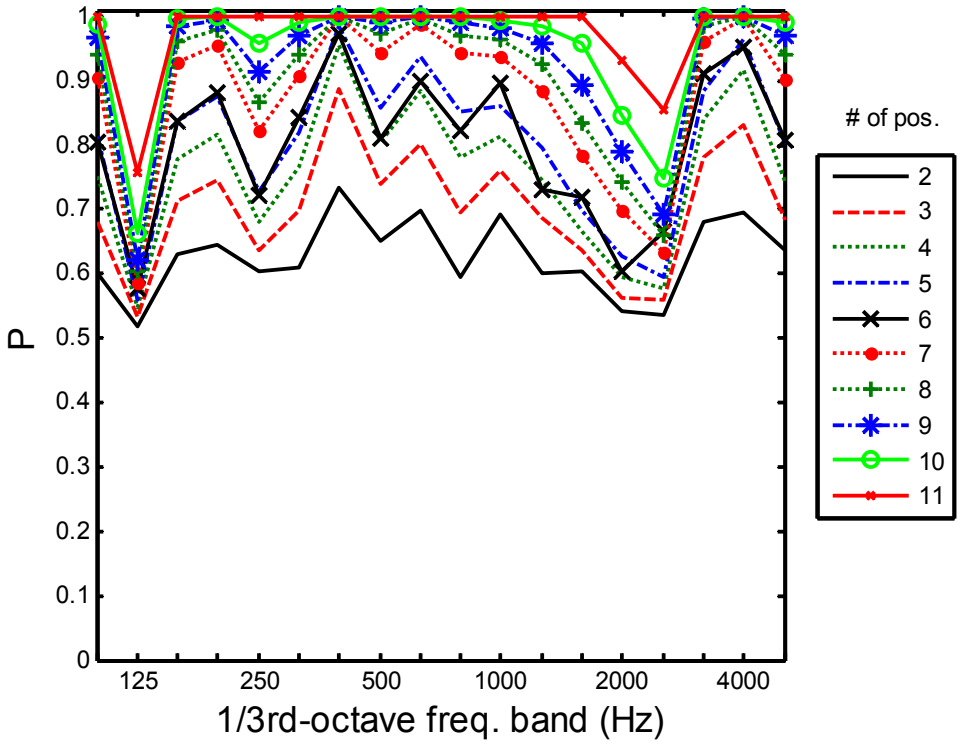

FIG. 3.15. Probability of lower variation in ED vs. p^2 for a given number of positions, in the large chamber with chairs.

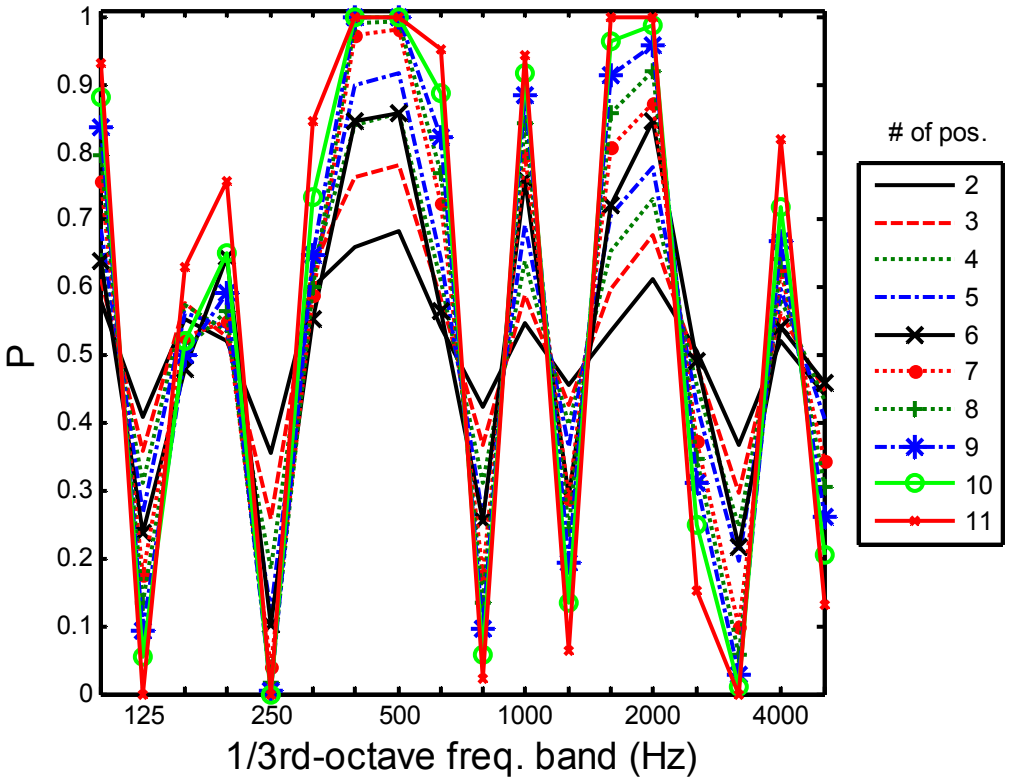

FIG. 3.16. Probability of lower variation in u^2 vs. ED for a given number of positions, in the large chamber with chairs.

3.1.4 Measurements in Small Chamber and Classroom

This series of T_{60} measurements and comparisons was repeated in the small chamber and classroom. Table 3.1 lists the T_{60} averages and standard deviations for all measurements. For each frequency band, the averages and standard deviations of T_{60} in each scenario are grouped together. The "L" columns are measurements taken in the large chamber. The "S" columns are measurements taken in the small chamber. The "C" columns are measurements taken in the classroom. For each frequency band, the rows "P", "U", and "E" refer to p^2, u^2, and ED. Boxes colored in yellow show the smallest standard deviation between the three quantities for a given frequency band.

TABLE 3.1. T_{60} averages and standard deviations for all cases in all rooms.

f (Hz)		Empty						Chairs						Fiberglass					
		L		S		C		L		S		C		L		S		C	
		Avg	σ	Avg	σ	Avg	σ	Avg	σ	Avg	σ	Avg	σ	Avg	σ	Avg	σ	Avg	σ
100	P	9.50	0.69	4.26	0.29	0.71	0.11	8.69	0.94	3.65	0.39	0.75	0.13	7.08	0.28	3.17	0.38	0.82	0.22
	U	9.43	0.76	4.43	0.16	0.81	0.20	8.40	0.44	3.67	0.30	0.73	0.09	6.84	0.37	3.45	0.39	0.74	0.17
	E	9.39	0.40	4.44	0.20	0.76	0.17	8.63	0.59	3.78	0.19	0.72	0.09	6.98	0.22	3.42	0.38	0.77	0.17
125	P	10.1	0.77	3.65	0.75	0.75	0.12	8.53	0.63	2.93	0.39	0.77	0.06	5.70	0.29	2.57	0.47	0.78	0.11
	U	10.5	1.06	4.01	0.62	0.81	0.11	9.27	0.80	3.24	0.36	0.74	0.07	5.64	0.29	2.54	0.34	0.77	0.07
	E	10.4	0.63	4.06	0.52	0.76	0.10	9.06	0.60	3.12	0.32	0.75	0.06	5.69	0.24	2.58	0.38	0.76	0.05
160	P	7.17	0.34	2.80	0.36	0.78	0.09	6.29	0.43	2.67	0.27	0.73	0.08	4.41	0.17	1.92	0.21	0.70	0.10
	U	7.54	0.40	2.79	0.31	0.93	0.57	6.26	0.29	2.66	0.21	0.75	0.03	4.40	0.23	1.89	0.13	0.72	0.08
	E	7.34	0.25	2.80	0.33	0.88	0.42	6.33	0.29	2.69	0.23	0.73	0.04	4.41	0.19	1.92	0.17	0.71	0.06
200	P	8.05	0.41	3.66	0.28	0.81	0.07	6.66	0.34	2.94	0.14	0.78	0.07	3.62	0.19	1.83	0.23	0.70	0.11
	U	8.13	0.34	3.52	0.13	0.85	0.25	6.70	0.20	2.81	0.12	0.80	0.05	3.58	0.13	1.87	0.31	0.71	0.04
	E	8.10	0.36	3.61	0.22	0.85	0.20	6.68	0.20	2.87	0.08	0.80	0.05	3.60	0.15	1.87	0.25	0.70	0.06
250	P	8.86	0.25	4.55	0.33	0.85	0.09	6.87	0.20	2.94	0.19	0.84	0.05	3.31	0.15	1.60	0.15	0.70	0.07
	U	8.98	0.30	4.65	0.30	0.86	0.04	6.90	0.22	2.85	0.12	0.82	0.06	3.33	0.11	1.63	0.09	0.68	0.03
	E	8.94	0.23	4.61	0.27	0.85	0.05	6.89	0.15	2.89	0.14	0.82	0.03	3.32	0.11	1.60	0.11	0.69	0.04
315	P	8.71	0.15	5.23	0.37	0.84	0.06	6.68	0.21	3.02	0.15	0.78	0.07	2.86	0.10	1.44	0.13	0.63	0.05
	U	8.73	0.17	5.19	0.22	0.84	0.05	6.74	0.12	3.04	0.12	0.76	0.07	2.90	0.09	1.40	0.06	0.63	0.03
	E	8.73	0.14	5.22	0.27	0.83	0.03	6.72	0.14	3.03	0.11	0.77	0.06	2.88	0.07	1.41	0.05	0.63	0.03
400	P	8.48	0.18	4.57	0.12	0.70	0.04	6.15	0.18	2.80	0.19	0.68	0.06	2.53	0.06	1.34	0.10	0.55	0.04
	U	8.53	0.09	4.52	0.07	0.70	0.04	6.10	0.05	2.72	0.13	0.68	0.04	2.52	0.05	1.35	0.06	0.57	0.02
	E	8.51	0.11	4.54	0.07	0.70	0.03	6.12	0.08	2.75	0.15	0.68	0.04	2.52	0.04	1.34	0.06	0.56	0.03
500	P	8.49	0.15	4.67	0.10	0.60	0.03	5.81	0.14	2.65	0.12	0.62	0.04	2.35	0.05	1.22	0.06	0.52	0.03
	U	8.45	0.08	4.74	0.08	0.62	0.02	5.79	0.05	2.62	0.07	0.60	0.02	2.34	0.03	1.22	0.07	0.53	0.03
	E	8.47	0.10	4.71	0.07	0.61	0.01	5.80	0.08	2.64	0.07	0.61	0.02	2.34	0.03	1.22	0.05	0.52	0.02
630	P	8.33	0.10	4.92	0.09	0.56	0.03	5.66	0.10	2.65	0.05	0.56	0.02	2.19	0.07	1.18	0.08	0.50	0.03
	U	8.41	0.07	4.99	0.05	0.56	0.02	5.72	0.05	2.68	0.04	0.55	0.02	2.17	0.03	1.20	0.03	0.51	0.04
	E	8.37	0.07	4.96	0.04	0.56	0.03	5.70	0.06	2.67	0.04	0.55	0.02	2.18	0.04	1.18	0.05	0.50	0.03
800	P	8.09	0.08	4.76	0.08	0.57	0.02	5.69	0.06	2.66	0.05	0.55	0.02	2.11	0.04	1.14	0.05	0.52	0.03
	U	8.20	0.03	4.88	0.04	0.56	0.02	5.70	0.06	2.63	0.03	0.54	0.01	2.11	0.04	1.13	0.04	0.53	0.02
	E	8.15	0.04	4.83	0.04	0.56	0.02	5.69	0.05	2.64	0.03	0.54	0.01	2.11	0.03	1.13	0.04	0.52	0.02
1000	P	7.55	0.09	4.46	0.07	0.57	0.03	5.35	0.06	2.52	0.05	0.53	0.03	2.00	0.04	1.10	0.03	0.54	0.03
	U	7.56	0.06	4.64	0.04	0.57	0.03	5.40	0.02	2.52	0.02	0.53	0.02	2.00	0.03	1.10	0.03	0.55	0.02
	E	7.56	0.06	4.56	0.04	0.57	0.03	5.37	0.03	2.52	0.03	0.53	0.02	2.00	0.03	1.10	0.03	0.55	0.02
1250	P	6.68	0.09	3.97	0.09	0.56	0.03	5.07	0.06	2.44	0.05	0.55	0.03	1.94	0.05	1.08	0.03	0.55	0.03
	U	6.70	0.04	4.15	0.02	0.57	0.05	5.06	0.05	2.46	0.03	0.54	0.02	1.93	0.02	1.06	0.03	0.56	0.02
	E	6.69	0.05	4.07	0.04	0.57	0.03	5.06	0.04	2.45	0.04	0.54	0.02	1.94	0.03	1.07	0.02	0.55	0.02
1600	P	5.60	0.07	3.35	0.08	0.53	0.02	4.50	0.06	2.18	0.03	0.52	0.03	1.85	0.03	1.03	0.04	0.54	0.02
	U	5.64	0.04	3.51	0.02	0.57	0.11	4.51	0.04	2.18	0.03	0.52	0.02	1.85	0.02	1.02	0.03	0.53	0.02
	E	5.62	0.05	3.44	0.04	0.54	0.03	4.50	0.05	2.18	0.02	0.52	0.02	1.85	0.02	1.03	0.03	0.53	0.02
2000	P	4.77	0.07	2.95	0.07	0.53	0.02	4.06	0.05	1.98	0.03	0.52	0.03	1.78	0.04	1.00	0.02	0.54	0.02
	U	4.81	0.03	3.14	0.02	0.54	0.03	4.08	0.03	1.99	0.03	0.52	0.02	1.79	0.02	1.00	0.02	0.54	0.02
	E	4.79	0.04	3.06	0.03	0.54	0.02	4.07	0.04	1.99	0.02	0.52	0.02	1.78	0.03	1.00	0.02	0.54	0.02
2500	P	3.95	0.05	2.50	0.07	0.55	0.02	3.60	0.03	1.75	0.03	0.53	0.02	1.68	0.03	0.95	0.02	0.54	0.03
	U	4.01	0.03	2.68	0.02	0.56	0.12	3.60	0.03	1.76	0.03	0.53	0.02	1.67	0.03	0.95	0.02	0.54	0.02
	E	3.98	0.03	2.61	0.03	0.55	0.05	3.60	0.03	1.76	0.03	0.53	0.02	1.67	0.02	0.95	0.02	0.54	0.02
3150	P	3.18	0.05	2.06	0.06	0.54	0.03	3.05	0.03	1.49	0.04	0.54	0.02	1.51	0.04	0.89	0.02	0.53	0.03
	U	3.18	0.03	2.21	0.02	0.58	0.15	3.05	0.02	1.50	0.03	0.54	0.02	1.52	0.02	0.89	0.01	0.54	0.02
	E	3.18	0.03	2.15	0.03	0.56	0.06	3.05	0.02	1.50	0.03	0.54	0.02	1.52	0.03	0.89	0.01	0.54	0.02
4000	P	2.49	0.05	1.69	0.05	0.53	0.03	2.54	0.05	1.24	0.04	0.54	0.03	1.35	0.03	0.81	0.03	0.52	0.03
	U	2.53	0.03	1.82	0.01	0.63	0.32	2.57	0.02	1.25	0.04	0.54	0.02	1.36	0.02	0.81	0.02	0.53	0.03
	E	2.51	0.03	1.77	0.02	0.62	0.27	2.56	0.03	1.25	0.04	0.54	0.02	1.36	0.02	0.81	0.02	0.54	0.03
5000	P	1.85	0.03	1.34	0.04	0.52	0.04	2.03	0.03	1.01	0.03	0.54	0.03	1.14	0.03	0.71	0.02	0.51	0.03
	U	1.86	0.02	1.45	0.02	0.62	0.32	2.02	0.02	1.03	0.03	0.53	0.02	1.14	0.02	0.71	0.02	0.51	0.02
	E	1.86	0.02	1.40	0.02	0.60	0.27	2.03	0.02	1.02	0.03	0.53	0.02	1.14	0.02	0.71	0.02	0.52	0.02

Tables 3.2 through 3.7 detail the probability results mentioned previously. Table 3.2 lists the probabilities where the T60 standard deviations are smaller with a given number of positions of particle velocity magnitude or ED than with 12 pressure positions, in the large chamber. The data is grouped in columns according to the number of positions used, where "U" is particle velocity magnitude, and "ED" is ED. It is also grouped in rows according to the frequency band of interest, where "E" represents the chamber without absorption present, "C" represents measurements involving the upholstered chairs, and "F" represents measurements involving the fiberglass absorption. Table 3.3 is extremely similar to Table 3.2, except in this case the probabilities are of T60 standard deviations which are smaller with particle velocity magnitude or ED than with pressure, using the same number of positions. Tables 3.4 and 3.5 show results obtained from the small chamber, while Tables 3.6 and 3.7 show results obtained from the classroom.

The tables show the general characteristic that ED is consistently a better quantity to use under both diffuse and non-diffuse conditions. It also suggests that u^2 is a suitable quantity to use above the Schroeder frequency, in which case its performance is comparable to ED.

TABLE 3.2. Probabilities for lower standard deviations of T_{60} using a given number of u^2 or ED positions, vs. 12 p^2 positions, in the large chamber.

f		$P(\sigma_{x(n)} < \sigma_{p(12)})$																			
(Hz)	n	2		3		4		5		6		7		8		9		10		11	
	x	U	ED	U	ED	U	ED	U	ED	U	ED	U	ED	U	ED	U	ED	U	ED	U	ED
100	E	0.6	0.9	0.5	1	0.5	1	0.4	1	0.5	1	0.3	1	0.3	1	0.3	1	0.2	1	0.2	1
	F	1	0.9	1	0.9	1	1	1	1	1	1	1	1	1	1	1	1	1	1	1	1
	C	0.5	0.8	0.4	0.8	0.3	0.8	0.2	0.8	0.3	0.9	0.1	1	0.1	1	0.1	1	0	1	0	1
125	E	0.5	0.8	0.4	0.7	0.2	0.7	0.2	0.7	0.1	0.6	0.1	0.9	0	1	0	1	0	1	0	1
	F	0.6	0.7	0.5	0.7	0.4	0.6	0.3	0.6	0.3	0.7	0.2	0.6	0.1	0.6	0.1	0.7	0.1	0.7	0.1	1
	C	0.7	0.8	0.6	0.7	0.5	0.8	0.6	0.7	0.5	0.7	0.5	0.9	0.5	0.8	0.4	1	0.3	1	0.3	1
160	E	0.6	0.8	0.4	0.9	0.3	1	0.3	1	0.3	1	0.2	1	0.1	1	0.1	1	0	1	0	1
	F	0.8	0.8	0.9	0.9	0.9	1	1	1	1	1	1	1	1	1	1	1	1	1	1	1
	C	0.5	0.5	0.3	0.4	0.2	0.3	0.1	0.3	0	0.4	0	0.2	0	0.2	0	0.1	0	0.1	0	0
200	E	0.7	0.7	0.7	0.7	0.8	0.7	0.9	0.7	0.9	0.7	1	0.7	1	0.7	1	0.9	1	1	1	1
	F	0.9	0.9	0.9	0.9	1	1	1	1	1	1	1	1	1	1	1	1	1	1	1	1
	C	0.8	0.7	0.9	0.8	1	0.9	1	0.9	1	1	1	1	1	1	1	1	1	1	1	1
250	E	0.5	0.7	0.5	0.6	0.3	0.6	0.3	0.6	0.2	0.7	0.2	0.7	0.2	0.7	0.1	0.7	0	0.8	0	1
	F	0.5	0.8	0.5	0.8	0.4	0.9	0.3	0.9	0.5	1	0.3	1	0.2	1	0.2	1	0.1	1	0.1	1
	C	0.8	0.8	0.9	0.9	0.9	1	1	1	1	1	1	1	1	1	1	1	1	1	1	1
315	E	0.6	0.7	0.5	0.6	0.4	0.6	0.3	0.7	0.2	0.7	0.2	0.8	0.2	0.8	0.1	0.9	0.1	1	0	1
	F	0.9	0.9	0.8	1	1	1	1	1	1	1	1	1	1	1	1	1	1	1	1	1
	C	0.8	0.9	0.7	0.9	0.6	0.9	0.7	1	0.8	1	0.8	1	0.8	1	0.9	1	1	1	1	1
400	E	1	0.9	1	0.9	1	1	1	1	1	1	1	1	1	1	1	1	1	1	1	1
	F	1	1	1	1	1	1	1	1	1	1	1	1	1	1	1	1	1	1	1	1
	C	0.8	0.9	0.8	0.9	0.7	0.9	0.6	1	0.8	1	0.6	1	0.6	1	0.8	1	1	1	1	1
500	E	0.9	0.8	1	0.9	1	1	1	1	1	1	1	1	1	1	1	1	1	1	1	1
	F	1	0.9	1	1	1	1	1	1	1	1	1	1	1	1	1	1	1	1	1	1
	C	0.8	0.9	0.8	0.9	0.9	1	0.8	1	0.9	1	1	1	1	1	1	1	1	1	1	1
630	E	0.8	0.9	0.9	0.9	0.9	1	0.9	1	0.9	1	1	1	1	1	1	1	1	1	1	1
	F	1	0.9	1	1	1	1	1	1	1	1	1	1	1	1	1	1	1	1	1	1
	C	1	0.9	1	0.9	1	1	1	1	1	1	1	1	1	1	1	1	1	1	1	1
800	E	1	1	1	1	1	1	1	1	1	1	1	1	1	1	1	1	1	1	1	1
	F	0.7	0.8	0.6	0.9	0.7	0.9	0.6	1	0.5	1	0.5	1	0.5	1	0.5	1	0.6	1	0.7	1
	C	0.6	0.8	0.7	0.8	0.7	0.9	0.8	0.8	0.8	0.9	0.9	1	0.9	1	1	1	1	1	1	1
1000	E	0.8	0.9	0.9	1	0.9	1	1	1	1	1	1	1	1	1	1	1	1	1	1	1
	F	1	0.9	1	1	1	1	1	1	1	1	1	1	1	1	1	1	1	1	1	1
	C	0.8	0.8	0.8	0.9	0.9	1	0.9	1	0.9	1	1	1	1	1	1	1	1	1	1	1
1250	E	1	0.9	1	0.9	1	1	1	1	1	1	1	1	1	1	1	1	1	1	1	1
	F	0.7	0.8	0.8	0.9	0.8	1	0.8	1	0.8	1	1	1	1	1	1	1	1	1	1	1
	C	0.9	0.8	1	0.9	1	1	1	1	1	1	1	1	1	1	1	1	1	1	1	1
1600	E	0.9	0.8	0.9	0.9	1	0.9	1	1	1	1	1	1	1	1	1	1	1	1	1	1
	F	0.9	0.7	0.9	0.8	1	0.8	1	0.7	1	0.7	1	0.8	1	1	1	1	1	1	1	1
	C	0.9	0.9	1	1	1	1	1	1	1	1	1	1	1	1	1	1	1	1	1	1
2000	E	1	0.9	1	1	1	1	1	1	1	1	1	1	1	1	1	1	1	1	1	1
	F	0.9	0.7	0.9	0.8	1	0.7	1	0.8	1	0.8	1	0.9	1	0.9	1	1	1	1	1	1
	C	1	0.8	1	0.8	1	0.7	1	0.7	1	0.7	1	1	1	1	1	1	1	1	1	1
2500	E	0.9	0.9	1	0.9	1	1	1	1	1	1	1	1	1	1	1	1	1	1	1	1
	F	0.7	0.7	0.6	0.7	0.5	0.7	0.5	0.7	0.6	0.7	0.6	0.7	0.5	0.7	0.5	0.7	0.3	0.8	0.2	1
	C	0.7	0.9	0.7	0.9	0.7	0.9	0.7	1	0.7	1	0.7	1	0.7	1	0.7	1	0.8	1	1	1
3150	E	1	1	1	1	1	1	1	1	1	1	1	1	1	1	1	1	1	1	1	1
	F	0.8	0.9	0.8	1	0.9	1	0.9	1	1	1	1	1	1	1	1	1	1	1	1	1
	C	1	0.9	1	1	1	1	1	1	1	1	1	1	1	1	1	1	1	1	1	1
4000	E	1	0.9	1	1	1	1	1	1	1	1	1	1	1	1	1	1	1	1	1	1
	F	1	1	1	1	1	1	1	1	1	1	1	1	1	1	1	1	1	1	1	1
	C	0.8	0.8	0.9	0.8	1	0.9	1	1	1	1	1	1	1	1	1	1	1	1	1	1
5000	E	1	0.9	1	0.9	1	1	1	1	1	1	1	1	1	1	1	1	1	1	1	1
	F	0.8	0.8	0.8	0.9	0.8	1	0.8	1	0.9	1	1	1	1	1	1	1	1	1	1	1
	C	0.7	0.8	0.7	0.8	0.8	0.9	0.8	0.9	0.8	0.9	0.9	1	1	1	1	1	1	1	1	1
Avg	E	0.8	0.8	0.8	0.9	0.8	0.9	0.8	0.9	0.8	0.9	0.8	0.9	0.7	1	0.7	1	0.7	1	0.7	1
	F	0.8	0.8	0.8	0.9	0.8	0.9	0.8	0.9	0.8	0.9	0.8	0.9	0.8	1	0.8	1	0.8	1	0.8	1
	C	0.8	0.8	0.8	0.8	0.8	0.9	0.8	0.9	0.8	0.9	0.8	0.9	0.8	0.9	0.8	0.9	0.8	0.9	0.8	0.9

TABLE 3.3. Probabilities for lower standard deviations of T_{60} using a given number of u^2 or ED positions, vs. the same number of p^2 positions, in the large chamber.

f		$P(\sigma_{x(n)} < \sigma_{p(n)})$																			
(Hz)	n	2		3		4		5		6		7		8		9		10		11	
	x	U	ED	U	ED	U	ED	U	ED	U	ED	U	ED	U	ED	U	ED	U	ED	U	ED
100	E	0.5	0.6	0.5	0.8	0.4	0.8	0.4	0.9	0.4	0.9	0.4	1	0.3	1	0.3	1	0.2	1	0.1	1
	F	0.7	0.6	0.8	0.7	0.8	0.8	0.9	0.8	0.9	0.8	1	0.9	1	0.9	1	1	1	1	1	1
	C	0.4	0.6	0.4	0.7	0.3	0.7	0.2	0.8	0.3	0.8	0.1	0.9	0.1	0.9	0.1	0.9	0	1	0	1
125	E	0.4	0.6	0.3	0.6	0.3	0.7	0.2	0.7	0.2	0.7	0.1	0.8	0.1	0.8	0	0.9	0	0.9	0	1
	F	0.4	0.5	0.4	0.5	0.4	0.5	0.3	0.6	0.3	0.6	0.2	0.6	0.2	0.6	0.1	0.6	0.1	0.7	0.1	0.8
	C	0.5	0.5	0.5	0.6	0.5	0.6	0.5	0.6	0.4	0.6	0.5	0.7	0.5	0.7	0.5	0.8	0.5	0.8	0.4	0.9
160	E	0.4	0.6	0.4	0.7	0.3	0.7	0.3	0.8	0.3	0.8	0.2	0.9	0.2	0.9	0.1	1	0.1	1	0	1
	F	0.7	0.6	0.7	0.7	0.8	0.8	0.8	0.8	0.8	0.8	0.9	0.9	1	1	1	1	1	1	1	1
	C	0.4	0.5	0.3	0.4	0.2	0.4	0.2	0.4	0.1	0.3	0.1	0.3	0	0.2	0	0.2	0	0.1	0	0
200	E	0.5	0.5	0.5	0.5	0.6	0.5	0.6	0.6	0.6	0.6	0.7	0.6	0.7	0.7	0.8	0.7	0.8	0.8	0.9	0.9
	F	0.7	0.6	0.8	0.7	0.8	0.8	0.9	0.9	0.9	0.9	1	1	1	1	1	1	1	1	1	1
	C	0.6	0.6	0.7	0.6	0.8	0.7	0.8	0.7	0.8	0.7	0.9	0.8	0.9	0.9	1	0.9	1	0.9	1	1
250	E	0.4	0.5	0.4	0.5	0.3	0.5	0.3	0.5	0.3	0.6	0.2	0.6	0.2	0.6	0.1	0.6	0	0.7	0	0.8
	F	0.5	0.6	0.4	0.6	0.4	0.7	0.4	0.7	0.4	0.7	0.3	0.8	0.3	0.9	0.3	0.9	0.2	1	0.1	1
	C	0.5	0.6	0.6	0.6	0.7	0.7	0.7	0.7	0.8	0.8	0.8	0.9	0.9	0.9	0.9	0.9	1	1	1	1
315	E	0.4	0.5	0.4	0.5	0.4	0.5	0.4	0.6	0.3	0.6	0.3	0.6	0.3	0.7	0.2	0.8	0.1	0.8	0	0.9
	F	0.7	0.6	0.7	0.7	0.8	0.8	0.8	0.8	0.8	0.8	0.9	0.9	1	0.9	1	1	1	1	1	1
	C	0.5	0.6	0.6	0.7	0.6	0.7	0.6	0.8	0.6	0.8	0.7	0.9	0.7	0.9	0.8	1	0.8	1	0.9	1
400	E	0.7	0.7	0.8	0.8	0.9	0.8	1	0.9	0.9	0.9	1	1	1	1	1	1	1	1	1	1
	F	0.8	0.7	0.9	0.9	1	1	1	1	1	1	1	1	1	1	1	1	1	1	1	1
	C	0.6	0.6	0.6	0.7	0.6	0.7	0.6	0.8	0.7	0.7	0.6	0.8	0.7	0.9	0.7	0.9	0.8	1	0.9	1
500	E	0.7	0.6	0.8	0.7	0.9	0.8	0.9	0.9	0.9	0.9	1	1	1	1	1	1	1	1	1	1
	F	0.8	0.7	0.9	0.7	1	0.8	1	0.9	1	0.8	1	0.9	1	1	1	1	1	1	1	1
	C	0.6	0.7	0.7	0.7	0.7	0.8	0.8	0.9	0.9	0.9	0.8	1	0.9	1	0.9	1	1	1	1	1
630	E	0.6	0.6	0.6	0.6	0.6	0.7	0.7	0.7	0.7	0.8	0.8	0.8	0.8	0.9	0.8	0.9	0.9	0.9	0.9	1
	F	0.7	0.7	0.8	0.8	0.9	0.9	1	0.9	0.9	0.9	1	1	1	1	1	1	1	1	1	1
	C	0.8	0.7	0.9	0.7	0.9	0.8	1	0.9	1	0.9	1	0.9	1	1	1	1	1	1	1	1
800	E	0.8	0.7	0.9	0.8	0.9	0.9	1	0.9	1	0.9	1	1	1	1	1	1	1	1	1	1
	F	0.5	0.6	0.6	0.7	0.6	0.8	0.6	0.9	0.5	0.8	0.5	0.9	0.5	1	0.6	1	0.6	1	0.7	1
	C	0.5	0.6	0.5	0.6	0.5	0.7	0.5	0.7	0.5	0.7	0.6	0.8	0.7	0.8	0.7	0.9	0.8	0.9	0.9	0.9
1000	E	0.7	0.7	0.8	0.8	0.8	0.9	0.9	0.9	0.9	0.9	1	1	1	1	1	1	1	1	1	1
	F	0.7	0.7	0.8	0.8	0.9	0.8	0.9	0.9	1	0.9	1	0.9	1	1	1	1	1	1	1	1
	C	0.6	0.6	0.7	0.7	0.7	0.7	0.7	0.8	0.8	0.8	0.8	0.9	0.9	0.9	0.9	0.9	0.9	1	1	1
1250	E	0.7	0.6	0.8	0.7	0.9	0.8	1	0.8	1	0.9	1	0.9	1	0.9	1	1	1	1	1	1
	F	0.6	0.6	0.6	0.7	0.7	0.7	0.7	0.8	0.5	0.7	0.8	0.9	0.8	0.9	0.8	1	0.9	1	0.9	1
	C	0.7	0.6	0.9	0.7	0.9	0.8	1	0.9	1	0.9	1	1	1	1	1	1	1	1	1	1
1600	E	0.6	0.6	0.7	0.7	0.8	0.7	0.8	0.8	0.9	0.8	0.9	0.9	0.9	0.9	1	0.9	1	1	1	1
	F	0.7	0.6	0.7	0.6	0.8	0.7	0.9	0.7	0.9	0.7	1	0.8	1	0.8	1	0.9	1	1	1	1
	C	0.7	0.7	0.8	0.8	0.8	0.8	0.9	0.9	0.9	0.9	1	1	1	1	1	1	1	1	1	1
2000	E	0.8	0.7	0.9	0.8	0.9	0.9	1	0.9	1	0.9	1	1	1	1	1	1	1	1	1	1
	F	0.6	0.5	0.7	0.6	0.8	0.6	0.8	0.6	0.9	0.6	0.9	0.7	0.9	0.7	1	0.8	1	0.8	1	0.9
	C	0.6	0.6	0.7	0.7	0.8	0.7	0.9	0.7	0.9	0.7	0.9	0.7	1	0.8	1	0.8	1	0.9	1	0.9
2500	E	0.7	0.6	0.8	0.7	0.8	0.7	0.9	0.8	0.9	0.8	0.9	0.8	1	0.9	1	0.9	1	1	1	1
	F	0.5	0.5	0.5	0.6	0.5	0.6	0.5	0.6	0.6	0.7	0.5	0.6	0.4	0.7	0.4	0.7	0.3	0.7	0.2	0.9
	C	0.5	0.6	0.5	0.7	0.5	0.8	0.6	0.8	0.5	0.8	0.6	0.9	0.7	0.9	0.7	1	0.8	1	0.9	1
3150	E	0.7	0.7	0.7	0.7	0.8	0.8	0.9	0.9	0.9	0.9	0.9	1	1	1	1	1	1	1	1	1
	F	0.6	0.7	0.6	0.8	0.7	0.8	0.7	0.9	0.8	0.9	0.8	1	0.9	1	0.9	1	1	1	1	1
	C	0.8	0.7	0.9	0.8	1	0.9	1	0.9	1	1	1	1	1	1	1	1	1	1	1	1
4000	E	0.7	0.6	0.8	0.7	0.9	0.8	0.9	0.9	0.9	0.9	1	0.9	1	1	1	1	1	1	1	1
	F	0.7	0.7	0.9	0.8	0.9	0.9	1	1	1	1	1	1	1	1	1	1	1	1	1	1
	C	0.6	0.6	0.7	0.7	0.8	0.7	0.9	0.8	0.7	0.7	0.9	0.9	1	0.9	1	1	1	1	1	1
5000	E	0.7	0.6	0.7	0.6	0.8	0.7	0.8	0.7	0.9	0.8	0.9	0.9	0.9	0.9	1	1	1	1	1	1
	F	0.6	0.6	0.6	0.7	0.7	0.7	0.7	0.8	0.7	0.8	0.8	0.9	0.8	0.9	0.9	1	0.9	1	1	1
	C	0.5	0.6	0.6	0.6	0.6	0.7	0.7	0.7	0.7	0.8	0.8	0.8	0.8	0.9	0.9	0.9	0.9	1	0.9	1
Avg	E	0.6	0.6	0.6	0.7	0.7	0.7	0.7	0.8	0.7	0.8	0.7	0.9	0.7	0.9	0.7	0.9	0.7	0.9	0.7	1
	F	0.6	0.6	0.7	0.7	0.7	0.8	0.8	0.8	0.8	0.8	0.8	0.9	0.8	0.9	0.8	0.9	0.8	1	0.8	1
	C	0.6	0.6	0.6	0.7	0.7	0.7	0.7	0.8	0.7	0.8	0.7	0.8	0.7	0.9	0.8	0.9	0.8	0.9	0.8	0.9

TABLE 3.4. Probabilities for lower standard deviations of T_{60} using a given number of u^2 or ED positions, vs. 12 p^2 positions, in the small chamber.

f		$P(\sigma_{x(n)} < \sigma_{p(12)})$																			
(Hz)	n	2		3		4		5		6		7		8		9		10		11	
	x	U	ED	U	ED	U	ED	U	ED	U	ED	U	ED	U	ED	U	ED	U	ED	U	ED
100	E	0.9	0.8	1	0.9	1	1	1	1	1	1	1	1	1	1	1	1	1	1	1	1
	F	0.8	1	0.9	1	0.8	1	0.9	1	0.9	1	1	1	1	1	1	1	1	1	1	1
	C	0.7	0.6	0.5	0.7	0.5	0.5	0.6	0.5	0.6	0.6	0.5	0.5	0.4	0.5	0.5	0.5	0.4	0.3	0.3	0.3
125	E	0.8	0.8	0.8	0.9	0.8	1	0.8	1	0.9	1	0.9	1	1	1	1	1	1	1	1	1
	F	0.5	0.7	0.6	0.8	0.7	0.8	0.7	0.9	0.7	0.9	0.8	1	0.9	1	1	1	1	1	1	1
	C	0.9	0.7	0.9	0.7	1	0.8	1	0.8	1	0.8	1	1	1	1	1	1	1	1	1	1
160	E	0.7	0.7	0.7	0.6	0.7	0.7	0.7	0.7	0.8	0.8	0.8	0.8	0.9	0.8	1	0.8	1	1	1	1
	F	0.8	0.7	0.8	0.7	0.8	0.7	0.8	0.7	0.8	0.7	0.9	0.8	1	0.8	1	0.9	1	1	1	1
	C	0.9	0.8	0.9	0.8	1	0.8	1	0.8	1	0.9	1	1	1	1	1	1	1	1	1	1
200	E	1	0.8	1	0.8	1	0.8	1	0.8	1	0.8	1	0.9	1	1	1	1	1	1	1	1
	F	0.7	0.9	0.7	0.9	0.7	1	0.8	1	0.9	1	0.9	1	0.9	1	1	1	1	1	1	1
	C	0.6	0.7	0.5	0.6	0.5	0.5	0.4	0.6	0.5	0.7	0.4	0.4	0.3	0.3	0.3	0.3	0.2	0.2	0.1	0.1
250	E	0.8	0.7	0.7	0.7	0.7	0.8	0.6	0.9	0.5	0.8	0.5	0.9	0.6	1	0.8	1	1	1	1	1
	F	1	0.8	1	0.8	1	0.9	1	1	1	1	1	1	1	1	1	1	1	1	1	1
	C	0.9	0.8	0.8	0.9	0.9	0.8	1	1	1	0.9	1	1	1	1	1	1	1	1	1	1
315	E	0.9	0.8	1	0.9	1	1	1	1	1	1	1	1	1	1	1	1	1	1	1	1
	F	0.8	0.8	0.8	0.8	0.7	0.9	0.6	0.9	0.5	0.9	0.4	1	0.5	1	1	1	1	1	1	1
	C	1	1	1	1	1	1	1	1	1	1	1	1	1	1	1	1	1	1	1	1
400	E	0.9	1	1	1	1	1	1	1	1	1	1	1	1	1	1	1	1	1	1	1
	F	0.8	0.7	0.9	0.8	0.9	0.8	1	0.9	1	0.9	1	1	1	1	1	1	1	1	1	1
	C	0.9	0.9	1	0.9	1	1	1	1	1	1	1	1	1	1	1	1	1	1	1	1
500	E	0.8	0.8	0.8	0.9	0.8	0.9	0.8	0.9	0.7	0.9	1	1	1	1	1	1	1	1	1	1
	F	0.9	0.9	1	0.9	1	1	1	1	1	1	1	1	1	1	1	1	1	1	1	1
	C	0.6	0.8	0.5	0.8	0.4	0.8	0.4	0.8	0.3	0.7	0.3	0.9	0.2	1	0.2	1	0.2	1	0.1	1
630	E	0.9	1	1	1	1	1	1	1	1	1	1	1	1	1	1	1	1	1	1	1
	F	0.8	0.8	0.8	0.8	0.9	0.9	1	1	0.9	1	1	1	1	1	1	1	1	1	1	1
	C	1	0.9	1	1	1	1	1	1	1	1	1	1	1	1	1	1	1	1	1	1
800	E	1	1	1	1	1	1	1	1	1	1	1	1	1	1	1	1	1	1	1	1
	F	0.9	0.9	1	1	1	1	1	1	1	1	1	1	1	1	1	1	1	1	1	1
	C	0.7	0.7	0.7	0.7	0.8	0.7	0.8	0.7	0.9	0.9	1	0.9	1	0.9	1	1	1	1	1	1
1000	E	0.9	0.9	1	1	1	1	1	1	1	1	1	1	1	1	1	1	1	1	1	1
	F	1	0.9	1	1	1	1	1	1	1	1	1	1	1	1	1	1	1	1	1	1
	C	0.6	0.7	0.6	0.7	0.5	0.8	0.5	0.8	0.4	0.8	0.5	0.9	0.5	1	0.5	1	0.4	1	0.3	1
1250	E	1	1	1	1	1	1	1	1	1	1	1	1	1	1	1	1	1	1	1	1
	F	0.9	0.8	0.9	0.8	1	0.9	1	1	1	1	1	1	1	1	1	1	1	1	1	1
	C	0.8	0.9	0.7	1	0.8	1	0.9	1	0.9	1	1	1	1	1	1	1	1	1	1	1
1600	E	1	1	1	1	1	1	1	1	1	1	1	1	1	1	1	1	1	1	1	1
	F	0.7	0.7	0.8	0.8	0.7	0.8	0.7	0.9	0.6	0.9	0.7	1	0.8	1	1	1	1	1	1	1
	C	0.8	0.8	0.8	0.7	0.8	0.8	0.8	0.8	0.9	0.9	0.9	0.9	1	1	1	1	1	1	1	1
2000	E	1	1	1	1	1	1	1	1	1	1	1	1	1	1	1	1	1	1	1	1
	F	0.7	0.8	0.7	0.8	0.7	0.9	0.7	0.9	0.6	1	0.7	1	0.7	1	0.8	1	1	1	1	1
	C	0.7	0.8	0.6	0.9	0.5	1	0.6	1	0.5	1	0.7	1	0.7	1	0.6	1	0.8	1	1	1
2500	E	1	1	1	1	1	1	1	1	1	1	1	1	1	1	1	1	1	1	1	1
	F	0.6	0.7	0.5	0.6	0.4	0.6	0.3	0.6	0.2	0.5	0.3	0.6	0.3	0.6	0.3	0.6	0.2	0.6	0.2	0.8
	C	0.7	0.8	0.7	0.9	0.7	0.9	0.8	1	0.7	1	0.8	1	0.9	1	1	1	1	1	1	1
3150	E	1	1	1	1	1	1	1	1	1	1	1	1	1	1	1	1	1	1	1	1
	F	0.8	0.9	0.8	1	0.8	1	0.9	1	1	1	1	1	1	1	1	1	1	1	1	1
	C	0.9	0.9	0.9	1	1	1	1	1	1	1	1	1	1	1	1	1	1	1	1	1
4000	E	1	1	1	1	1	1	1	1	1	1	1	1	1	1	1	1	1	1	1	1
	F	0.6	0.7	0.5	0.7	0.5	0.7	0.5	0.7	0.5	0.6	0.4	0.7	0.4	0.8	0.4	0.9	0.3	1	0.3	1
	C	0.8	0.8	0.8	0.9	0.8	1	0.8	1	0.9	1	0.9	1	1	1	1	1	1	1	1	1
5000	E	1	0.9	1	1	1	1	1	1	1	1	1	1	1	1	1	1	1	1	1	1
	F	0.6	0.6	0.6	0.5	0.5	0.4	0.5	0.4	0.4	0.4	0.4	0.4	0.3	0.3	0.3	0.3	0.2	0.2	0.1	0.1
	C	0.8	0.8	0.7	0.8	0.8	0.9	0.9	0.9	0.8	0.8	0.9	1	1	1	1	1	1	1	1	1
Avg	E	0.9	0.9	0.9	0.9	0.9	0.9	0.9	1	0.9	1	1	1	1	1	1	1	1	1	1	1
	F	0.8	0.8	0.8	0.8	0.8	0.9	0.8	0.9	0.8	0.9	0.8	0.9	0.8	0.9	0.9	0.9	0.9	0.9	0.9	0.9
	C	0.8	0.8	0.8	0.8	0.8	0.8	0.8	0.9	0.8	0.9	0.8	0.9	0.8	0.9	0.8	0.9	0.8	0.9	0.8	0.9

TABLE 3.5. Probabilities for lower standard deviations of T_{60} using a given number of u^2 or ED positions, vs. the same number of p^2 positions, in the small chamber.

f		$P(\sigma_{x(n)} < \sigma_{p(n)})$																			
(Hz)	n	2		3		4		5		6		7		8		9		10		11	
	x	U	ED	U	ED	U	ED	U	ED	U	ED	U	ED	U	ED	U	ED	U	ED	U	ED
100	E	0.7	0.6	0.8	0.7	0.9	0.8	0.9	0.9	0.9	0.9	1	1	1	1	1	1	1	1	1	1
	F	0.6	0.7	0.6	0.9	0.7	0.9	0.7	1	0.7	1	0.8	1	0.9	1	0.9	1	1	1	1	1
	C	0.5	0.5	0.5	0.5	0.5	0.5	0.5	0.5	0.5	0.6	0.5	0.5	0.5	0.5	0.5	0.5	0.4	0.5	0.4	0.5
125	E	0.6	0.6	0.6	0.7	0.7	0.8	0.7	0.9	0.8	0.9	0.8	1	0.9	1	0.9	1	1	1	1	1
	F	0.5	0.5	0.6	0.6	0.6	0.7	0.6	0.7	0.5	0.7	0.7	0.8	0.7	0.9	0.8	0.9	0.8	0.9	0.8	1
	C	0.6	0.6	0.6	0.6	0.7	0.7	0.8	0.7	0.8	0.7	0.9	0.8	0.9	0.8	0.9	0.9	1	0.9	1	0.9
160	E	0.6	0.5	0.6	0.6	0.6	0.6	0.7	0.6	0.6	0.6	0.7	0.7	0.8	0.7	0.8	0.8	0.9	0.8	1	0.9
	F	0.6	0.5	0.6	0.6	0.7	0.6	0.7	0.6	0.7	0.6	0.8	0.7	0.9	0.7	0.9	0.8	1	0.8	1	0.9
	C	0.7	0.6	0.8	0.6	0.8	0.7	0.9	0.7	0.8	0.7	1	0.8	1	0.9	1	0.9	1	1	1	1
200	E	0.7	0.6	0.8	0.6	0.9	0.6	0.9	0.7	0.9	0.7	1	0.7	1	0.8	1	0.8	1	0.9	1	0.9
	F	0.5	0.7	0.6	0.8	0.6	0.8	0.6	0.9	0.6	0.9	0.7	1	0.8	1	0.8	1	0.9	1	0.9	1
	C	0.5	0.5	0.5	0.5	0.4	0.5	0.4	0.5	0.5	0.6	0.3	0.4	0.3	0.4	0.2	0.3	0.2	0.2	0.1	0.1
250	E	0.5	0.5	0.5	0.6	0.5	0.6	0.6	0.7	0.6	0.7	0.6	0.8	0.6	0.8	0.7	0.8	0.7	0.9	0.8	0.9
	F	0.7	0.6	0.7	0.6	0.8	0.7	0.9	0.8	0.9	0.8	1	0.9	1	0.9	1	0.9	1	1	1	1
	C	0.7	0.6	0.8	0.7	0.8	0.8	0.9	0.8	0.9	0.8	1	0.9	1	0.9	1	1	1	1	1	1
315	E	0.7	0.6	0.8	0.7	0.9	0.7	0.9	0.8	1	0.9	1	0.9	1	0.9	1	1	1	1	1	1
	F	0.7	0.6	0.7	0.7	0.7	0.7	0.6	0.7	0.6	0.7	0.6	0.8	0.7	0.9	0.7	0.9	0.8	1	0.9	1
	C	0.8	0.8	0.9	0.9	0.9	0.9	1	1	1	1	1	1	1	1	1	1	1	1	1	1
400	E	0.6	0.7	0.7	0.8	0.8	0.8	0.8	0.9	0.8	0.9	0.9	0.9	1	1	1	1	1	1	1	1
	F	0.6	0.6	0.7	0.6	0.8	0.7	0.8	0.8	0.8	0.8	0.9	0.8	1	0.9	1	0.9	1	1	1	1
	C	0.7	0.7	0.8	0.8	0.8	0.8	0.9	0.9	0.9	0.9	1	1	1	1	1	1	1	1	1	1
500	E	0.6	0.6	0.7	0.7	0.8	0.8	0.8	0.9	0.7	0.8	0.9	1	0.9	1	1	1	1	1	1	1
	F	0.6	0.7	0.7	0.7	0.8	0.8	0.8	0.8	0.9	0.8	0.9	0.9	1	0.9	1	1	1	1	1	1
	C	0.4	0.5	0.4	0.6	0.4	0.6	0.4	0.6	0.3	0.6	0.3	0.7	0.3	0.8	0.2	0.8	0.2	0.9	0.1	0.9
630	E	0.6	0.7	0.7	0.8	0.8	0.9	0.9	0.9	0.9	1	0.9	1	1	1	1	1	1	1	1	1
	F	0.6	0.6	0.7	0.7	0.7	0.8	0.8	0.8	0.7	0.8	0.9	0.9	0.9	1	1	1	1	1	1	1
	C	0.7	0.6	0.8	0.7	0.9	0.8	0.9	0.8	0.9	0.8	1	0.9	1	1	1	1	1	1	1	1
800	E	0.7	0.7	0.8	0.9	0.9	0.9	0.9	1	0.9	1	1	1	1	1	1	1	1	1	1	1
	F	0.7	0.7	0.8	0.8	0.9	0.9	0.9	0.9	0.9	0.9	1	1	1	1	1	1	1	1	1	1
	C	0.5	0.5	0.6	0.6	0.7	0.7	0.8	0.7	0.8	0.8	0.9	0.8	0.9	0.9	1	0.9	1	1	1	1
1000	E	0.7	0.7	0.7	0.8	0.8	0.8	0.8	0.9	0.8	0.8	0.9	0.9	1	1	1	1	1	1	1	1
	F	0.8	0.7	0.9	0.7	0.9	0.8	1	0.9	1	0.9	1	1	1	1	1	1	1	1	1	1
	C	0.5	0.5	0.5	0.6	0.5	0.6	0.5	0.7	0.5	0.7	0.5	0.8	0.5	0.8	0.5	0.8	0.5	0.9	0.6	0.9
1250	E	0.9	0.8	1	0.9	1	1	1	1	1	1	1	1	1	1	1	1	1	1	1	1
	F	0.7	0.7	0.8	0.7	0.9	0.8	0.9	0.8	0.9	0.8	1	0.9	1	0.9	1	1	1	1	1	1
	C	0.6	0.7	0.6	0.8	0.6	0.9	0.7	0.9	0.8	0.9	0.8	1	0.8	1	0.9	1	0.9	1	1	1
1600	E	0.9	0.8	1	0.9	1	1	1	1	1	1	1	1	1	1	1	1	1	1	1	1
	F	0.6	0.6	0.6	0.6	0.6	0.7	0.6	0.7	0.5	0.6	0.7	0.8	0.7	0.8	0.8	0.9	0.8	1	0.9	1
	C	0.6	0.6	0.6	0.6	0.7	0.7	0.7	0.7	0.8	0.7	0.8	0.8	0.9	0.8	0.9	0.9	1	0.9	1	1
2000	E	0.9	0.8	1	0.9	1	0.9	1	1	1	1	1	1	1	1	1	1	1	1	1	1
	F	0.5	0.6	0.5	0.6	0.6	0.7	0.6	0.7	0.4	0.6	0.6	0.8	0.7	0.9	0.7	0.9	0.8	1	0.8	1
	C	0.5	0.6	0.5	0.7	0.5	0.7	0.5	0.7	0.6	0.8	0.6	0.8	0.7	0.8	0.7	0.9	0.8	0.9	0.9	1
2500	E	0.9	0.8	1	0.9	1	1	1	1	1	1	1	1	1	1	1	1	1	1	1	1
	F	0.5	0.5	0.5	0.5	0.4	0.5	0.4	0.5	0.4	0.5	0.4	0.5	0.3	0.6	0.3	0.6	0.2	0.6	0.1	0.8
	C	0.5	0.6	0.5	0.6	0.6	0.7	0.6	0.7	0.5	0.7	0.7	0.8	0.7	0.9	0.7	0.9	0.8	0.9	0.9	1
3150	E	0.8	0.7	0.9	0.8	1	0.9	1	1	1	1	1	1	1	1	1	1	1	1	1	1
	F	0.6	0.6	0.7	0.8	0.8	0.9	0.8	0.9	0.8	0.9	0.9	1	1	1	1	1	1	1	1	1
	C	0.7	0.7	0.8	0.8	0.8	0.8	0.9	0.9	0.9	0.9	1	1	1	1	1	1	1	1	1	1
4000	E	0.9	0.7	1	0.9	1	0.9	1	1	1	1	1	1	1	1	1	1	1	1	1	1
	F	0.5	0.5	0.5	0.6	0.5	0.6	0.5	0.6	0.5	0.6	0.5	0.6	0.5	0.7	0.5	0.7	0.5	0.8	0.5	0.9
	C	0.6	0.6	0.6	0.7	0.7	0.8	0.7	0.8	0.9	0.9	0.8	0.9	0.8	1	0.9	1	0.9	1	1	1
5000	E	0.7	0.7	0.8	0.8	0.9	0.9	0.9	0.9	0.9	0.9	1	1	1	1	1	1	1	1	1	1
	F	0.5	0.5	0.5	0.5	0.5	0.4	0.4	0.4	0.4	0.4	0.3	0.4	0.3	0.3	0.2	0.3	0.2	0.2	0.1	0.1
	C	0.6	0.6	0.6	0.7	0.7	0.7	0.8	0.8	0.8	0.8	0.8	0.9	0.9	0.9	0.9	1	1	1	1	1
Avg	E	0.7	0.7	0.8	0.8	0.8	0.8	0.9	0.9	0.9	0.9	0.9	0.9	0.9	0.9	1	1	1	1	1	1
	F	0.6	0.6	0.7	0.7	0.7	0.7	0.7	0.8	0.7	0.7	0.8	0.8	0.8	0.9	0.8	0.9	0.8	0.9	0.8	0.9
	C	0.6	0.6	0.6	0.7	0.7	0.7	0.7	0.8	0.7	0.8	0.8	0.8	0.8	0.8	0.8	0.9	0.8	0.9	0.8	0.9

TABLE 3.6. Probabilities for lower standard deviations of T_{60} using a given number of u^2 or ED positions, vs. 12 p^2 positions, in the classroom.

f		$P(\sigma_{x(n)} < \sigma_{p(12)})$																			
(Hz)	n	2		3		4		5		6		7		8		9		10		11	
	x	U	ED	U	ED	U	ED	U	ED	U	ED	U	ED	U	ED	U	ED	U	ED	U	ED
100	E	0.7	0.6	0.6	0.5	0.5	0.5	0.4	0.4	0.3	0.4	0.4	0.3	0.3	0.3	0.3	0.3	0.2	0.2	0.1	0.1
	F	0.9	0.9	0.9	0.9	0.9	0.9	1	1	1	0.9	1	1	1	1	1	1	1	1	1	1
	C	0.8	0.7	0.8	0.8	0.8	0.9	0.8	1	0.8	1	1	1	1	1	1	1	1	1	1	1
125	E	0.7	0.7	0.7	0.8	0.7	0.7	0.7	0.7	0.6	0.7	0.6	0.7	0.7	0.8	0.7	1	0.9	1	1	1
	F	0.5	0.6	0.4	0.6	0.4	0.5	0.2	0.4	0.2	0.4	0.1	0.4	0.1	0.3	0	0.3	0	0.3	0	0.2
	C	0.9	1	0.9	1	1	1	1	1	1	1	1	1	1	1	1	1	1	1	1	1
160	E	0.7	0.6	0.7	0.6	0.7	0.5	0.6	0.5	0.5	0.4	0.4	0.4	0.3	0.3	0.3	0.3	0.2	0.2	0.1	0.1
	F	1	0.9	1	1	1	1	1	1	1	1	1	1	1	1	1	1	1	1	1	1
	C	0.8	0.9	0.7	0.8	0.7	0.9	0.8	1	0.8	1	0.7	1	0.9	1	1	1	1	1	1	1
200	E	0.7	0.7	0.6	0.6	0.6	0.6	0.6	0.5	0.5	0.4	0.4	0.4	0.3	0.3	0.3	0.3	0.2	0.2	0.1	0.1
	F	0.8	0.9	0.8	0.9	0.9	1	1	1	1	1	1	1	1	1	1	1	1	1	1	1
	C	1	1	1	1	1	1	1	1	1	1	1	1	1	1	1	1	1	1	1	1
250	E	1	1	1	1	1	1	1	1	1	1	1	1	1	1	1	1	1	1	1	1
	F	0.6	0.8	0.6	0.8	0.5	0.8	0.4	0.8	0.6	0.9	0.4	0.9	0.3	1	0.3	1	0.2	1	0.1	1
	C	1	1	1	1	1	1	1	1	1	1	1	1	1	1	1	1	1	1	1	1
315	E	0.7	0.9	0.8	1	0.9	1	0.9	1	0.9	1	1	1	1	1	1	1	1	1	1	1
	F	0.7	0.7	0.6	0.7	0.6	0.7	0.6	0.7	0.7	0.8	0.6	0.8	0.7	0.9	0.7	1	0.8	1	1	1
	C	0.9	0.8	1	0.9	1	1	1	1	1	1	1	1	1	1	1	1	1	1	1	1
400	E	0.7	0.8	0.6	0.9	0.6	0.9	0.6	0.9	0.5	1	0.6	1	0.6	1	0.5	1	0.6	1	0.6	1
	F	0.9	0.9	1	0.9	1	1	1	1	1	1	1	1	1	1	1	1	1	1	1	1
	C	1	0.8	1	0.9	1	1	1	1	1	1	1	1	1	1	1	1	1	1	1	1
500	E	0.9	0.9	1	1	1	1	1	1	1	1	1	1	1	1	1	1	1	1	1	1
	F	1	0.9	1	1	1	1	1	1	1	1	1	1	1	1	1	1	1	1	1	1
	C	0.7	0.8	0.8	0.8	0.7	0.8	0.6	0.8	0.5	0.7	0.5	1	0.6	1	0.7	1	1	1	1	1
630	E	0.8	0.7	0.9	0.8	0.9	1	0.9	1	1	1	1	1	1	1	1	1	1	1	1	1
	F	0.7	0.8	0.6	0.8	0.6	0.9	0.6	0.8	0.5	0.8	0.4	1	0.3	1	0.3	1	0.2	1	0.2	1
	C	0.6	0.6	0.4	0.6	0.3	0.5	0.2	0.4	0.2	0.3	0.1	0.4	0.1	0.3	0	0.4	0	0.3	0	0.2
800	E	0.7	0.6	0.7	0.7	0.6	0.7	0.6	0.7	0.8	0.8	0.7	0.8	0.7	0.8	0.8	0.8	0.8	1	1	1
	F	0.9	0.9	0.9	1	1	1	1	1	1	1	1	1	1	1	1	1	1	1	1	1
	C	0.7	0.8	0.7	0.8	0.6	0.8	0.6	0.9	0.6	0.9	0.7	1	0.7	1	0.8	1	1	1	1	1
1000	E	0.7	0.8	0.6	0.8	0.5	1	0.5	1	0.5	1	0.5	1	0.5	1	0.5	1	0.5	1	0.7	1
	F	0.8	0.9	1	0.9	1	0.9	1	1	1	1	1	1	1	1	1	1	1	1	1	1
	C	0.7	0.7	0.7	0.8	0.7	0.7	0.7	0.7	0.6	0.6	0.7	0.7	0.6	0.7	0.6	0.9	0.8	1	1	1
1250	E	0.7	0.8	0.7	0.7	0.7	0.7	0.6	0.8	0.5	0.7	0.4	0.8	0.3	0.9	0.3	1	0.2	1	0.1	1
	F	0.9	0.8	0.8	0.8	1	0.9	1	0.9	1	1	1	1	1	1	1	1	1	1	1	1
	C	0.8	0.8	0.7	0.8	0.7	0.9	0.7	0.9	0.7	0.9	0.7	1	0.8	1	0.9	1	1	1	1	1
1600	E	0.5	0.6	0.3	0.5	0.2	0.5	0.2	0.4	0.2	0.4	0.1	0.2	0.1	0.2	0	0.2	0	0.2	0	0.1
	F	0.8	0.8	0.8	0.8	0.8	0.8	0.9	0.9	1	0.9	1	1	1	1	1	1	1	1	1	1
	C	0.7	0.7	0.6	0.7	0.6	0.6	0.6	0.6	0.6	0.7	0.6	0.6	0.5	0.6	0.6	0.6	0.6	0.7	0.6	1
2000	E	0.7	0.8	0.7	0.9	0.6	1	0.6	1	0.5	1	0.4	1	0.3	1	0.3	1	0.2	1	0.1	1
	F	0.9	0.9	1	0.9	1	1	1	1	1	1	1	1	1	1	1	1	1	1	1	1
	C	0.7	0.8	0.7	0.8	0.7	0.8	0.8	0.8	0.8	0.8	0.7	0.9	0.8	1	1	1	1	1	1	1
2500	E	0.6	0.6	0.4	0.5	0.4	0.4	0.3	0.5	0.4	0.4	0.2	0.3	0.2	0.2	0.1	0.3	0	0.2	0	0.1
	F	0.8	0.8	0.9	0.9	0.9	0.9	0.9	0.9	0.9	1	1	1	1	1	1	1	1	1	1	1
	C	0.9	0.8	0.9	0.8	1	0.8	1	0.9	1	0.8	1	1	1	1	1	1	1	1	1	1
3150	E	0.7	0.6	0.6	0.6	0.5	0.5	0.5	0.5	0.5	0.4	0.4	0.4	0.3	0.3	0.3	0.3	0.2	0.2	0.1	0.1
	F	0.7	0.7	0.8	0.5	0.8	0.5	0.7	0.5	0.8	0.5	0.8	0.4	0.9	0.4	1	0.4	1	0.3	1	0.3
	C	1	0.8	1	0.8	1	0.9	1	1	1	1	1	1	1	1	1	1	1	1	1	1
4000	E	0.5	0.5	0.5	0.4	0.4	0.3	0.3	0.2	0.3	0.3	0.2	0.1	0.2	0.1	0.1	0.1	0	0	0.1	0
	F	0.8	0.8	0.8	0.8	0.7	0.8	0.7	0.8	0.8	0.9	0.9	1	1	1	1	1	1	1	1	1
	C	0.7	0.7	0.7	0.7	0.7	0.6	0.7	0.6	0.7	0.5	0.8	0.4	0.8	0.4	1	0.3	1	0.2	1	0.2
5000	E	0.5	0.5	0.5	0.3	0.3	0.2	0.2	0.2	0.2	0.1	0.2	0.1	0.1	0.1	0	0	0	0	0	0
	F	0.8	0.8	0.9	0.9	1	1	1	1	1	1	1	1	1	1	1	1	1	1	1	1
	C	0.9	0.9	0.9	0.9	1	1	1	1	1	1	1	1	1	1	1	1	1	1	1	1
Avg	E	0.7	0.7	0.7	0.7	0.6	0.7	0.6	0.7	0.6	0.7	0.5	0.6	0.5	0.6	0.5	0.6	0.5	0.6	0.5	0.6
	F	0.8	0.8	0.8	0.8	0.8	0.9	0.8	0.9	0.9	0.9	0.8	0.9	0.8	0.9	0.8	0.9	0.8	0.9	0.8	0.9
	C	0.8	0.8	0.8	0.8	0.8	0.8	0.8	0.9	0.8	0.8	0.8	0.9	0.8	0.9	0.9	0.9	0.9	0.9	0.9	0.9

TABLE 3.7. Probabilities for lower standard deviations of T_{60} using a given number of u^2 or ED positions, vs. the same number of p^2 positions, in the classroom.

f		$P(\sigma_{x(n)} < \sigma_{p(n)})$																			
(Hz)	n	2		3		4		5		6		7		8		9		10		11	
	x	U	ED	U	ED	U	ED	U	ED	U	ED	U	ED	U	ED	U	ED	U	ED	U	ED
100	E	0.5	0.5	0.5	0.4	0.4	0.4	0.4	0.4	0.3	0.3	0.3	0.3	0.3	0.2	0.2	0.2	0.1	0.1	0.1	0.1
	F	0.6	0.6	0.7	0.7	0.7	0.7	0.8	0.8	0.8	0.8	0.8	0.8	0.9	0.9	0.9	0.9	1	1	1	1
	C	0.5	0.6	0.6	0.6	0.6	0.7	0.7	0.7	0.7	0.7	0.8	0.8	0.8	0.9	0.9	0.9	0.9	1	1	1
125	E	0.5	0.6	0.5	0.6	0.6	0.6	0.6	0.6	0.7	0.7	0.6	0.7	0.7	0.8	0.7	0.8	0.8	0.9	0.9	0.9
	F	0.4	0.4	0.3	0.4	0.3	0.4	0.3	0.4	0.2	0.4	0.2	0.4	0.2	0.4	0.1	0.3	0	0.2	0	0.1
	C	0.7	0.8	0.8	0.9	0.8	1	0.9	1	1	1	1	1	1	1	1	1	1	1	1	1
160	E	0.4	0.4	0.4	0.4	0.4	0.4	0.4	0.3	0.3	0.3	0.3	0.3	0.3	0.2	0.2	0.2	0.1	0.1	0.1	0.1
	F	0.8	0.8	0.9	0.9	1	0.9	1	1	1	1	1	1	1	1	1	1	1	1	1	1
	C	0.5	0.6	0.5	0.6	0.5	0.7	0.6	0.7	0.6	0.8	0.6	0.8	0.7	0.8	0.7	0.8	0.8	0.9	0.9	0.9
200	E	0.5	0.5	0.6	0.5	0.5	0.5	0.5	0.5	0.4	0.4	0.4	0.4	0.3	0.3	0.2	0.2	0.2	0.2	0.1	0.1
	F	0.7	0.7	0.7	0.8	0.8	0.8	0.8	0.9	0.8	0.9	0.9	1	1	1	1	1	1	1	1	1
	C	0.8	0.7	0.9	0.8	1	0.9	1	0.9	1	0.9	1	1	1	1	1	1	1	1	1	1
250	E	0.8	0.7	0.9	0.8	1	0.9	1	0.9	1	0.9	1	1	1	1	1	1	1	1	1	1
	F	0.5	0.7	0.5	0.7	0.5	0.7	0.4	0.7	0.5	0.8	0.3	0.8	0.3	0.9	0.2	0.9	0.2	1	0.1	1
	C	0.8	0.7	0.9	0.8	1	0.9	1	0.9	1	1	1	1	1	1	1	1	1	1	1	1
315	E	0.6	0.7	0.7	0.8	0.7	0.9	0.7	0.9	0.7	1	0.8	1	0.9	1	0.9	1	1	1	1	1
	F	0.5	0.6	0.5	0.6	0.5	0.6	0.5	0.6	0.5	0.7	0.6	0.7	0.6	0.7	0.6	0.8	0.7	0.9	0.8	0.9
	C	0.6	0.6	0.6	0.6	0.7	0.7	0.7	0.7	0.6	0.6	0.9	0.8	0.9	0.9	0.9	0.9	1	0.9	1	1
400	E	0.5	0.6	0.5	0.7	0.5	0.8	0.5	0.8	0.6	0.9	0.6	0.9	0.6	1	0.6	1	0.6	1	0.7	1
	F	0.6	0.6	0.7	0.7	0.8	0.8	0.8	0.8	0.9	0.9	0.9	0.9	1	1	1	1	1	1	1	1
	C	0.7	0.6	0.8	0.7	0.8	0.7	0.9	0.8	0.9	0.8	1	0.9	1	0.9	1	1	1	1	1	1
500	E	0.6	0.7	0.7	0.8	0.7	0.8	0.8	0.9	0.7	0.8	0.9	0.9	0.9	1	1	1	1	1	1	1
	F	0.7	0.7	0.8	0.8	0.8	0.8	0.9	0.9	0.9	0.9	1	0.9	1	1	1	1	1	1	1	1
	C	0.6	0.6	0.6	0.7	0.6	0.7	0.6	0.8	0.5	0.7	0.6	0.9	0.7	0.9	0.7	1	0.8	1	0.9	1
630	E	0.6	0.6	0.7	0.6	0.8	0.7	0.8	0.8	0.8	0.8	0.9	0.9	1	0.9	1	1	1	1	1	1
	F	0.6	0.6	0.6	0.7	0.5	0.7	0.5	0.7	0.4	0.6	0.4	0.8	0.4	0.9	0.4	0.9	0.3	0.9	0.3	1
	C	0.4	0.5	0.4	0.5	0.3	0.5	0.3	0.4	0.2	0.3	0.2	0.4	0.1	0.4	0.1	0.3	0	0.3	0	0.2
800	E	0.5	0.5	0.6	0.6	0.6	0.6	0.6	0.6	0.7	0.7	0.7	0.7	0.7	0.7	0.7	0.8	0.8	0.8	0.9	0.9
	F	0.6	0.7	0.7	0.8	0.8	0.9	0.9	1	0.9	1	1	1	1	1	1	1	1	1	1	1
	C	0.6	0.6	0.6	0.6	0.6	0.7	0.6	0.8	0.5	0.7	0.7	0.9	0.7	0.9	0.8	0.9	0.8	1	1	1
1000	E	0.5	0.6	0.5	0.6	0.5	0.7	0.5	0.8	0.5	0.8	0.5	0.9	0.5	0.9	0.6	0.9	0.6	1	0.7	1
	F	0.6	0.6	0.7	0.7	0.8	0.8	0.8	0.8	0.9	0.9	0.9	0.9	1	0.9	1	1	1	1	1	1
	C	0.5	0.6	0.6	0.6	0.6	0.6	0.6	0.6	0.5	0.6	0.6	0.7	0.6	0.7	0.7	0.8	0.8	0.9	0.9	0.9
1250	E	0.6	0.6	0.6	0.6	0.6	0.6	0.5	0.6	0.5	0.6	0.4	0.7	0.3	0.7	0.2	0.8	0.2	0.8	0.1	0.9
	F	0.7	0.6	0.7	0.7	0.8	0.7	0.9	0.8	0.9	0.8	0.9	0.9	1	0.9	1	1	1	1	1	1
	C	0.4	0.5	0.4	0.5	0.4	0.6	0.5	0.6	0.6	0.7	0.6	0.7	0.7	0.7	0.7	0.8	0.8	0.9	0.9	0.9
1600	E	0.4	0.4	0.3	0.4	0.2	0.4	0.2	0.3	0.2	0.3	0.1	0.3	0.1	0.2	0	0.2	0	0.1	0	0.1
	F	0.6	0.6	0.7	0.7	0.7	0.7	0.8	0.8	0.8	0.8	0.9	0.9	0.9	0.9	1	0.9	1	1	1	1
	C	0.5	0.5	0.5	0.5	0.5	0.6	0.6	0.6	0.5	0.5	0.6	0.6	0.6	0.6	0.6	0.6	0.6	0.7	0.7	0.8
2000	E	0.5	0.6	0.5	0.7	0.5	0.8	0.5	0.8	0.4	0.8	0.4	0.9	0.3	0.9	0.2	1	0.2	1	0.1	1
	F	0.7	0.7	0.8	0.7	0.9	0.8	0.9	0.8	0.9	0.9	1	0.9	1	1	1	1	1	1	1	1
	C	0.5	0.6	0.6	0.7	0.7	0.7	0.7	0.8	0.7	0.8	0.8	0.9	0.8	0.9	0.9	1	1	1	1	1
2500	E	0.4	0.5	0.4	0.4	0.3	0.4	0.3	0.4	0.3	0.3	0.2	0.3	0.2	0.2	0.1	0.2	0.1	0.1	0.1	0.1
	F	0.6	0.6	0.7	0.7	0.8	0.7	0.8	0.8	0.9	0.9	0.9	0.9	0.9	0.9	1	1	1	1	1	1
	C	0.6	0.6	0.7	0.7	0.7	0.7	0.8	0.7	0.8	0.7	0.9	0.8	0.9	0.8	1	0.9	1	0.9	1	1
3150	E	0.5	0.5	0.5	0.4	0.5	0.4	0.4	0.4	0.4	0.3	0.3	0.3	0.3	0.3	0.2	0.2	0.2	0.1	0.1	0.1
	F	0.6	0.5	0.6	0.5	0.7	0.5	0.7	0.5	0.7	0.4	0.8	0.4	0.8	0.4	0.9	0.4	0.9	0.4	1	0.3
	C	0.7	0.6	0.8	0.6	0.9	0.7	0.9	0.7	0.9	0.8	1	0.8	1	0.9	1	0.9	1	0.9	1	1
4000	E	0.4	0.4	0.4	0.4	0.3	0.3	0.3	0.3	0.3	0.3	0.2	0.2	0.2	0.1	0.1	0.1	0.1	0	0	0
	F	0.6	0.6	0.6	0.6	0.6	0.7	0.7	0.7	0.7	0.8	0.7	0.8	0.8	0.8	0.8	0.9	0.9	0.9	0.9	1
	C	0.6	0.5	0.6	0.6	0.6	0.5	0.6	0.5	0.7	0.6	0.7	0.5	0.7	0.4	0.8	0.4	0.9	0.3	0.9	0.2
5000	E	0.4	0.4	0.3	0.3	0.3	0.2	0.3	0.2	0.2	0.1	0.2	0.1	0.1	0.1	0.1	0	0	0	0	0
	F	0.6	0.6	0.7	0.6	0.7	0.7	0.7	0.7	0.8	0.8	0.8	0.8	0.9	0.8	0.9	0.9	0.9	0.9	1	1
	C	0.7	0.6	0.8	0.7	0.8	0.8	0.9	0.9	0.9	0.9	1	1	1	1	1	1	1	1	1	1
Avg	E	0.5	0.5	0.5	0.6	0.5	0.6	0.5	0.6	0.5	0.6	0.5	0.6	0.5	0.6	0.5	0.6	0.5	0.6	0.5	0.5
	F	0.6	0.6	0.7	0.7	0.7	0.7	0.7	0.8	0.7	0.8	0.8	0.8	0.8	0.8	0.8	0.9	0.8	0.9	0.8	0.9
	C	0.6	0.6	0.6	0.7	0.7	0.7	0.7	0.7	0.7	0.7	0.8	0.8	0.8	0.8	0.8	0.8	0.8	0.9	0.9	0.9

3.2 Absorption Coefficients

The sound absorption for both test materials were calculated according to the procedures outlined in ISO 354, which are highlighted in chapter 2. The surface area of the planar fiberglass insulation absorber, including the edges, was 10.65 m^2 for the large chamber, 6.11 m^2 for the small chamber, and 9.54 m^2 for the classroom. Calculations were obtained from impulse responses for 12 positions. From the T_{60} results, it was shown that half of the number of ED positions was sufficient to obtain comparable results with p^2. Thus, six u^2 and ED positions were randomly chosen for calculation of the absorption coefficients. Figures 3.23 through 3.25 show the absorption coefficient α_s results obtained in the large chamber, small chamber, and classroom. According to ISO 9613-1, the accuracy of the calculated pure-tone attenuation coefficient α is estimated to be ± 10% for atmospheric variables within these ranges: 0.05% to 5% for molar concentration of water vapor, -20 ºC to 50 ºC for air temperature, and less than 200 kPa for atmospheric pressure.[26] The 10 % accuracy window was calculated based on α obtained from squared pressure measurements. In other words, the window is calculated from the values 1.1α and 0.9α.

It can be seen that the similarities in T_{60} for each energy quantity extend to the absorption coefficient measurements. That is, for each room, the results will be very similar no matter which quantity is used. Based on smaller variations of T_{60} for both u^2 and ED, fewer positions could be used to obtain the same absorption coefficients. In this case, the number was reduced by one-half. The large and small chamber measurements are very similar, with some differences at lower frequencies. It is very apparent that results obtained in the classroom are not accurate. The data from the T_{60} measurements

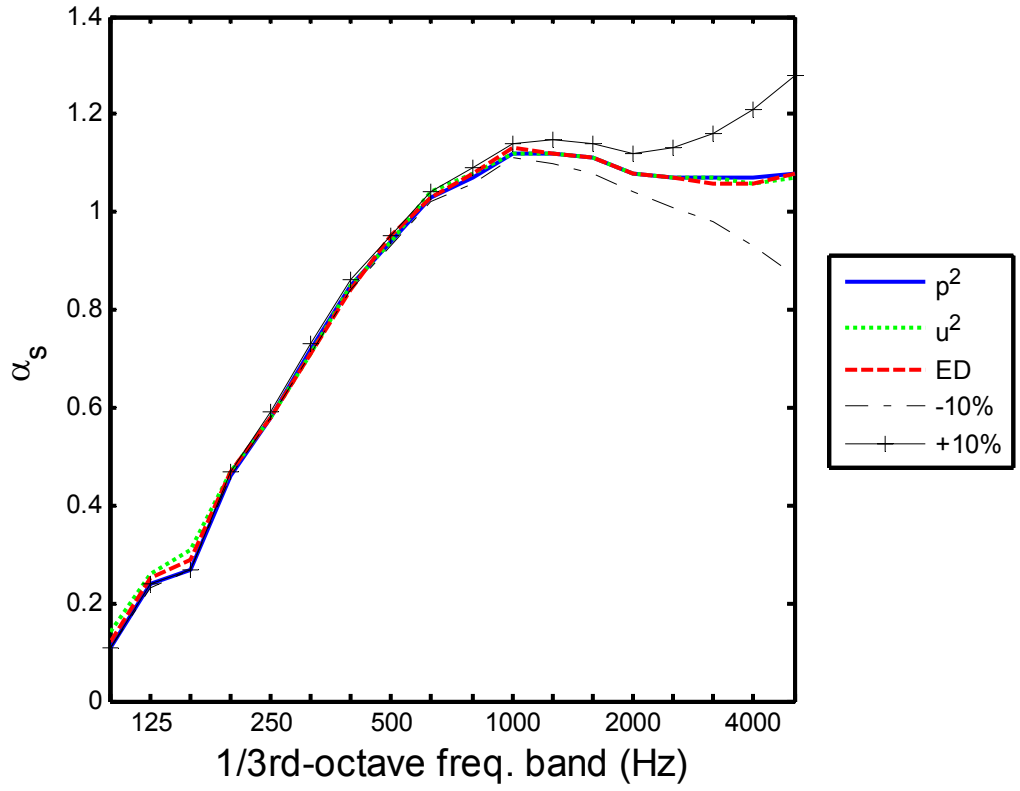

FIG. 3.23. Measured absorption coefficients of 5 cm fiberglass in the large chamber.

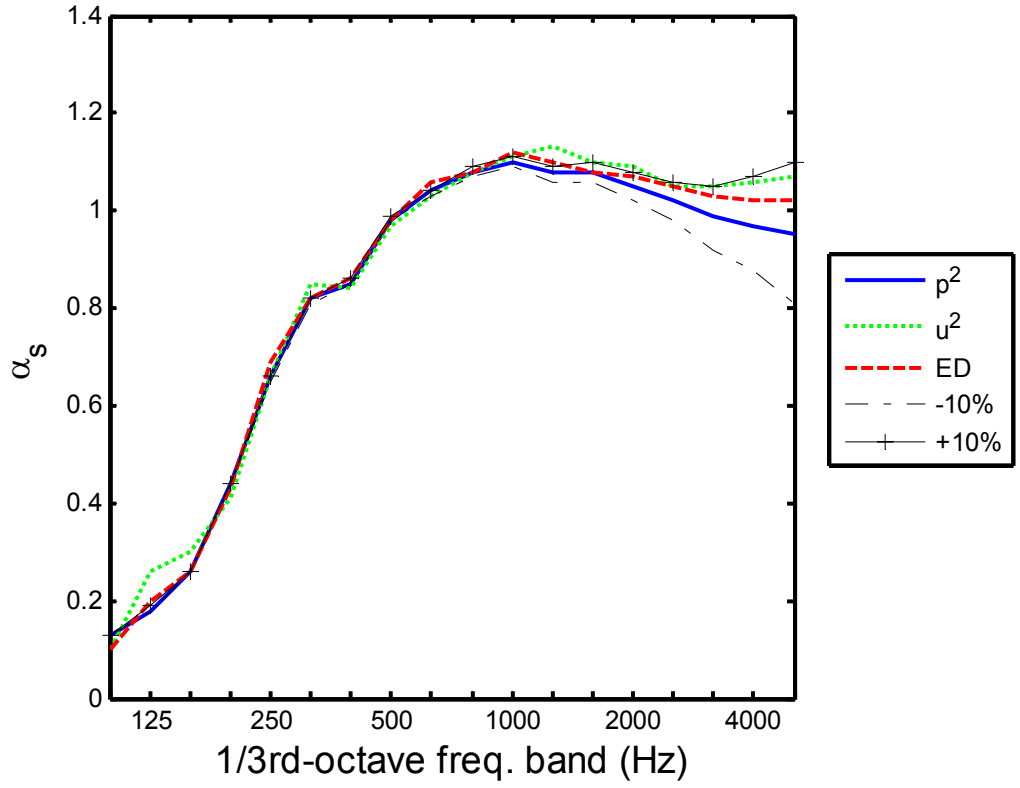

FIG. 3.24. Measured absorption coefficients of 5 cm fiberglass in the small chamber.

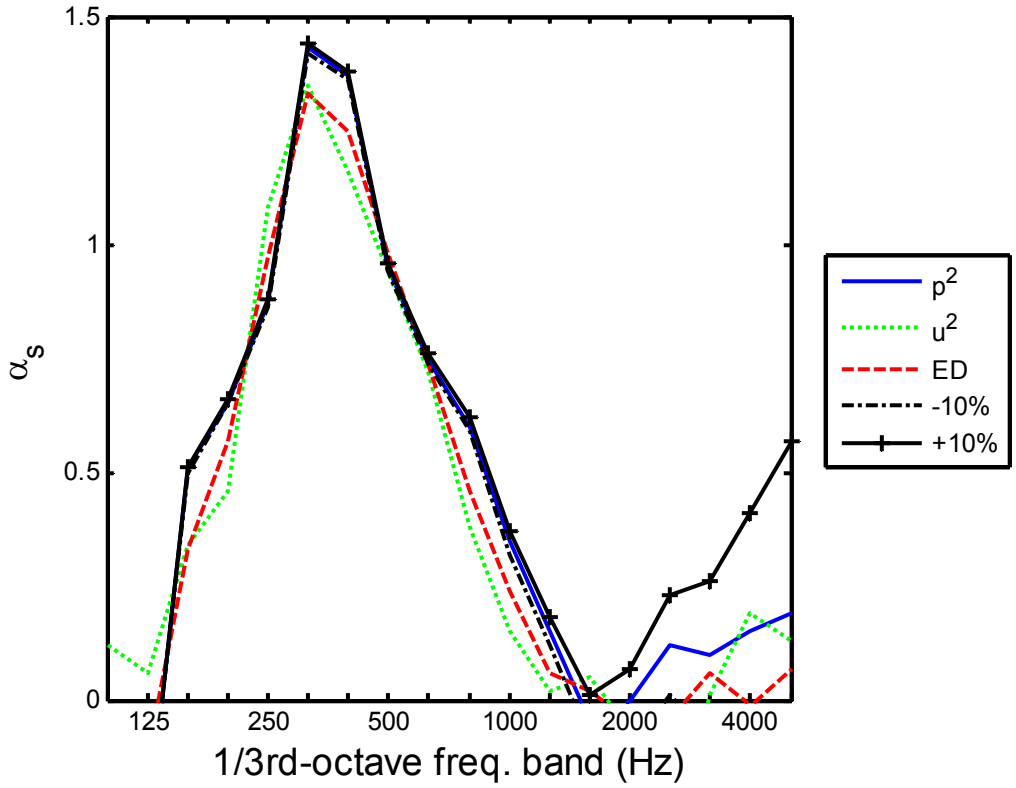

FIG. 3.25. Measured absorption coefficients of 5 cm fiberglass in the classroom.

of the classroom listed in Table 3.1 show that spatial variation is not really the cause. Two possibilities for the inaccuracies are the lack of a diffuse field for all 1/3rd-octave frequency bands and insufficient change in total absorption when the test material is present. The fiberglass insulation was first placed on the floor, in the center of the carpeted room. The T_{60} values were similar at high frequencies in both the empty and occupied measurements. At these frequencies, the total absorption of the room was not affected appreciably by the covering of the carpet with the fiberglass. The measurement was performed again with 2 cm thick particle board covering the sample region on the carpentry for both the empty and occupied states. When the fiberglass insulation was put into the room, it rested on top of the fiberboard. The results were similar as shown in Fig. 3.26. A comparison of ratios of total absorption area with and without the test

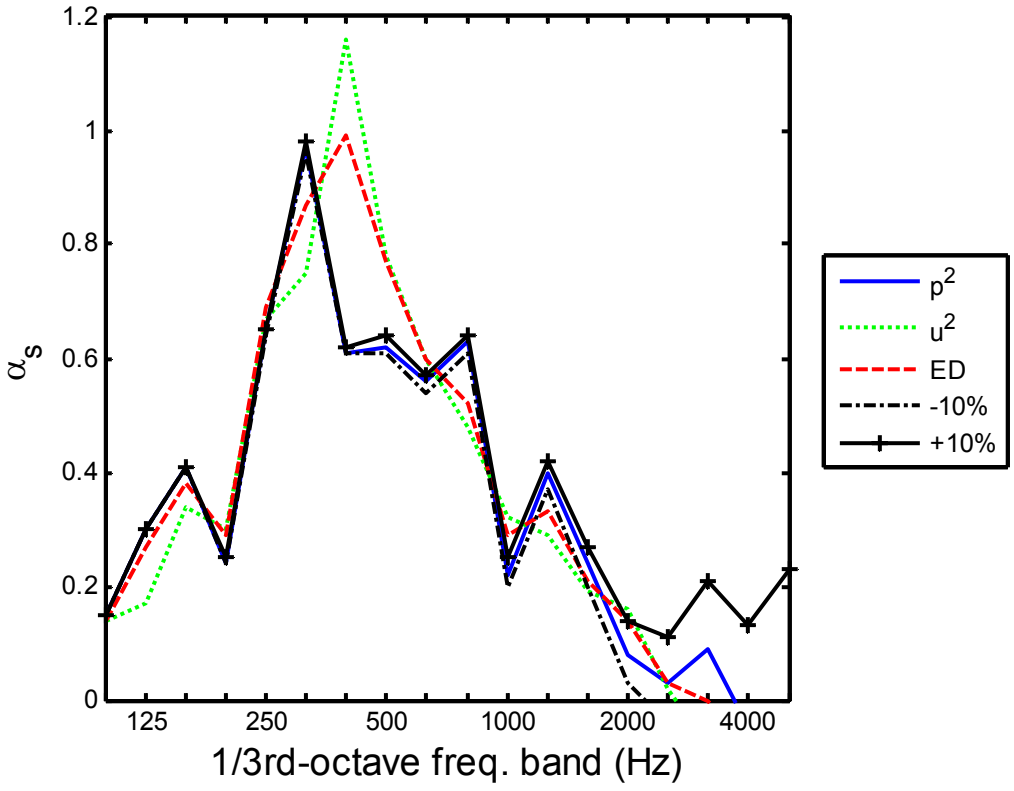

FIG. 3.26. Measured absorption coefficients of 5 cm fiberglass in the classroom with fiberboard.

material in the classroom shows that the percent increase of the total absorption area when the test material was added was very small. When the test material was present, a maximum of 22% increase in total absorption area was observed. In comparison, the same test material positioned in both the large and small reverberation chambers yielded an absorption area increase of over 350%. Thus, the small change in absorption may be one reason for the inaccurate measurements in the classroom. Furthermore, because of the lack of diffusivity of the room, it cannot be assumed that energy incident at the receiver positions comes from all possible directions and with random phases. The results are admittedly inconclusive and require further investigation.

The second test sample was the three identical office chairs. The measured absorption coefficients for each field quantity are displayed in Figs. 3.27 through 3.29.

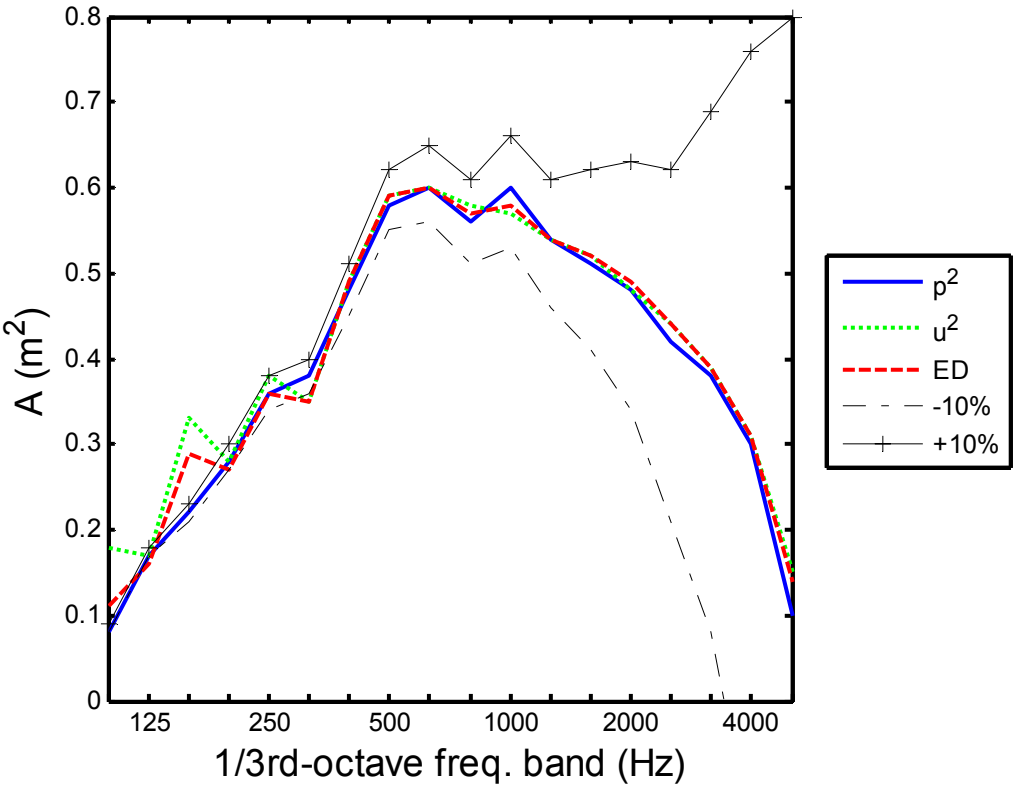

FIG. 3.27. Measured absorption coefficients of office chairs in the large chamber.

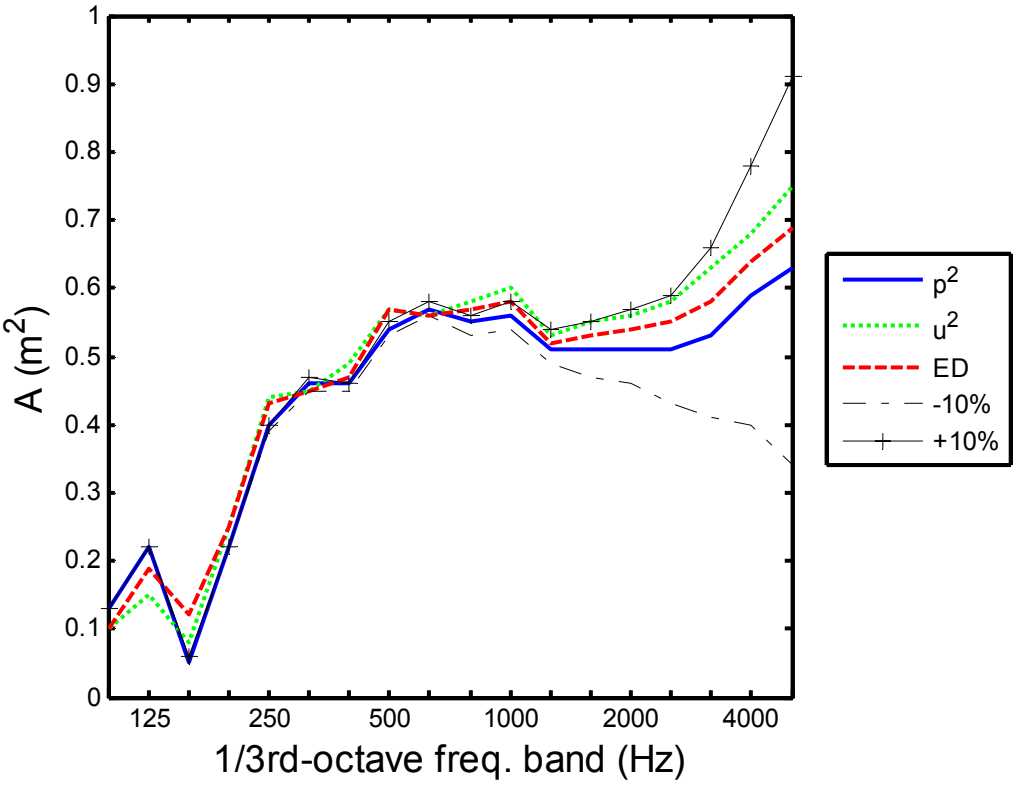

FIG. 3.28. Measured absorption coefficients of office chairs in the small chamber.

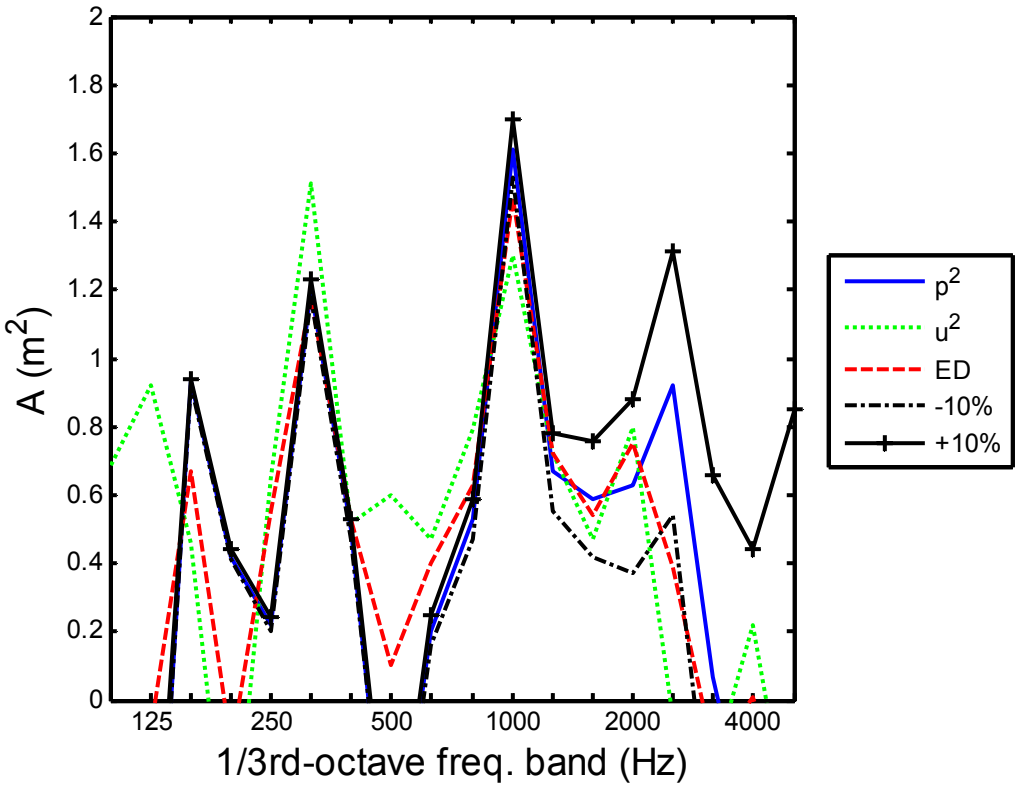

FIG. 3.29. Measured absorption coefficients of office chairs in the classroom.

The measurements taken in the small chamber were difficult due to the geometry of the room. Care was taken to allow sufficient space between the chairs as well as the room boundaries and microphones. However, the positioning was not ideal according to ISO 354 specifications. In other words, the chairs could not be adequately spaced from each other and still maintain enough distance from the room walls, diffusers, and microphones.

By comparison, the measured values at higher frequencies are much different in the small chamber versus the large chamber. It is unclear why such large differences exist. Inaccuracies due to atmospheric absorption are more significant at higher frequencies for larger chambers, but there seems to be something else that is causing this difference. It would seem that the data from the small chamber is more believable. Like

the measurements of fiberglass, the data from the classroom measurements is very inaccurate.

3.3 Sound Power

A Brüel and Kjaer 4204 Reference Sound Source was used for all sound power measurements. Six receiver positions and one source position were chosen in the large chamber and the classroom. The small chamber measurements consisted of two source positions and three receiver positions. The spatially averaged SPL, SVL, and SEDL values were obtained and used to determine the sound power of the source. Figure 3.30 shows the sound power measurements taken in the large chamber, with the standard deviations in Fig. 3.31. Measurements taken in the small chamber and classroom are shown in Figs. 3.32-3.35. Included in the standard deviation plots are the allowed

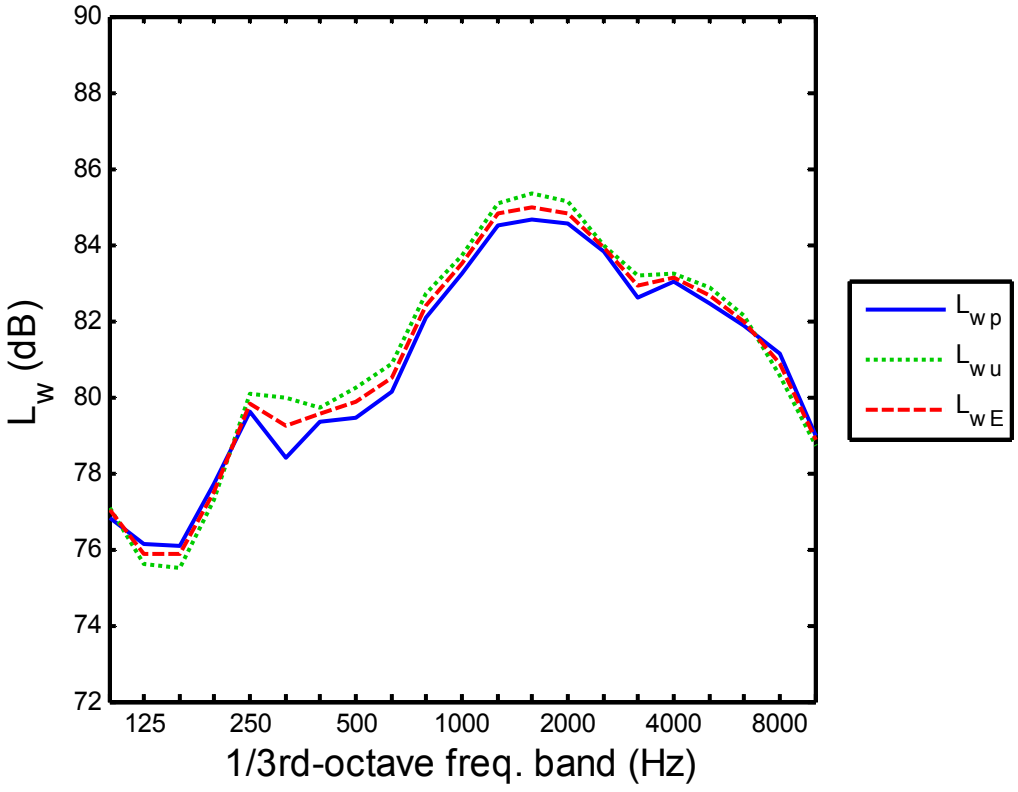

FIG. 3.30. Sound power measurements in the large chamber.

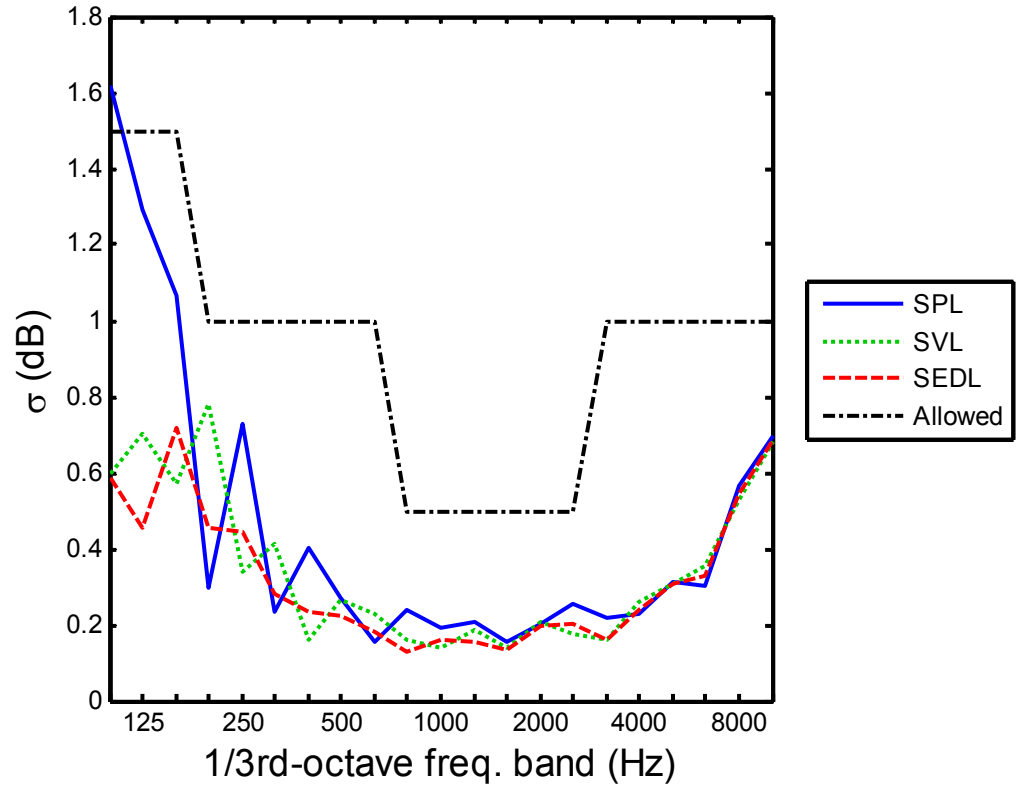

FIG. 3.31. Standard deviation of sound power measurements in the large chamber.

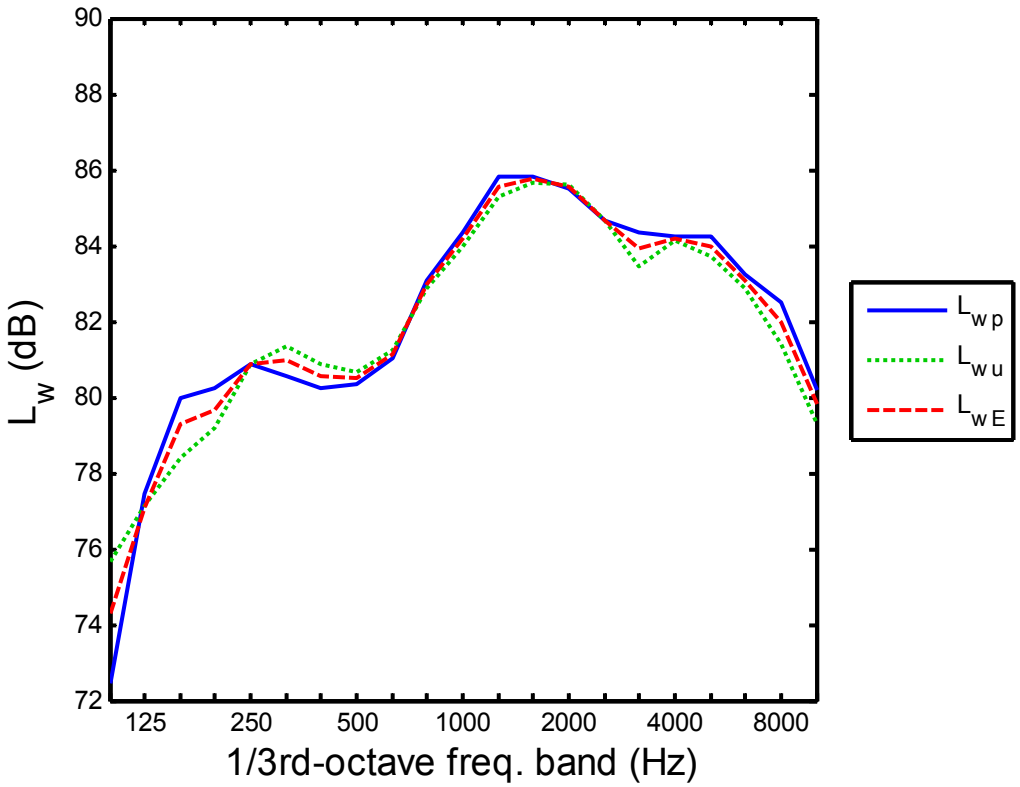

FIG. 3.32. Sound power measurements in the small chamber.

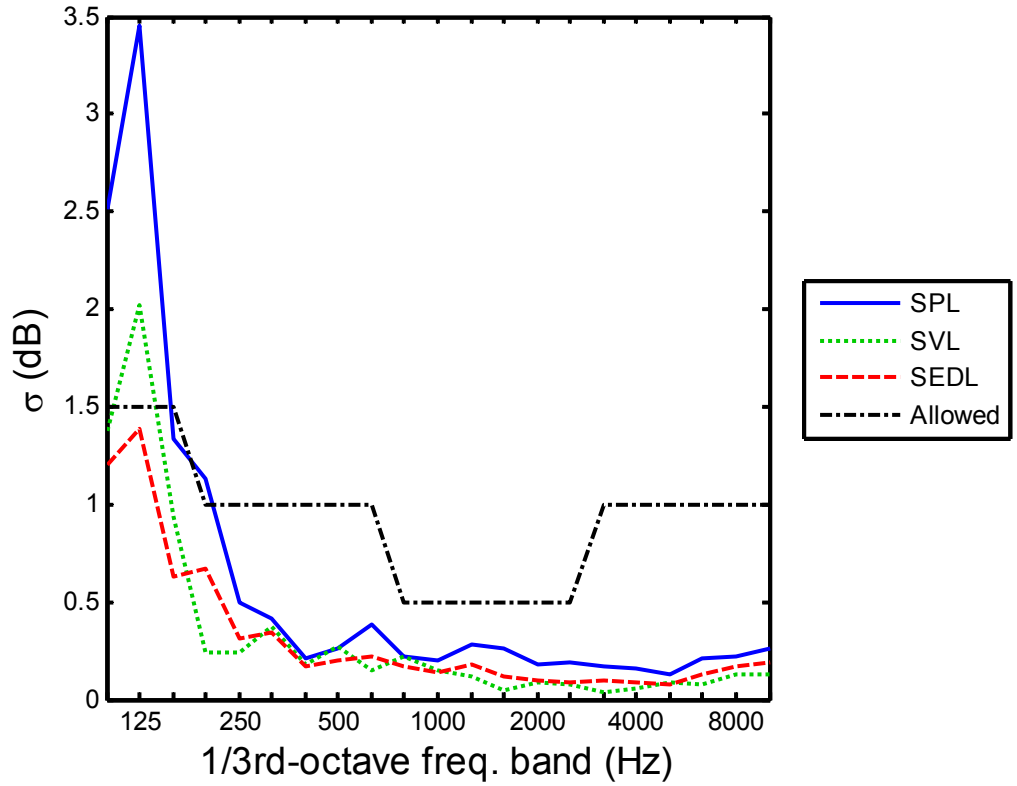

FIG. 3.33. Measured and allowed standard deviations of sound power in the small chamber.

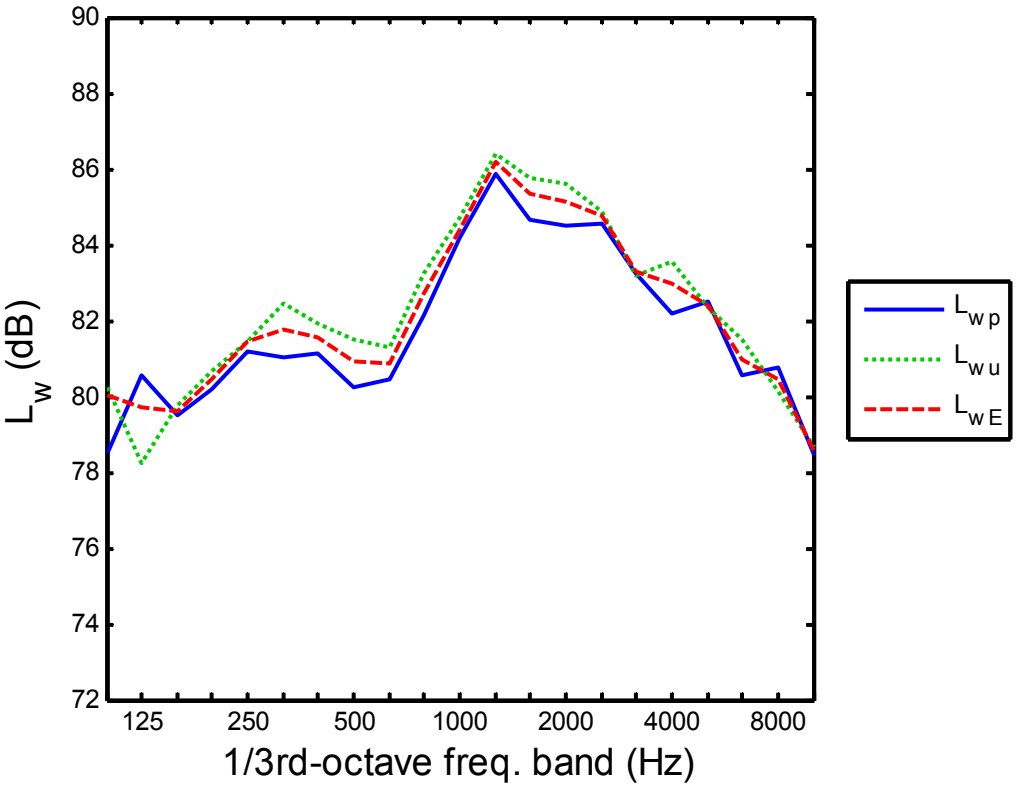

FIG. 3.34. Sound power measurements in the classroom.

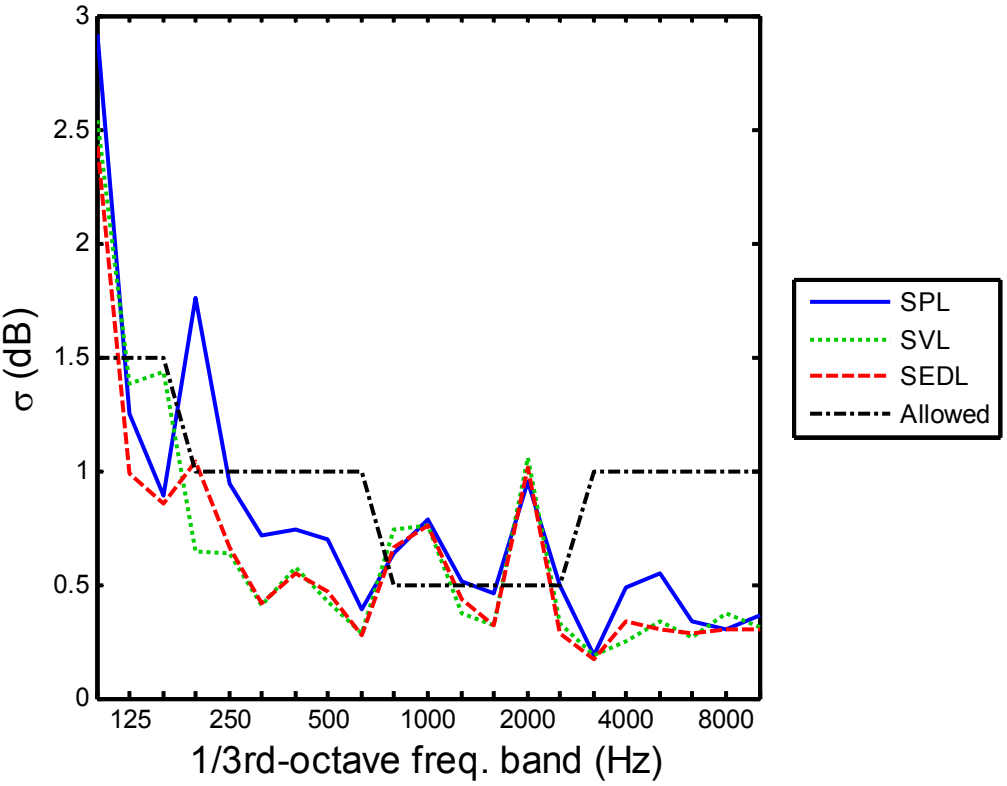

FIG. 3.35. Measured and allowed standard deviations of sound power in the classroom.

standard deviations according to ISO 3741. If the measured standard deviations exceed the allowed values, more source and/or receiver positions are necessary.

In all room measurements, the sound power levels obtained from SPL, SVL, and SEDL are similar for the same room. Measurements between different rooms show slight variations in the results. Of further interest are the standard deviations of the measured values. In the large chamber, the standard deviation of the sound power level determined by SPL exceeds the allowed deviation at the lower frequencies. As stated before, this problem is due to low modal overlap, and would likely be solved with the addition of low-frequency absorbers. Standard deviation of sound power values determined from SVL and SEDL perform much better at these lower frequencies. This suggests that the addition of low-frequency absorbers may not be necessary if sound power is determined

by particle velocity magnitude or ED instead of pressure.

Similar results in standard deviation are observed in the measurements taken in the small chamber. As expected, the standard deviation of the sound power level determined by SPL is poor at the lower frequencies. Standard deviations determined by SVL yield slightly better results. Surprisingly, the results from SEDL are outstanding at the lower frequencies. This suggests that ED measurements could be used to accurately calculate low-frequency sound power levels of sources in a smaller room with inadequate modal overlap.

Sound power measurements taken in the classroom were surprisingly more useful than sound absorption measurements taken in the same room. The results in Fig. 3.34 bear a strong resemblance to those in Figs. 3.30 and 3.32, from measurements in the two reverberation chambers. The performance of ED vs. pressure, shown in Fig. 3.35, is also encouraging. While the room is obviously not optimized for diffuse field measurements, the SEDL consistently has lower variation than SPL. The SVL measurements also perform in a pattern seen in other measurements; its variation is comparable to SEDL at higher frequencies, but a bit unpredictable at lower frequencies. The cause of the standard deviation peaks at 1 kHz and 2 kHz for all quantities is unknown. It is possibly due to background tonal noise present in the room. Although receiver positions were spaced at adequate distances, high variation in the 100 Hz band was observed. It was most likely caused by strong modal patterns which exist because of insufficient absorption and/or diffusers at that frequency band.

3.4 Conclusions

Based on the observations in a qualified reverberation chamber, ED measurements provide a more accurate way to measure T_{60} than traditional p^2 measurements. This observation extended to other rooms as well. For frequencies above the Schroeder frequency, the number of ED measurements necessary is about half the required number of p^2 measurements. This illustrates the increased uniformity of the ED field in a three-dimensional space.

The performance of u^2 was a surprising observation. While not quite as consistent as ED, it generally performed much better than p^2. In some cases, it even seemed to outperform ED, however this was shown statistically to not be the case. An analytical investigation is discussed in the following chapter.

Because T_{60} values are a major part of obtaining the random-incidence absorption coefficient of a test material, it follows that each energy quantity is capable of delivering accurate results in a diffuse field. Since greater field uniformity exists for both kinetic and total energy density, fewer receiver positions are necessary to obtain the same results. Room volume is shown to affect the measurements at higher frequencies. Measurements taken in a non reverberant room show the importance of ideal sound field conditions for obtaining accurate results.

In a reverberation chamber, the calculation of sound power can be determined by the spatially averaged SPL, SVL, or SEDL. For this experiment, the use of SVL and SEDL resulted in lower spatial variation, but calculated sound power levels slightly higher than those obtained by SPL. These differences depend on frequency. For a chamber with adequate volume, low-frequency absorbers may not be necessary for

frequencies below the Schroeder frequency if the SVL or SEDL is used. A room with smaller volume may prohibit the spacing of receivers at a distance of half-wavelength for lower frequencies, especially if only one source position is used. In a nonreverberant room, SEDL still performs better than SPL, although the standard deviations may still exceed the allowed values specified in ISO 3741.

CHAPTER 4 – ANALYTICAL VERIFICATION OF RESULTS

To verify results from experimental measurements taken in the reverberation chamber, a Matlab program was developed to simulate the room response. Using modal analysis, the spatial variation for several acoustic quantities was obtained and compared. Using the Green's function for a monopole source in a rectangular room, the pressure can be calculated for any point. Using the Cartesian coordinate system, a given volume V, wave number k, and damping factor δ_N, the pressure at a point (x,y,z) is[1]

$$\hat{p}(x,y,z) = j\rho_0 ck\hat{Q}\sum_{N=0}^{\infty}\frac{\psi_N(x_0,y_0,z_0)\psi_N(x,y,z)}{\left(k^2 - k_N^2 - j2k_N\frac{\delta_N}{c}\right)V\Lambda_N}, \tag{4.1}$$

where

$$\Lambda_N = \frac{1}{\varepsilon_l\varepsilon_m\varepsilon_n}, \tag{4.2}$$

and

$$\varepsilon_i = \begin{cases} 1, i = 0 \\ 2, i \neq 0 \end{cases}, \tag{4.3}$$

and where $\hat{Q}$ is the complex volume velocity amplitude of the source, and ψ_N is the Nth eigenfunction corresponding to a solution to the homogeneous Helmholtz equation with the form

$$\psi_N(x,y,z) = \cos\left(\frac{n_x\pi}{L_x}x\right)\cos\left(\frac{n_y\pi}{L_y}y\right)\cos\left(\frac{n_z\pi}{L_z}z\right), \tag{4.4}$$

and where n_x, n_y, and n_z are nonnegative integers, $N = (n_x, n_y, n_z)$, and L_x, L_y, and L_z are the dimensions of the room in meters. The k_N are the eigenvalues of the room corresponding to its natural frequencies, given by

$$k_N = \pi\sqrt{\left(\frac{n_x}{L_x}\right)^2 + \left(\frac{n_y}{L_y}\right)^2 + \left(\frac{n_z}{L_z}\right)^2}\,. \tag{4.5}$$

The value of δ_N is approximated by the relationship[1]

$$\delta_N = \frac{cA}{8V} = \frac{c\sum_i \alpha_i S_i}{8V}, \tag{4.6}$$

where α_i is the absorption coefficient of the i^{th} surface of the room, S_i is the i^{th} surface area, and A is the total absorption.

The particle velocity for any direction, s, can be obtained as a closed form solution by using Euler's equation for a fluid in motion, such that

$$u_s = -\frac{1}{j\omega\rho_0}\frac{\partial p}{\partial s}. \tag{4.7}$$

Using Eq. (4.1), the Cartesian components of the particle velocity $\hat{u}_x$, $\hat{u}_y$, and $\hat{u}_z$ are obtained as

$$\hat{u}_x(x,y,z) = -\frac{1}{j\omega\rho_0}\, j\rho_0 ck\hat{Q}\sum_{N=0}^{\infty}\frac{\psi_N(x_0,y_0,z_0)\dfrac{d}{dx}\psi_N(x,y,z)}{\left(k^2 - k_N^2 - j2k_N\dfrac{\delta_N}{c}\right)V\Lambda_N}, \tag{4.8}$$

$$u_y(x,y,z) = -\frac{1}{j\omega\rho_0}\, j\rho_0 ck\hat{Q}\sum_{N=0}^{\infty}\frac{\psi_N(x_0,y_0,z_0)\dfrac{d}{dy}\psi_N(x,y,z)}{\left(k^2 - k_N^2 - j2k_N\dfrac{\delta_N}{c}\right)V\Lambda_N}, \tag{4.9}$$

$$u_z(x,y,z) = -\frac{1}{j\omega\rho_0}\, j\rho_0 ck\hat{Q}\sum_{N=0}^{\infty}\frac{\psi_N(x_0,y_0,z_0)\dfrac{d}{dz}\psi_N(x,y,z)}{\left(k^2 - k_N^2 - j2k_N\dfrac{\delta_N}{c}\right)V\Lambda_N}, \tag{4.10}$$

where

$$\frac{d}{dx}\psi_N(x,y,z) = -\frac{n_x\pi}{L_x}\sin\left(\frac{n_x\pi}{L_x}x\right)\cos\left(\frac{n_y\pi}{L_y}y\right)\cos\left(\frac{n_z\pi}{L_z}z\right), \tag{4.11}$$

$$\frac{d}{dy}\psi_N(x,y,z) = -\frac{n_y\pi}{L_y}\sin\left(\frac{n_y\pi}{L_y}y\right)\cos\left(\frac{n_x\pi}{L_x}x\right)\cos\left(\frac{n_z\pi}{L_z}z\right), \tag{4.12}$$

$$\frac{d}{dz}\psi_N(x,y,z) = -\frac{n_z\pi}{L_z}\sin\left(\frac{n_z\pi}{L_z}z\right)\cos\left(\frac{n_x\pi}{L_x}x\right)\cos\left(\frac{n_y\pi}{L_y}y\right). \tag{4.13}$$

The vector particle velocity can be obtained by combining the three terms, by

$$\hat{\vec{u}} = \hat{u}_x\vec{e}_x + \hat{u}_y\vec{e}_y + \hat{u}_z\vec{e}_z\,. \tag{4.14}$$

The time-averaged kinetic energy density is then obtained by

$$w_k = \frac{1}{4}\rho_0\hat{\vec{u}}\cdot\hat{\vec{u}}^* = \frac{1}{4}\rho_0\left(\left|\hat{u}_x\right|^2 + \left|\hat{u}_y\right|^2 + \left|\hat{u}_z\right|^2\right). \tag{4.15}$$

The potential energy density is obtained by

$$w_p = \frac{1}{4}\frac{\left|\hat{p}\right|^2}{\rho_0 c^2} = \frac{1}{4}\frac{\hat{p}\hat{p}^*}{\rho_0 c^2}\,. \tag{4.16}$$

The total energy density is the sum of the kinetic and potential energy density components, such that

$$w_t = w_k + w_p \tag{4.17}$$

4.1 Numerical Model

In order to accurately describe the spatial variation of the three-dimensional field, several receiver locations had to be used. While it is difficult and time consuming to perform actual measurements, it is relatively simple to simulate the measurement using a

computer model. The dimensions used in the model were 5 m x 6 m x 7 m, similar to the dimensions of the large chamber.

The number of modes required to accurately describe the sound field at and below a given frequency is estimated by[1]

$$N(f) \approx \frac{4\pi V f^3}{3c^3} + \frac{\pi f^2}{2c^2}(L_x L_y + L_x L_z + L_y L_z) + \frac{f}{2c}(L_x + L_y + L_z). \qquad (4.18)$$

This value increases dramatically as frequency increases. As such, it is very time consuming to accurately represent the sound field at higher frequencies. For this numerical analysis, the value of 5000 Hz was chosen as the highest frequency of concern, which corresponds to over 7.5 million natural frequencies. All natural frequencies up to 5612 Hz (the upper band limit for the 5kHz 1/3rd-octave band) were obtained, sorted in ascending order, and stored for later use in numerical analyses.

In this model, an absorption coefficient of 0.02 was chosen for all room surfaces, at all frequencies of interest. This value corresponded to a T_{60} value of 7.9 s, and a modal bandwidth of 0.27 Hz. The spatial variation was calculated for the 1/3rd-octave frequency band from 100 Hz to 5000 Hz, with 1 Hz resolution. All modes that fell within nearly 10 times the modal bandwidth at each frequency were used to compute the results. The source strength $\hat{Q}$ was set to unity. The source position was located in the lower corner of the room (x_0 = 5 m, y_0 = 6 m, z_0 = 0 m) Field quantities were calculated at 0.1 m increments in x, y, and z, 1 m away from each wall, and 2 m away from the source, yielding 52111 positions. Each cross-section in z was saved in a separate Matlab file for later extraction and analysis. Each file included pressure, vector velocity magnitude, potential energy density, kinetic energy density, and total energy density.

The data was grouped into two scenarios: variation for the entire volume, and variation for each cross-section in elevation. The variables affecting the outcome were room dimensions, source position, frequency, and elevation in cross-section. In order to equitably compare variation, the standard deviation was obtained by normalization of the data by the mean value of each quantity. This results in a new average value of 1 and a unitless standard deviation.

4.2 Numerical Results

Figure 4.1 shows the standard deviations of the sound field, with the source in the corner, for potential, kinetic, and total ED, normalized by their mean values, in 1/3rd-octave bands. As has been shown in experimental measurements, both kinetic and total ED outperform potential ED. The performances of kinetic and total ED are quite similar.

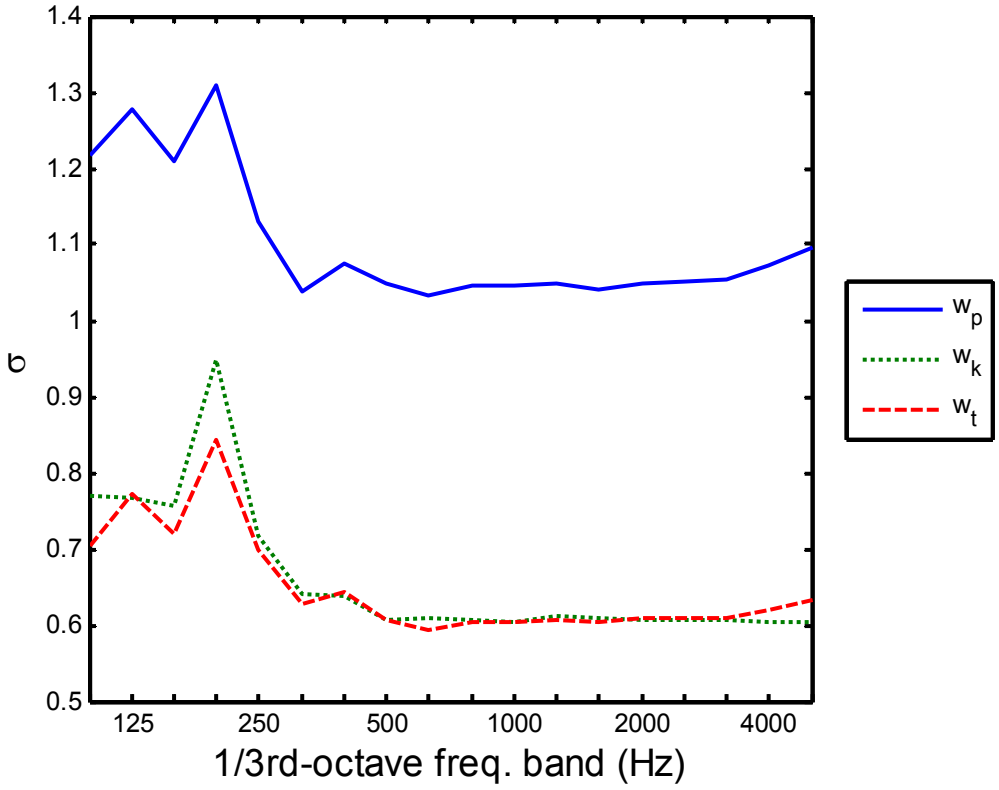

FIG. 4.1. Standard deviation for normalized potential, kinetic, and total ED. Source in the corner.

An F-test for unequal variances[32] reveals that for a 99% confidence level, the standard deviations between kinetic and total ED are statistically equal, except in a few cases where total ED is better. While this result does not hold at the 4 kHz and 5 kHz 1/3rd-octave bands, it may be that the analytical model becomes less accurate at higher frequencies for real-valued wavenumbers.[33] Figure 4.2 shows the spatial variation in the z = 3 m, for the 125 Hz 1/3rd-octave band. The cross-section measurements are similar to the results for the entire volume.

4.3 Effect of Uncertainty Error due to Atmospheric Conditions

As explained earlier, measurement uncertainty in reverberation chambers comes from many sources. One of these variables is the atmospheric conditions of the room. For the measurements, these parameters are obtained by a weather station, which measures temperature, relative humidity, and barometric pressure. The displayed values each had a margin of error for the specific instrument used. The question to be answered is, to what degree does this margin of error affect the measurements?

The margin of error of the Weather Station is ±1 °C, ±7 % RH, and ±700 Pa. All three values are used to obtain the air attenuation coefficient α. This coefficient is based on a theoretical calculation of the relaxation frequencies of nitrogen and oxygen, which calculation is detailed in ISO 9613 and is accurate to ±10%. Of the three atmospheric values, temperature most strongly affects the speed of sound. An uncertainty of ±1 °C results in a variation of ±0.6 m/s. The uncertainty present in the air attenuation coefficient has considerable effect on the equivalent absorption area at frequencies above

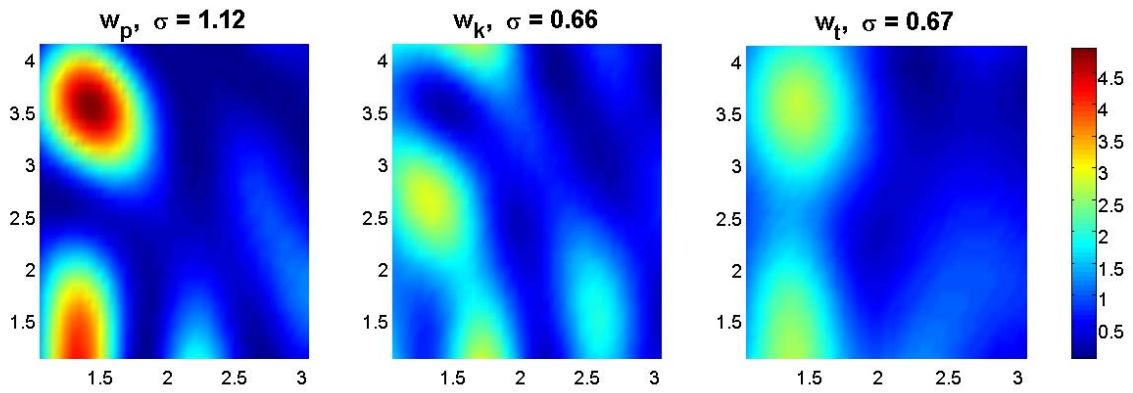

FIG. 4.2. Spatial variation for potential, kinetic, and total ED in the z = 3 m plane, at 125 Hz.

1 kHz. For example, the error value of α at 5kHz for fiberglass absorption in the large chamber is ±0.21, according to the 10% accuracy limit. In comparison, the error value of α due to an uncertainty of ±1 °C alone is ±0.08. Accordingly, it seems that the uncertainty of the atmospheric values is not as significant as that obtained from the standard.

The effects are further accentuated in the calculation of energy density, which uses both ρ_0 and c. The uncertainties of the three atmospheric values results in an overall uncertainty of ±0.013 kg/m^3 for ρ_0. Thus, the energy density impulse response can introduce additional errors in the measured T_{60}, an issue absent in the squared pressure impulse response. This also affects the sound power level obtained from the SEDL by ±0.1 dB. Are these effects negligible? Since T_{60}, absorption coefficients, and sound power are based on spatially averaged values, some effects may be averaged out. Furthermore, T_{60} measurements are traditionally truncated to the nearest hundredth of a second, sound absorption coefficients are set to two decimal places, and sound power levels are rounded to the nearest 0.1 dB. Other errors exist from theoretical assumptions alone. As has been stated before, reproducibility of reverberation chamber measurements

is still under investigation. The combined uncertainties from several factors in these measurements probably has a larger effect than ρ_0 and c variation.

CHAPTER 5 – CONCLUSIONS

The application of total acoustic energy density (ED) to reverberation chamber measurements has demonstrated its effectiveness in comparison with squared pressure. The fundamental characteristic that causes its improved performance is its greater spatial uniformity over an enclosed sound field. Because reverberation chamber measurements suffer from uncertainties due partly to approximations of the diffuse field model, it was hoped that ED might be used to reduce measurement error and also simplify the process.

5.1 Sound Absorption

Results from T_{60} measurements show greater spatial uniformity of energy decay using the ED impulse response. It was shown that the variation for ED was roughly half of that for squared pressure in a large qualified reverberation chamber. This suggests that fewer source-receiver positions are necessary to obtain an adequate sample of the sound field. It also suggests that low-frequency measurements are more accurate using ED. Similar results were obtained in a small reverberation chamber and in a classroom.

Because sound absorption calculations are obtained from T_{60} values, it follows that ED can be used to successfully obtain sound absorption measurements in a diffuse field. Results in both the large and small chambers show similar values of the coefficients compared to those obtained from squared pressure. The measured results in the classroom, however, were unsuccessful, likely due to the small change in total absorption after the test material was placed in the room, as well as the lack of a diffuse sound field.

5.2 Sound Power

The sound power level of a reference sound source was measured using both squared pressure and ED methods. Under steady-state conditions, ED was shown to have greater spatial uniformity than squared pressure. This was observed in all three rooms. The large chamber, not yet fitted with low-frequency absorption, did not meet ISO requirements for variation at low frequencies (100 Hz) with squared pressure, when one source position and six receiver positions were used. However, variation in ED was lower than the maximum allowable values. This was encouraging because it meant that the low-frequency absorption did not need to be installed for the ED measurements. Otherwise the chamber could not have been used for broadband sound power tests without more source and receiver positions. Results in the small chamber showed that standard deviation values obtained from ED at low frequencies met the ISO requirements, despite using a room with a smaller volume than suggested. The inclusion of the factors ρ_0 and c add some uncertainty to sound energy density level (SEDL) measurements by ± 0.06 dB, due to the instrumentation used in obtaining values for the atmospheric variables.

5.3 Particle Velocity

The total ED measurements of this work, with relatively small spatial standard deviations relied on both pressure and particle velocity. The work revealed that the squared vector magnitude of the particle velocity alone resulted in much smaller variations than squared pressure for both T_{60} values and spatially averaged sound levels. Surprisingly, this variation was quite similar to that of total ED. In some cases, the measured variation was slightly better than ED, especially at higher frequencies.

However, this observation was tested and found to be statistically insignificant. Sometimes, particularly at the lower frequencies, variation in particle velocity was worse than squared pressure. Thus, while not as consistent as ED, the particle velocity measurements suggest that kinetic ED alone may be a viable approach to reducing measurement error.

5.4 Realization of Objectives

Based on the results of this research, ED was shown to successfully measure sound absorption and sound power in a reverberation chamber. It was also shown to extend the usable low-frequency range of a large reverberation chamber, without the need for additional absorption. Thus, there is apparently no need to reconfigure the chamber for different types of measurements when using ED. The possibility of extending the usable low-frequency range in a smaller reverberation chamber was also realized. Usable sound power data was also obtained in a nonreverberant room, even though the variation in measured values did not meet ISO standards. Accurate measurements of sound absorption in a nonreverberant room were unsuccessful in this study.

5.5 Recommendations for Future Work

This study used a discrete number of measurement positions according to ISO 354 and 3741. A thorough investigation of the sound field in a small enclosure without diffusers would be beneficial for determining whether accurate low-frequency measurements could be obtained in such a space. This could be done by sampling the ED sound field using many more data points than required in the standards.

This study of reverberation chamber measurements was limited to sound power and sound absorption. Other types of measurements should be explored, such as sound transmission and sound scattering.

REFERENCES

[1] H. Kuttruff, *Room Acoustics* (Spon Press, NY), 4th ed., 2000.

[2] M. Schroeder, "The Schroeder frequency revisited," J. Acoust. Soc. Am. **99**, 3240-3421 (1996).

[3] W. Sabine, *Collected Papers on Acoustics* (Dover Publications, NY), 1964.

[4] J. Tichy and P. Baade, "Effect of rotating diffusers and sampling techniques on sound-pressure averaging in reverberation rooms," J. Acoust. Soc. Am. **56**, 137-143 (1974).

[5] ISO 3741:1999(E). Acoustics – Determination of sound power levels of noise sources using sound pressure – Precision methods for reverberation rooms (International Organization for Standardization, Geneva).

[6] R. V. Waterhouse, "Interference patterns in reverberant sound fields," J. Acoust. Soc. Am. **27**, 247-258 (1955).

[7] A. Schaffner, "Accurate estimation of the mean sound pressure level in enclosures," J. Acoust. Soc. Am. **106** (2), 823-827 (1999).

[8] M. Vorlander, "Revised relation between the sound power and the average sound pressure level in rooms and the consequences for acoustic measurements," Acustica, **81**, 332-343 (1995).

[9] T. J. Schultz, "Persisting questions in steady-state measurements of noise power and sound absorption," J. Acoust. Soc. Am. **54**, 978-981 (1973).

[10] ISO/DIS 17497-1. Acoustics – Measurement of the sound scattering properties of surfaces – Part 1: Measurement of the random-incidence scattering coefficient in a reverberation room (International Organization for Standardization, Geneva).

[11] R. V. Waterhouse, "Statistical Properties of Reverberant Sound Fields," J. Acoust. Soc. Am. **43**, 1436-1444 (1968).

[12] D. Lubman, "Distribution of Reverberant Sound in Large Rooms," J. Acoust. Soc. Am. **39**, 1266 (A) (1968).

[13] ISO 354:2003. Acoustics – Measurement of sound absorption in a reverberation room. (International Organization for Standardization, Geneva).

[14] C. Eyring, "Reverberation time in dead rooms," J. Acoust. Soc. Am. **1**, 217-214 (1930).

[15] M. Hodgson, "On measures to increase sound-field diffuseness and the applicability of diffuse-field theory," J. Acoust. Soc. Am. **95** (6), 3651-3654 (1994).

[16] M. Schroeder, "New method of measuring reverberation time," J. Acoust. Soc. Am. **37**, 409-412 (1965).

[17] I. Wolff and F. Massa, "Use of pressure gradient microphones for acoustical measurements," J. Acoust. Soc. Am. **4**, 217-234 (1933).

[18] F. Fahy, "Measurement of acoustic intensity using the cross-spectral density of two microphone signals," J. Acoust. Soc. Am. **62**, 1057-1059 (1977).

[19] J. Ghan, "Expression for the estimation of time-averaged acoustic energy density using the two-microphone method (L)," J. Acoust. Soc. Am. **113**, 2404-2407 (2003).

[20] G. W. Elko, "An acoustic vector-field probe with calculable obstacle bias," Proc. Noise-Con 91 (7) 525-532 (1991).

[21] http://www.microflown.com/r&d_publications.htm

[22] J. Parkins, S. Sommerfeldt, and J. Tichy, "Narrowband and broadband active control in an enclosure using the acoustic energy density," J. Acoust. Soc. Am. **108**, 192-203 (2000).

[23] A. Duval, "In situ impedance and absorption coefficient measurements compared to poro-elastic simulation in free, diffuse or semi-statistical fields using microflown p-u probes," DAGA (2006).

[24] D. Bonsi, D. Gonzalez, and D. Stanzial, "Quadraphonic impulse responses for acoustic enhancement of audio tracks: measurement and analysis," Forum Acusticum, 335-340 (2005).

[25] S. Rollins, The Salt Lake Tabernacle: acoustic characterization and study of spatial variation, M.S. Thesis, Brigham Young University, 2005, pp. 126-129.

[26] ISO 9613-1:1993(E). Acoustics – Attenuation of sound during propagation outdoors – Part 1: Calculation of the absorption of sound by the atmosphere (International Organization for Standardization, Geneva).

[27] ASTM C423-00. Standard Test Method for Sound Absorption and Sound Absorption Coefficients by the Reverberation Room Method (West Conshohocken).

[28] ISO 9295:1988. Acoustics - Measurement of high-frequency noise emitted by computer and business equipment (International Organization for Standardization, Geneva).

[29] A. Pierce, *Acoustics, An Introduction to Its Physical Principles and Applications* (Acoustical Society of America, NY), 1994.

[30] G. Mange, "The effect of mean free path on reverberation room measurement of absorption and absorption coefficients," Noise Control Engineering Journal, **53** (6), 268-270 (2005).

[31] ANSI S1.1-1994. Acoustical terminology (American National Standards Institute, New York).

[32] G. Keller, *Applied Statistics with Microsoft® Excel* (Wadworth Group, CA), 2001.

[33] Private conversation with Buye Xu, August 14, 2006.

APPENDIX (Matlab code)

EDIIR.m

```
%T60 Measurements using ED and Integrated Impulse Response Method
%adapted from code written by Sarah Rollins

clear all;close all;clc;
warning('off', 'all')
T60p = zeros(18,12); T60uv = zeros(18,12); T60ED = zeros(18,12);
room = input('Room (1-Large,2-Small,3-Classroom) - ');
if room == 1
   V = 203.92; S = 255.72; rm = ('LG');
elseif room == 2
   V = 61.28; S = 99.02; rm = ('SM');
elseif room == 3
   V = 235.16; S = 250.42; rm = ('RG');
end
tempmat = input('Test Material (1-Empty, 2-Fiberglass, 3-Chairs) - ');
if tempmat == 1
   material = ('Empty');
elseif tempmat == 2
   material = ('Fiber');
elseif tempmat == 3
   material = ('Chair');
end
Tc = input('Temperature in Celsius - ');% Celsius Temperature
hr = input('Relative Humidity (decimal) - ');
P = input('Barometric Pressure in Pa - ');
T = Tc+273.15; %Kelvin
%parameters to find speed of sound and air density
Rd = 287.05; %coefficient of dry air
Rv = 461.495;%coefficient of humid air
a0 = 331.5024; a1 = 0.603055; a2 = -0.000528; a3 = 51.471935; a4 = 0.1495874;
a5 = -0.000782; a6 = -0.000000182; a7 = 3.73E-08; a8 = -2.93E-10;
a9 = -85.20931; a10 =       -0.228525; a11 = 0.0000591; a12 = -2.835149;
a13 = -2.15E-13; a14 = 29.179762; a15 = 0.000486;
xc = 0.000314;
B = P;   %atmospheric pressure, notation same as ISO 3741
B0 = 101325;
psv =exp(1.2811805*10^-5*T^2-1.9509874*10^-2*T+34.04926034-6.3536311*10^3/T);
Pv = psv*hr; Pd = P-Pv; fe = 1.00062+3.14E-8*P+5.6E-7*T^2;
xw = hr*fe*psv/P;   %for speed of sound calculation
c = a0 + a1*Tc + a2*Tc^2 + (a3 + a4*Tc + a5*Tc^2)*xw + (a6 + a7*Tc + a8*Tc^2)*P + (a9 + a10*Tc +
a11*Tc^2)*xc + a12*xw^2 + a13*P^2 + a14*xc^2 + a15*xw*P*xc;
rho = (Pd/(Rd*T))+(Pv/(Rv*T));

k=1;
s=what; numfiles=length(s.mat);
fc=[100 125 160 200 250 315 400 500 630 800 1000 1250 1600 2000 2500 3150 4000 5000]; %1/3 oct-
band center freqs
numoct=length(fc); %number of 1/3 octave band filters
n=1;
for k=1:numfiles/4 % processes 4 files at a time (p,ux,uy,uz)
```

```
    if k<10
       pos = ['0' num2str(k)];
    else
       pos = num2str(k);
    end
    pIRfile = load(char(s.mat(k))); % load the pressure file
    S_Rate = pIRfile.samplingfrequency;
    ep = pIRfile.data;
    tms = (1:length(ep))/S_Rate*1000; %time in ms
    uxIRfile = load(char(s.mat(k+12))); eux = uxIRfile.data;
    uyIRfile = load(char(s.mat(k+24))); euy = uyIRfile.data;
    uzIRfile = load(char(s.mat(k+36))); euz = uzIRfile.data;
    fprintf(['Using files: ' char(s.mat(k)) ', ' char(s.mat(k+12)) ', ' char(s.mat(k+24)), ', ' char(s.mat(k+36)),
'\n']);
    %Correct for sensitivities in the frequency domain
    N = length(ep);
    fs = S_Rate;
    dt =1/fs;
    t=0:dt:dt*(N-1);
    tmax = max(t);
    df = 1/tmax;
    f = 0:df:fs;
    fss = f(1:N/2+1);  %single sided freq.
    %Calibrated sensitivities given by the manufacturer
    Mpss = 0.0153./sqrt(1+(56./fss).^2);
    Muxss = 0.066*(rho*c)./(sqrt(1+(102./fss).^2).*sqrt(1+(fss./1200).^2).*sqrt(1+(fss./13000).^2));
    Muyss = 0.067*(rho*c)./(sqrt(1+(102./fss).^2).*sqrt(1+(fss./1200).^2).*sqrt(1+(fss./13000).^2));
    Muzss = 0.086*(rho*c)./(sqrt(1+(103./fss).^2).*sqrt(1+(fss./1200).^2).*sqrt(1+(fss./13000).^2));
    Mp = [Mpss,Mpss(length(Mpss)-1:-1:2)];
    Mux = [Muxss,Muxss(length(Muxss)-1:-1:2)];
    Muy = [Muyss,Muyss(length(Muyss)-1:-1:2)];
    Muz = [Muzss,Muzss(length(Muzss)-1:-1:2)];

    epfft = fft(ep); pfft = epfft; pfft(2:N) = epfft(2:N)./Mp(2:N)'; p = ifft(pfft);
    euxfft = fft(eux); uxfft = euxfft; uxfft(2:N) = euxfft(2:N)./Mux(2:N)'; ux = ifft(uxfft);
    euyfft = fft(euy); uyfft = euyfft; uyfft(2:N) = euyfft(2:N)./Muy(2:N)'; uy = ifft(uyfft);
    euzfft = fft(euz); uzfft = euzfft; uzfft(2:N) = euzfft(2:N)./Muz(2:N)'; uz = ifft(uzfft);

    % Filter out the unneeded low frequency content (Anything below 50 Hz)
    [b,a] = butter(2,50/24000,'high');
    p = filtfilt(b,a,p); ux = filtfilt(b,a,ux); uy = filtfilt(b,a,uy); uz = filtfilt(b,a,uz);
    %process data for each 1/3rd octave band
    for m = 1:numoct
       fprintf([num2str(fc(m)) ','])
       [b,a] = oct3dsgn(fc(m),S_Rate,3);
       p_filt = filter(b,a,p); ux_filt = filter(b,a,ux); uy_filt = filter(b,a,uy); uz_filt=filter(b,a,uz);
       %square the filtered signals
       p_filtsq = p_filt.^2; ux_filtsq = ux_filt.^2; uy_filtsq = uy_filt.^2; uz_filtsq = uz_filt.^2;
       %calculate energy quantities from squared signals
       uvsq = (ux_filtsq + uy_filtsq + uz_filtsq);  %particle velocity magnitude
       ED = 1/2*rho*(uvsq + p_filtsq/(rho*c).^2);
       T60p(m,n) = t60_dn_b(S_Rate,p_filtsq);
       T60uv(m,n) = t60_dn_b(S_Rate,uvsq);
       T60ED(m,n) = t60_dn_b(S_Rate,ED);
    end
```

```
   if mod(k,1)==0
      fprintf('Calculating RT...\n')
   end
   n = n+1;
end

%Compute averages and variation
pavg = mean(T60p,2); uavg = mean(T60uv,2); Eavg = mean(T60ED,2);
pstd = std(T60p,0,2); ustd = std(T60uv,0,2); Estd = std(T60ED,0,2);
%plot averages and deviations for each quantity
figure
plot([pavg';uavg';Eavg']','LineWidth',2)
xlim([1,18])
set(gca,'xtick',1:18);
set(gca,'Xticklabel',{'','125','','','250','','','500','','','1000','','','2000','','','4000',''});
set(gcf,'Color',[1,1,1])
xlabel('1/3 octave freq. band','Fontsize',14)
ylabel('T_6_0','Fontsize',14)
title('Average T_6_0 from 12 positions','Fontsize',16)

figure
plot([pstd';ustd';Estd']','LineWidth',2)
xlim([1,18])
set(gca,'xtick',1:18);
set(gca,'Xticklabel',{'','125','','','250','','','500','','','1000','','','2000','','','4000',''});
set(gcf,'Color',[1,1,1])
legend('p^2','u^2','ED')
xlabel('1/3 octave freq. band','Fontsize',14)
ylabel('\sigma','Fontsize',14)
title('Standard Deviation of T_6_0 from 12 positions','Fontsize',16)
save pavg pavg
save uavg uavg
save Eavg Eavg
save T60p T60p
save T60ED T60ED
save T60uv T60uv
```

EDpower.m

```
%Energy Density measurements for Sound Power

clear all;close all;clc;
warning('off', 'all')
room = input('Room (1-Large,2-Small,3-Classroom) - ');
if room == 1
   V = 203.92; S = 255.72; RT = load('T15\\T15large.mat'); rm = ('BnK_Lg');%open appropriate folder
elseif room == 2
   V = 61.28; S = 99.02; RT = load('T15\\T15small.mat'); rm = ('BnK_Sm');
elseif room == 3
   V = 235.16; S = 250.42; RT = load('T15\\T15reg.mat'); rm = ('BnK_Rg');
end
Tc = input('Temperature (Celsius) \n'); % Celsius Temperature
hr = input('Humidity (decimal) \n');
P= input('Pressure (Pa) \n');
Rd = 287.05;
Rv = 461.495;
%parameters to find speed of sound
a0 = 331.5024; a1= 0.603055; a2 = -0.000528; a3 = 51.471935; a4 = 0.1495874; a5 = -0.000782;
a6 = -0.000000182; a7 = 3.73E-08; a8 = -2.93E-10; a9 = -85.20931; a10 = -0.228525;
a11 = 0.0000591; a12 = -2.835149; a13 = -2.15E-13; a14 = 29.179762; a15 = 0.000486;
xc = 0.000314;
allowed = [1.5 1.5 1.5 1 1 1 1 1 1 .5 .5 .5 .5 .5 .5 1 1 1 1 1 1];
B = P;   %atmospheric pressure, notation same as ISO 3741
B0 = 101325;
T = Tc+273.15; %Kelvin
psv =exp(1.2811805*10^-5*T^2-1.9509874*10^-2*T+34.04926034-6.3536311*10^3/T);
Pv = psv*hr; Pd = P-Pv;
fe = 1.00062+3.14E-8*P+5.6E-7*T^2;
xw = hr*fe*psv/P;   %for speed of sound calculation
c = a0 + a1*Tc + a2*Tc^2 + (a3 + a4*Tc + a5*Tc^2)*xw + (a6 + a7*Tc + a8*Tc^2)*P + (a9 + a10*Tc +
a11*Tc^2)*xc + a12*xw^2 + a13*P^2 + a14*xc^2 + a15*xw*P*xc;
rho = (Pd/(Rd*T))+(Pv/(Rv*T));
AE=55.26/c*V./RT.Eavg; %ISO 3741 p. 15 eq.12
Au=55.26/c*V./RT.uavg; Ap=55.26/c*V./RT.pavg;
s=what;
folder = [s.path '\' rm];
ss=what(folder);
numfiles=length(ss.mat);
fc=[100 125 160 200 250 315 400 500 630 800 1000 1250 1600 2000 2500 3150 4000 5000 6300 8000
10000]; %1/3 oct-band center freqs
numoct=length(fc); %number of 1/3 octave band filters
fs = 24000; %using 4 channel DAT
S_Rate=fs;
pref = 20e-6;   % pascals
uref = pref/(rho*c);    % m/s   1 Pa* = 1 Pa/(m/s)
Eref = rho/2*uref^2 + pref^2/(2*rho*c^2);
for k=1:numfiles
   g=char(ss.mat(k)); % get the file name and convert
   %it into a character string
   fname=1;
   while ((g(fname))~='.') % search through the string
```

```
      %and figure out where the .mat starts
      fname=fname+1;
   end
   g=g(1:fname-1);% get rid of the .mat extension
   filedata=load([folder '\' g]);
   filedata=getfield(filedata,g);
   tms=(1:length(filedata))/S_Rate*1000; %time in ms
   ts = (1:length(filedata))/S_Rate; %time in s
   fprintf(['Using file: ' char(ss.mat(k)) '\n']);
   ep = filedata(1,:); eux = filedata(2,:); euy = filedata(3,:); euz = filedata(4,:);
   %%%%%%% CORRECT FOR SENSITIVITIES IN FREQ DOMAIN %%%%%%%%
   N = length(filedata);
   dt =1/fs; t=0:dt:dt*(N-1); tmax = max(t); df = 1/tmax; f=0:df:fs;
   fss = f(1:N/2+1);  %single sided freq.
   %Calibrated sensitivities given by the manufacturer
   Mpss = .0153./sqrt(1+(56./fss).^2);
   Muxss=0.066*(rho*c)./(sqrt(1+(102./fss).^2).*sqrt(1+(fss./1200).^2).*sqrt(1+(fss./13000).^2));
   Muyss=0.067*(rho*c)./(sqrt(1+(102./fss).^2).*sqrt(1+(fss./1200).^2).*sqrt(1+(fss./13000).^2));
   Muzss=0.086*(rho*c)./(sqrt(1+(103./fss).^2).*sqrt(1+(fss./1200).^2).*sqrt(1+(fss./13000).^2));
   Mp=[Mpss,Mpss(length(Mpss)-1:-1:2)];
   Mux=[Muxss,Muxss(length(Muxss)-1:-1:2)];
   Muy=[Muyss,Muyss(length(Muyss)-1:-1:2)];
   Muz=[Muzss,Muzss(length(Muzss)-1:-1:2)];

   epfft=fft(ep); pfft = epfft; pfft(2:N) = epfft(2:N)./Mp(2:N); p = ifft(pfft);
   euxfft=fft(eux); uxfft = euxfft; uxfft(2:N) = euxfft(2:N)./Mux(2:N); ux = ifft(uxfft);
   euyfft=fft(euy); uyfft = euyfft; uyfft(2:N) = euyfft(2:N)./Muy(2:N); uy = ifft(uyfft);
   euzfft=fft(euz); uzfft = euzfft; uzfft(2:N) = euzfft(2:N)./Muz(2:N); uz = ifft(uzfft);
   %%%% FILTER OUT THE UNNEEDED LOW FREQUENCY CONTENT (Anything below 50 Hz)
   [b,a]=butter(2,50/12000,'high');
   p = filtfilt(b,a,p); ux = filtfilt(b,a,ux); uy = filtfilt(b,a,uy); uz = filtfilt(b,a,uz);
   %this for loop process data for each 1/3rd octave band
   for m=1:numoct
      fprintf([num2str(fc(m)) ' '])
      [b,a]=oct3dsgn(fc(m),S_Rate,3);   %filter the data into 1/3rd oct bands
      p_filt=filter(b,a,p); ux_filt=filter(b,a,ux); uy_filt=filter(b,a,uy); uz_filt=filter(b,a,uz);
      %square the filtered signals
      p_filtsq = p_filt.^2; ux_filtsq = ux_filt.^2; uy_filtsq = uy_filt.^2; uz_filtsq = uz_filt.^2;
      %calculate energy quantities from squared signals
      uvsq = (ux_filtsq + uy_filtsq + uz_filtsq);  %vector velocity sq, summed from squared values
      ED = rho/2*uvsq + p_filtsq/(2*rho*c^2);
      %calculate SPL,SVL,ED(log)
      pint = mean(p_filtsq); uint = mean(uvsq); EDint = mean(ED);
      Lp = 10*log10(pint/pref^2); Lu = 10*log10(uint/uref^2); LE = 10*log10(EDint/Eref);
      Lparray(k,m) = Lp; Luarray(k,m) = Lu; LEarray(k,m) = LE;
   end
   fprintf('\n')
end
pmean = mean(Lparray); pstdev = std(Lparray);
umean = mean(Luarray); ustdev = std(Luarray);
EDmean = mean(LEarray); EDstdev = std(LEarray);
ptemp = 0; utemp = 0; Etemp = 0;
for q=1:6
   ptemp = ptemp + 10.^(.1*Lparray(q,:));
   utemp = utemp + 10.^(.1*Luarray(q,:));
   Etemp = Etemp + 10.^(.1*LEarray(q,:));
```

```
end
Lpbar = 10*log10(ptemp/6); Lubar = 10*log10(utemp/6); LEbar = 10*log10(Etemp/6);
Lwp = Lpbar + 10*log10(Ap)+4.34*Ap/S+10*log10(1+S*c./(8*V*fc))-
25*log10(427/400*sqrt(273/(273+Tc))*B/B0)-6;
Lwu = Lubar + 10*log10(Au)+4.34*Au/S+10*log10(1+S*c./(8*V*fc))-
25*log10(427/400*sqrt(273/(273+Tc))*B/B0)-6;
LwE = LEbar + 10*log10(AE)+4.34*AE/S+10*log10(1+S*c./(4*V*fc))-
25*log10(427/400*sqrt(273/(273+Tc))*B/B0)-6;
colvect=[0,0,0;0,.8,0;1,0,0;];
set(0,'Defaultaxescolororder',colvect);
set(0,'Defaultaxeslinestyleorder','-|:|--');
figure
plot([Lwp;Lwu;LwE;]','LineWidth',2)
title('Sound Power Level of B+K 4204 Reference Source','FontSize',16)
legend('L_w_p','L_w_u','L_w_E', 'Location', 'bestoutside')
xlabel('1/3rd-octave freq. band (Hz)','Fontsize',14)
xlim([1,21])
ylabel('L_w','Fontsize',14)
set(gca,'xtick',1:21);
set(gca,'Xticklabel',{'','125','','','250','','','500','','','1000','','','2000','','','4000','','','8000',''});
set(gcf,'Color',[1,1,1])
figure
plot([pstdev;ustdev;EDstdev;allowed]','LineWidth',2);
title('Standard Deviation of Measured Sound Power Level','FontSize',16)
legend('SPL','SVL','SEDL','Allowed');
xlabel('1/3rd-octave freq. band (Hz)','Fontsize',14)
xlim([1,21])
ylabel('\sigma','FontSize',14)
set(gca,'xtick',1:21);
set(gca,'Xticklabel',{'','125','','','250','','','500','','','1000','','','2000','','','4000','','','8000',''});
set(gcf,'Color',[1,1,1])
```

natfreq.m

```
Lx = 5; Ly = 6; Lz = 7; c = 343;
m = 1;

fndata = zeros(7,7546770);
for nx=0:164 %164 24
   for ny=0:197  %197 28
      for nz=0:230 %230 for 5680, allowing for 3rd oct with fc=5000Hz; 33
         fndata(1,m) = c/2*sqrt((nx/Lx)^2+(ny/Ly)^2+(nz/Lz)^2);
         fndata(2,m)=nx; fndata(3,m)=ny; fndata(4,m)=nz;
         if nx ==0
            fndata(5,m)=1;
         else
            fndata(5,m)=2;
         end
         if ny ==0
            fndata(6,m) = 1;
         else
            fndata(6,m) = 2;
         end
         if nz ==0
            fndata(7,m) = 1;
         else
            fndata(7,m) = 2;
         end
         m=m+1;
      end
   end
end
fndata = sortrows(fndata')';
```

oct3dsgn.m

```
function [B,A] = oct3dsgn(Fc,Fs,N);
% OCT3DSGN  Design of a one-third-octave filter.
%    [B,A] = OCT3DSGN(Fc,Fs,N) designs a digital 1/3-octave filter with
%    center frequency Fc for sampling frequency Fs.
%    The filter is designed according to the Order-N specification
%    of the ANSI S1.1-1986 standard. Default value for N is 3.
%    Warning: for meaningful design results, center frequency used
%    should preferably be in range Fs/200 < Fc < Fs/5.
%    Usage of the filter: Y = FILTER(B,A,X).
%
%    Requires the Signal Processing Toolbox.
%
%    See also OCT3SPEC, OCTDSGN, OCTSPEC.

% Author: Christophe Couvreur, Faculte Polytechnique de Mons (Belgium)
%         couvreur@thor.fpms.ac.be
% Last modification: Aug. 25, 1997, 2:00pm.

% References:
%    [1] ANSI S1.1-1986 (ASA 65-1986): Specifications for
%        Octave-Band and Fractional-Octave-Band Analog and
%        Digital Filters, 1993.

if (nargin > 3) | (nargin < 2)
  error('Invalide number of arguments.');
end
if (nargin == 2)
  N = 3;
end
if (Fc > 0.88*(Fs/2))
  error('Design not possible. Check frequencies.');
end

% Design Butterworth 2Nth-order one-third-octave filter
% Note: BUTTER is based on a bilinear transformation, as suggested in [1].
pi = 3.14159265358979;
f1 = Fc/(2^(1/6));
f2 = Fc*(2^(1/6));
Qr = Fc/(f2-f1);
Qd = (pi/2/N)/(sin(pi/2/N))*Qr;
alpha = (1 + sqrt(1+4*Qd^2))/2/Qd;
W1 = Fc/(Fs/2)/alpha;
W2 = Fc/(Fs/2)*alpha;
[B,A] = butter(N,[W1,W2]);
```

spatialvariation.m

```
% this program simulates the reverberation chamber used in experimental
% measurements.  using modal theory, the pressure solution is given for a
% source location and any receiver positions of interest.  the field is
% measured in cross sections of elevation, and for the entire volume.
% Variation for the quantities p^2, u^2, and ED are calculated for each
% cross-section and for the entire volume, for a given frequency.

clear all; close all; clc;
% load('fndata.mat');
%room dimensions
Lx=5; Lxinv=1/Lx;Ly=6; Lyinv=1/Ly;Lz=7; Lzinv=1/Lz;
V = Lx*Ly*Lz; c=343;
rho = 1.02; rhohf = rho*.25; Epconst = 1/(4*rho*c^2);
A=4.28; %using .02 for alpha for walls, floors and ceiling, calculated with S = 2*(Lx*Lz+Lx*Ly+Ly*Lz)
dn=c*A/(8*V); jdnpi = j*dn/pi;
%pressure field for a cross-section in elevation
x=1:.1:Lx-1; y=1:.1:Ly-1;
%Source position
x0=input('Source Position - x(m) '); y0=input('Source Position - y(m) '); z0=input('Source Position - z(m) ');
fw2=1; %2 Hz bandwidth, almost 10 times the modal bandwidth of .27 Hz
Q = 1; %constant volume velocity source
Ahat = j*rho*c^2*Q/(2*pi*V);
R=1;
for foct=[100 125 160 200 250 315 400 500 630 800 1000 1250 1600 2000 2500 3150 4000 5000]
   load(['fndata' num2str(foct) '.mat']);
   flow = floor(foct/2^(1/6));
   fhi = ceil(foct*2^(1/6));
   %looking at stdev of data, one cross-section at a time
   Epcurstd = zeros(1,41); Ekcurstd = zeros(1,41); Ecurstd = zeros(1,41);
   volEp = zeros(1,31*41*41); volEk = zeros(1,31*41*41); volE  = zeros(1,31*41*41);
   ele=1; %elevation counter
   volcount = 1;
   for z=2:0.1:Lz-1
      p = zeros(length(x),length(y)); ux  = zeros(length(x),length(y)); uy = zeros(length(x),length(y));
      uz = zeros(length(x),length(y)); usq = zeros(length(x),length(y)); Ep = zeros(length(x),length(y));
      Ek = zeros(length(x),length(y)); E = zeros(length(x),length(y));
      for f=flow:fhi
         b = find(f-fw2<=fndata(1,:) & fndata(1,:)<=f+fw2);
         Npart = fndata(2:7,b);
         fnpart = fndata(1,b);
         for N=1:size(Npart,2)   %add together portions from each nat freq
            B  = j/(rho*2*pi*f);
            xpsi = cos(Npart(1,N)*pi*x*Lxinv);
            x0psi = cos(Npart(1,N)*pi*x0*Lxinv);
            dxpsi = -sin(Npart(1,N)*pi*x*Lxinv)*Npart(1,N)*pi*Lxinv;
            ypsi = cos(Npart(2,N)*pi*y*Lyinv);
            y0psi = cos(Npart(2,N)*pi*y0*Lyinv);
            dypsi = -sin(Npart(2,N)*pi*y*Lyinv)*Npart(2,N)*pi*Lyinv;
            zpsi = cos(Npart(3,N)*pi*z*Lzinv);
            z0psi = cos(Npart(3,N)*pi*z0*Lzinv);
            dzpsi = -sin(Npart(3,N)*pi*z*Lzinv)*Npart(3,N)*pi*Lzinv;
            Linv = (Npart(4,N)*Npart(5,N)*Npart(6,N)); %enx, eny, enz
```

```
        psiS = x0psi*y0psi*z0psi;
        psiR = xpsi'*ypsi*zpsi;
        Almn=f*Ahat*Linv*psiS/(f^2-fnpart(N)^2-jdnpi*fnpart(N));
        p = p+Almn*psiR;
        ux = ux+B*Almn*dxpsi'*ypsi*zpsi;
        uy = uy+B*Almn*xpsi'*dypsi*zpsi;
        uz = uz+B*Almn*xpsi'*ypsi*dzpsi;
    end
end
usq = (ux.*conj(ux)+uy.*conj(uy)+uz.*conj(uz));
Ek = usq*rhohf; %kinetic ED
Ep = p.*conj(p)*Epconst; %potential ED
E = Ek + Ep; %Total Energy Density
clear p ux uy uz usq;
countA=1;
for m=1:size(Ep,1)
    for n=1:size(Ep,2)
        Epcur(countA)=Ep(m,n);
        Ekcur(countA)=Ek(m,n);
        Ecur(countA)=E(m,n);
        volEp(volcount)=Ep(m,n);
        volEk(volcount)=Ek(m,n);
        volE(volcount)=E(m,n);
        countA = countA+1;
        volcount=volcount+1;
    end
end
nEpcur = Epcur/mean(Epcur);          %normalize cross-section data by mean value
nEkcur = Ekcur/mean(Ekcur);
nEcur = Ecur/mean(Ecur);
nEp = Ep/mean(Epcur);
nEk = Ek/mean(Ekcur);
nE = E/mean(Ecur);
Epcurstd(ele) = std(nEpcur);         %standard deviation of cross-section data
Ekcurstd(ele) = std(nEkcur);
Ecurstd(ele) = std(nEcur);
figure
set(gcf,'Position',[96 386 560*3 420])
subplot(1,3,1)
surf(nEp)
shading interp
caxis([0 max(max(nEp))])
xlim([1 41])
ylim([1 31])
zlim([0 max(max(nEp))])
 title(['w_p,  \sigma = ' (num2str(Epcurstd(ele),'%6.2f'))],'Fontsize',16)
view(2)
xlabel(['\sigma = ' (num2str(Epcurstd(ele),'%6.2f'))],'Fontsize',14)
set(gca,'Xticklabel',{'1.5','2','2.5','3','3.5','4','4.5','5'});
set(gca,'Yticklabel',{'1.5','2','2.5','3','3.5','4'});
subplot(1,3,2)
surf(nEk)
shading interp
caxis([0 max(max(nEp))])
xlim([1 41])
ylim([1 31])
```

```
        set(gca,'Xticklabel',{'1.5','2','2.5','3','3.5','4','4.5','5'});
        set(gca,'Yticklabel',{'1.5','2','2.5','3','3.5','4'});
        zlim([0 max(max(nEk))])
        title(['w_k,  \sigma = ' (num2str(Ekcurstd(ele),'%6.2f'))],'Fontsize',16)
        view(2)
        xlabel(['\sigma = ' (num2str(Ekcurstd(ele),'%6.2f'))],'Fontsize',14)

        subplot(1,3,3)
        surf(nE)
        shading interp
        caxis([0 max(max(nEp))])
        xlim([1 41])
        ylim([1 31])
        set(gca,'Xticklabel',{'1.5','2','2.5','3','3.5','4','4.5','5'});
        set(gca,'Yticklabel',{'1.5','2','2.5','3','3.5','4'});
        zlim([0 max(max(nE))])
        title(['w_t,  \sigma = ' (num2str(Ecurstd(ele),'%6.2f'))],'Fontsize',16)
        view(2)
        xlabel(['\sigma = ' (num2str(Ecurstd(ele),'%6.2f'))],'Fontsize',14)
        H = colorbar;
        set(H,'Position',[.95 .11 .02 .81]);
        set(gcf,'Color',[1,1,1])
        clear Ep Ek E Epcur Ekcur Ecur nEpcur nEkcur nEcur;
        ele=ele+1;
    end
    nvolEp = volEp/mean(volEp);
    nvolEk = volEk/mean(volEk);
    nvolE = volE/mean(volE);
    volEpstd(R) = std(nvolEp);          %standard deviation of cross-section data
    volEkstd(R) = std(nvolEk);
    volEstd(R) = std(nvolE);
    fprintf(num2str(R))
    R=R+1;
    clear nvolEp nvolEk volEp volEk volE nvolE fndata
end
plot([volEpstd;volEkstd;volEstd]','LineWidth',2)
title('Normalized Standard Deviation of Energy Quantities','FontSize',16)
legend('w_p','w_k','w_t', 'Location', 'bestoutside')
xlabel('1/3rd-octave freq. band (Hz)','Fontsize',14)
xlim([1,18])
ylabel('\sigma (normalized)','Fontsize',14)
set(gca,'xtick',1:18);
set(gca,'Xticklabel',{'','125','','','250','','','500','','','1000','','','2000','','','4000',''});
set(gcf,'Color',[1,1,1])
```

t60_dn.m

```
function [RT] = t60_dn(S_Rate,IRdata)
%Code for calculating RT60 using Schroeder integration
%Impulse responses can be .wav files or .mat files
%after many tries...finished July 21, 2004, Sarah Rollins
%plot of integrated impulse response checked against
%plot from 't60.m', found on the Matlab website, by Micah Shepherd
%written by Christopher Brown, cbrown@phi.luc.edu
%data coming in is either a squared pressure,squared velocity component,
%squared velocity vector, or total Energy Density

fs=S_Rate;
N=length(IRdata);
dt=1/fs*1000; %delta t in ms
tms=(1:N)*dt;
logdata = 10*log10(IRdata./max(abs(IRdata)));

%find arrival of direct sound
dmean=max(logdata)-20; % direct sound must be at least 20 dB above the noise at
                       % the beginning of the IR
nn=find(logdata >= dmean);
direct=nn(1);

%find truncation point (where signal falls below noise level)
lastqu=round(.75*length(logdata));
nlev=max(logdata(lastqu:end));
nline=nlev*ones(size(tms));

%Skim across the envelope of the impulse response-finding the max value
    %in dm step size windows
    start500n=find(tms==500);
    dm=S_Rate/1000*50; %50 ms step size, looking for max
    mn=1;
    for m=start500n:dm:lastqu-1
       decaymax(mn)=max(logdata(m:m+dm-1));
       mn=mn+1;
    end

    %Find when the moving average of the log-squared IR drops below the max
    %of the noise
    dmm=1; %1 sample step size, looking for where IR drops belows noise level
    for mm=1:length(decaymax)/dmm
       decaymean = mean(decaymax((mm-1)*dmm+1:mm*dmm));
       if decaymean < nlev
          truncptn = start500n+dm*dmm*mm-dm*dmm;
          break;
       end
    end
    if exist('truncptn')==0
       fprintf('noise level not found')
       truncptn=length(logdata);
    end
```

```
starttime=direct;
endtime=truncptn(end);
tmspart=(1:endtime)*dt; %time in milliseconds, n/(FS/1000)
schrint(endtime:-1:1)=cumsum(IRdata(endtime:-1:1));
pschr=10*log10(schrint./max(abs(schrint)));
last4th=round(.75*length(pschr));
   dh=1;
   %Determine an approximation for the end of the linear part of the Schroeder curve
   for h=last4th:dh:length(pschr)
      temp(h)=abs(pschr(h)-pschr(h-dh));
      if temp(h) > abs(pschr(last4th)-(pschr(last4th-dh)))%+.03
         ends=h;
         break;
      else
         ends=length(pschr);
      end
   end
%Calculate the T60 from Schroeder curve between 5 dB down and 35 dB down
%unless the decay range is too small, then use 5 dB down to 25 dB down
%**REF: ISO 3382:1997(E), pp 9,14**
dBdown5=max(pschr)-5;
dBdown35=max(pschr)-35;
dBdown25=max(pschr)-25;
dBdown15=max(pschr)-15; %for Early Decay Time
dBdown10=max(pschr)-10;
dBdown20=max(pschr)-20;

if pschr(ends)>dBdown35
  dBdown=dBdown25;
else
  dBdown=dBdown35;
end

%Find the 5 dB down point
dif5=abs(pschr-dBdown5);
%Find the 25 dB down point
dift5=abs(pschr-dBdown);
fivedB=find(dif5==min(dif5));
tfivedB=find(dift5==min(dift5));

%Calculate T60 from Schroeder integration curve
%Find a and b for the least squares regression line
x=tms(fivedB:tfivedB);%(2400:4800);
y=pschr(fivedB:tfivedB);%(2400:4800);

N=length(x);%different N from index 'n' above
a=(mean(y)*sum(x.^2)-mean(x)*sum(x.*y))/(sum(x.^2)-N*mean(x)^2);
b=(sum(x.*y)-N*mean(x)*mean(y))/(sum(x.^2)-N*mean(x)^2);
regline=a+b*x;
T30=(max(pschr)-60-a)/b;
T60= T30/1000;

%    plot(pschr,'r')
%    hold on
%    plot(logdata,'b')
%    plot(fivedB,pschr(fivedB),'gx')
```

```
%     plot(tfivedB,pschr(tfivedB),'gx')
% %     hold on
% %     plot(tmsfull,regline,'g')
% %     xlim([0 endtime])
%     ylim([-60 0])
%     title(['T60: ' num2str(T60)])
clear pschr
clear schrint
RT=T30;
```